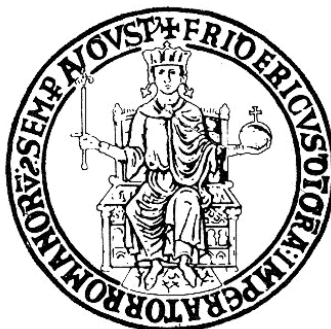


**UNIVERSITY OF NAPLES FEDERICO II**



**DEPARTMENT OF PHARMACY**

***PhD programme in Pharmaceutical Sciences***

*Plant extracts of industrial interest: phytochemical characterization  
and optimization of extraction methods*

**Masi Francesca**

**Coordinator**

**Prof. ROSARIA MELI**

**Tutor**

**Prof. ORAZIO TAGLIALATELA SCAFATI**

**Industrial tutor**

**Dr. ANTONELLA RIVA**

**XXXV CYCLE (2020-2022)**







## **Abstract**

---

Natural products have always played an important role in the pharmaceutical sciences both for their use as medicinal remedies and as a source of inspiration for drug discovery. In ancient times they were used in an unaltered state as concoctions or concentrated plant extracts for the treatment of ailments, but with the development of experimental procedures, the isolation and purification of the active ingredients from the phytocomplex have become a common practice. To date, the importance of natural products has been extensively recognized and natural sources have been significantly exploited in the development of new drugs, both as isolated natural products or their semi-synthetic derivatives. In addition, part of the drugs obtained by total synthesis have been inspired by the pharmacophore of active natural products.

In recent years the role of herbal extracts has slightly changed and, in addition to their use as drugs or source of drugs, also a "support tool" for personal well-being has become important. In this framework, natural products used as health support and alternative strategies have been widely encouraged by a great number of research and studies, due to the benefits that products of natural origin can bring to human health, as well as to mitigate health problems. However, the complexity of natural matrices and their chemical composition should be considered. In fact, nature does not provide products with a standardized composition, and in-depth studies of plant extracts are required in several research areas. From the chemical point of view, the implementation of extraction and purification protocols is indispensable to obtain high-quality

## ***Abstract***

standardized products, as well as the implementation of analytical techniques to investigate the phytochemical profile.

In this framework, the industrial PhD project was in collaboration with the industrial partner Indena Spa (Milan, Italy) and addressed both the characterization of commercial products obtained from different plant extracts and the development and optimization of the extraction method in the industrial laboratories.

The phytochemical investigation involved the characterization of two commercial products obtained from two different plant species: i) *Centella asiatica* and ii) *Rhodiola rosea*.

Thus, the second chapter of this thesis focuses on Centevita<sup>®</sup>, a nutraceutical extract obtained from the leaves of *C. asiatica*. It is standardized to 45% of triterpenes (glycosides), including mostly asiaticoside, madecassoside, asiatic acid, and madecassic acid. They represent the main bioactive compounds of the extract due to their antioxidant activity. My work first dealt with in the characterization of a previously unreported ursane saponin, that was called isomadecassoside, that emerged from preliminary analyses of a fraction enriched in madecassoside, obtained during the extract preparation of Centevita<sup>®</sup>. Then, the in-depth investigation of the full phytochemical profile of Centevita<sup>®</sup> through advanced analytical techniques resulted in the characterization of 24 secondary metabolites, including 10 polyphenols and 14 triterpenoids in the sapogenin or saponin form, and to the discovery of isoterminoloside, a new triglycoside saponin of the unprecedented 2 $\alpha$ , 3 $\beta$ , 6 $\beta$ , 23-tetrahydroxyolean-13(18)-en-28-oic acid (isoterminolic acid).

The third chapter reports on Rhodiola 5%, a nutraceutical extract obtained from the roots of *Rhodiola rosea*. It is standardized and purified to 5% of rosavins, the main bioactive compounds as tonic and adaptogen, and they include rosarin, rosavin, and rosin. The phytochemical investigation carried out resulted in: i) the characterization of 18 secondary metabolites including 13 polyphenols and 6 terpenoids, and ii) the discovery of rhodiosidin, a new compound, the first glycosylated derivative with both terpenoid and phenolic portions. In addition, the 5-lipoxygenase inhibition activity of the main components was characterized, revealing rosiridin, kenposide A and rosavins mainly responsible for the activity of the extract.

The fourth chapter reports on the preliminary studies and the relevant scientific activities carried out at Indena SpA laboratories for the development and optimization of a procedure to obtain a standardized nutraceutical extract enriched in annurcoic acid, a triterpene acid from *Malus domestica*. Apple biomass was chosen among the waste of industrial apple juice processing. It was first subjected to a phytochemical investigation allowing the identification of seven terpene acids including: annurcoic acid, tormentic acid, maslinic acid, corosolic acid, oleanolic acid, ursolic acid, and pomolic acid. The laboratory R&D activities led to the development of a seven-step procedure obtaining a standardized extract characterized by a high content of triterpene acids, of which annurcoic acid was the main component (25% w/w). In parallel, a further procedure was set up to obtain annurcoic acid to be used as a reference standard. The research process led to the isolation of

## ***Abstract***

annurcoic acid (85% w/w), together with two minor compounds: tormentic acid (3.4% w/w) and isomer A (2.6% w/w).

Results reported in this thesis have been in part already published in the following articles:

- Chianese, G., Masi, F., Cicia, D., Ciceri, D., Arpini, S., Falzoni, M., Pagano, E., Taglialatela-Scafati, O. (2021). Isomadecassoside, a new ursane-type triterpene glycoside from *Centella asiatica* leaves, reduces nitrite levels in LPS-stimulated macrophages. *Biomolecules*, 11(4), 494.

- Masi, F., Chianese, G., Peterlongo, F., Riva, A., Taglialatela-Scafati, O. (2022). Phytochemical profile of Centevita<sup>®</sup>, a *Centella asiatica* leaves extract, and isolation of a new oleanane-type saponin. *Fitoterapia*, 158, 105163.

## Table of contents

---

<b>Abstract</b> .....	<b>i</b>
<b>Table of contents</b> .....	<b>v</b>
<b>Chapter 1: Natural products towards drug discovery</b> .....	<b>1</b>
1.1 Natural products and human health .....	4
1.2 Techniques for natural product analyses .....	9
1.2.1 Mass spectrometry .....	10
1.2.1.1 Molecular Networking .....	13
1.2.2 Nuclear Magnetic Resonance .....	16
1.2.2.1 Determination of relative configuration .....	18
1.3 General experimental procedures .....	20
<b>References</b> .....	<b>22</b>
<b>Chapter 2: Phytochemical profile of Centevita<sup>®</sup> and its madecassoside-enriched fraction</b> .....	<b>31</b>
2.1 Introduction .....	31
2.1.1 Biosynthesis of centelloids .....	35
2.2 <i>Centella asiatica</i> as Centevita <sup>®</sup> .....	36
2.2.1 Phytochemical profile of madecassoside-rich fraction ..	38
2.2.2 Phytochemical profile of Centevita <sup>®</sup> .....	44
2.2.2.1 Structural elucidation of isoterminoloside .....	50
2.3 Conclusions .....	55
2.4 Experimental section .....	56
2.4.1 Plant material and extraction of Centevita <sup>®</sup> .....	56
2.4.2 Extraction and isolation of madecassoside-enriched fraction .....	56
2.4.3 LC-MS/MS and Molecular Networking .....	58
2.4.4 Chromatographic separation of Centevita <sup>®</sup> .....	59
<b>References</b> .....	<b>63</b>
<b>Appendix A: Spectral data of chapter 2</b> .....	<b>70</b>
<b>Chapter 3: Phytochemical profile of an industrial <i>Rhodiola rosea</i> extract</b> .....	<b>79</b>
3.1 Introduction .....	79
3.1.1 Biosynthesis of rosavins .....	81

## Table of contents

3.2 <i>Rhodiola rosea</i> as Rhodiola 5% .....	83
3.2.1 Dereplication of the extract .....	85
3.2.2 Structural elucidation of rhodiosidin .....	90
3.2.3 Pharmacological evaluation .....	93
3.3 Conclusion .....	95
3.4 Experimental section .....	96
2.4.1 Plant material and extraction of Rhodiola 5% .....	96
2.4.2 LC-MS/MS analysis .....	96
2.4.3 Chromatographic separation of Rhodiola 5% .....	97
2.4.4 Cell-free f-LO assay .....	99
2.4.5 Cell-based 5-LO assay in PMNL .....	99
<b>References .....</b>	<b>101</b>
<b>Appendix B: Spectral data of chapter 3 .....</b>	<b>109</b>
<b>Chapter 4: Towards an annurcoic acid-rich apple standardized extract .....</b>	<b>121</b>
4.1 Introduction .....	121
4.2 <i>Malus domestica</i> for the nutraceutical extract .....	125
4.2.1 Starting material and phytochemical profile of apple waste biomass .....	126
4.2.2 Annurcoic acid-enriched standardized extract: method development .....	128
4.2.3 Development of annurcoic acid reference standard ...	135
4.3 Conclusions .....	138
4.4 Experimental section .....	139
4.4.1 Starting material .....	139
4.4.2 HPLC-UV analysis .....	139
4.4.3 Chromatographic separations of raw extract from apple waste biomass .....	140
<b>References .....</b>	<b>142</b>
<b>Appendix C: Spectral data of chapter 4 .....</b>	<b>147</b>
<b>Chapter 5: Conclusions .....</b>	<b>153</b>

## **Chapter 1: Natural products towards drug discovery**

---

A natural product (NP) is a chemical compound or substance produced by a living organism (animals, plants, fungi, or microbes). Several NPs can have pharmacological or biological activity and can be clinically used either in crude form, typically in traditional medicines, or by chemical synthesis (semisynthesis or total synthesis), in the modern system.<sup>1,2</sup> In the field of medicinal chemistry, the definition of Natural products is usually restricted to organic compounds isolated from natural sources that are produced by the pathways of secondary metabolism. Different from primary metabolites (nucleic acids, proteins, fats, and carbohydrates), secondary metabolites can be considered as "dispensable" molecules for growth and development but "indispensable" for the interaction between different species and their survival and adaptation as they represent a valid weapon against predators or environmental stresses.<sup>3</sup>

Secondary metabolites are originated by enzymatically catalysed reactions roughly ascribable to four main pathways: acetate, mevalonate, shikimate pathways and of mixed origin. The precursor for these pathways comes from primary processes like glycolysis, Krebs cycle, amino acid metabolism and photosynthesis. These metabolic reactions produce intermediates such as mevalonic acid, acetyl coenzyme A (acetyl-CoA) and 1-deoxyxylulose-5-phosphate, that are rearranged to produce a countless number of natural compounds.

## *Chapter 1*

Therefore, each medicinal plant species has its own specificity, as well as different parts of the same plant (roots, stems, leaves, flowers, fruits, and seeds) can provide different secondary metabolites. In addition, the phytochemical profile of medicinal plants belonging to the same species can strongly vary depending on several environmental and anthropogenic factors (e.g. locations, climate changes, presence of biotic and abiotic stressors).

Since prehistoric times, a large part of the world population has relied on medicinal plants to treat different human diseases and they continue to be a significant source of therapeutically relevant compounds.<sup>4</sup> In fact, traditional natural medicines were widely used as concoctions or concentrated plant extracts without isolation of active compounds. Contrarily, since the nineteenth-century, advances in the technology field and the development of effective and reliable experimental procedures allowed the isolation and purification of the active principles from plants.<sup>5</sup> This modern concept of chemistry of natural products started with Friedrich Sertürner, who isolated morphine from opium in 1804. Other similar developments led to discovery of bioactive compounds such as: quinine (1820), cocaine (1859), tubocurarine (1935), among others. To date, the importance of natural products has been extensively recognized and natural sources have been significantly exploited. In fact, between 1981 and 2019, 33% of the newly approved drugs were natural products or their semi-synthetic derivatives, whereas 35% was obtained by total synthesis starting from the pharmacophore of an active natural product.<sup>6</sup>

However, in 2021, the Food and Drug Administration (FDA) has approved only four new drugs of natural origin: i) ibrexafungerp

(Brexafemme™), a triterpenoid antifungal drug, used for vulvovaginal candidiasis, ii) maribavir (Livtency™), a ribose-based antiviral drug, indicated for the treatment of post-transplant cytomegalovirus, iii) samidorphan (Lybalvi™), a morphine derivative, indicated for the treatment of schizophrenia or bipolar disorder, and iv) Nextstellis™, a combination of two steroids - drospirenone and estetrol - as oral contraceptive (**Figure 1.1**).

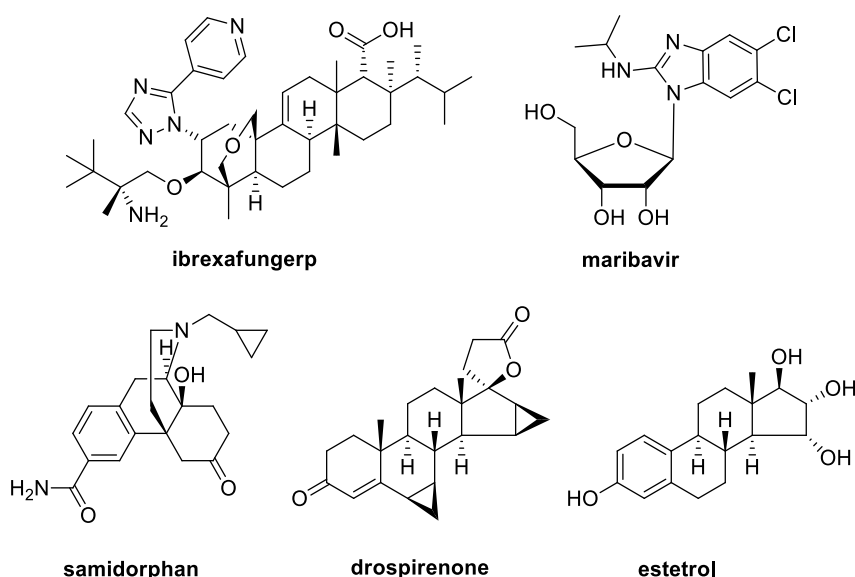


**Figure 1.1.** Structures of drugs inspired by natural products approved by FDA in 2021.

To analyse these data in the marketing of drugs of natural origin the impact that COVID-19 has had in the pharmaceutical sector must be taken into account.<sup>7</sup>

Nonetheless, natural products continue to play a key role in drug discovery not only for the high number of active compounds yet to be discovered but also for the huge chemodiversity observed among them, that represents a precious inspiration source for

## *Chapter 1*

synthetic derivatives.<sup>5</sup> In this regard, the wide structural variability of natural compounds can be explained through the fact that their structures are 'optimized' by evolution in order to interact with proteins and serve specific biological functions (e.g. regulation of endogenous defence mechanisms and the interaction with other organisms). This explains the high relevance of natural products for the treatment of cancer, infectious diseases, multiple sclerosis, and cardiovascular disorders.<sup>8</sup>

Although drug discovery from natural products could be arduous and time-consuming, the key factors for potential success are to find suitable strategies, pay more attention to the impact of new technologies, and assume a deep thinking and innovative spirit in the study of what the Nature can still offer.<sup>9</sup>

### **1.1 Natural products and human health**

Since ancient times, herbal extracts have been used as medicinal remedies for many human ailments. In recent years their role has slightly changed, in fact not only they are used as drugs or as a source of drugs, but also as "support tools" for personal well-being.

The increase in lifespan in association with the adoption of inappropriate lifestyle and eating habits have promoted the onset of a variety of diseases such as cardiovascular and neurodegenerative disorders, diabetes, cancer, obesity, osteoporosis, allergies, and dental problems.<sup>10</sup> These types of illnesses can occur even at an early age and one of the possible causes lies in an unbalanced diet.

In this framework, the benefits that products of natural origin can bring to human health, as well as to mitigate health problems, have been considered. Although the molecular-based mechanisms by which natural products can improve and preserve human health are extremely complex, their use as health support and alternative strategies has been widely encouraged by a great number of research and studies.<sup>11</sup>

The classification, as well as definition, of natural products that can provide benefits to human health, are still confused and contradictory. Nonetheless, a large variety of these products have been reported so far, including nutraceuticals, functional food, and medicinal foods.<sup>12</sup>

*Nutraceuticals* are all those products that are derived from food sources that can provide additional health benefits beyond basic nutritional value.<sup>13</sup> They have been defined as "a food (or part of a food) that gives medicinal or health benefits which help in the prevention and treatment of a disease".<sup>14</sup> Nutraceuticals can be classified in several ways based on i) their natural sources (e.g. products derived from plants, animals, minerals, and microbes), ii) mechanism of action (e.g. antibacterial, hypotensive, antioxidant, anti-inflammatory), and iii) chemical classes (e.g. amino acids and derivatives, carbohydrates and derivatives, fatty acids and lipids, isoprenoid derivatives or phenols).<sup>15,16</sup> Among these, the natural source of nutraceuticals is considered fundamental for their definition and marketing, therefore a further sub-classification can be made: isolated food nutrients (vitamins, minerals, amino acids, and fatty acids), herbals (herbs or botanical products as extracts) and dietary supplements (derived from other sources).<sup>17-19</sup>

## Chapter 1

Food nutrients (also known as phytonutrients) are a large category of natural chemicals including antioxidants, vitamins, that can be found in a wide variety of foods (grains, beans, fruits vegetables and herbs). They are secondary metabolites produced by plants for different purposes with specific nutritional functions, even if are not considered essential nutrients.<sup>20,21</sup>

Herbals are medicinal plants that have the aim of preventing different diseases thanks to the bioactive chemical compounds composition.<sup>22,23</sup> Herbs can be consumed as fresh or dried parts of the plant (or the whole plant) in very different ways: powders, standardized extracts, tinctures, capsules, and tablets.<sup>24</sup>

Dietary supplements are products that integrate the total daily intake of functional compounds (e.g. vitamins, minerals, proteins, and amino acids), without the effects of prevention and treatment of illnesses.<sup>25</sup> Although the food and drug administration (FDA) classifies dietary supplements as food, not as drug, many of them contain bioactive molecules with significant biological impact that may cause side effects when administered with specific drugs.

*Functional foods* are food products containing physiologically active constituents which act in the disease prevention since they are directly involved in the modulation of endocrine, immune, nerve, circulatory, and digestive systems.<sup>26</sup> Unlike nutraceuticals, functional foods include whole and fortified foods and enriched or enhanced dietary components that can reduce the risk of chronic disease and provide health benefits beyond the traditional nutrients it contains.<sup>13</sup> Probiotic yogurts, cholesterol-lowering spreads and foods fortified with additional nutrients such as omega-3 fatty acids are just some of the best-known products in this category.<sup>27</sup>

*Medicinal foods* are all those products administered to deal with specific diseases or health conditions for which distinctive nutritional requirements are required and established by medical evaluation (based on recognized scientific principle).<sup>28</sup> In fact, they are formulated to be consumed or administered internally under the strict supervision of a qualified operator.

Among all of these, *nutraceuticals* have received an unexpected worldwide response and their market is constantly growing. In fact, the current market trends in healthcare are focused on preventive health care strategies, rather than treatment and disease management. Thus, the nutraceutical industry is flourishing and diversifying rapidly (**Figure 1.2**). U.S. and China are the largest consumers of nutraceuticals, although above-average growth is expected for India, and Brazil over the coming decades.<sup>29</sup>

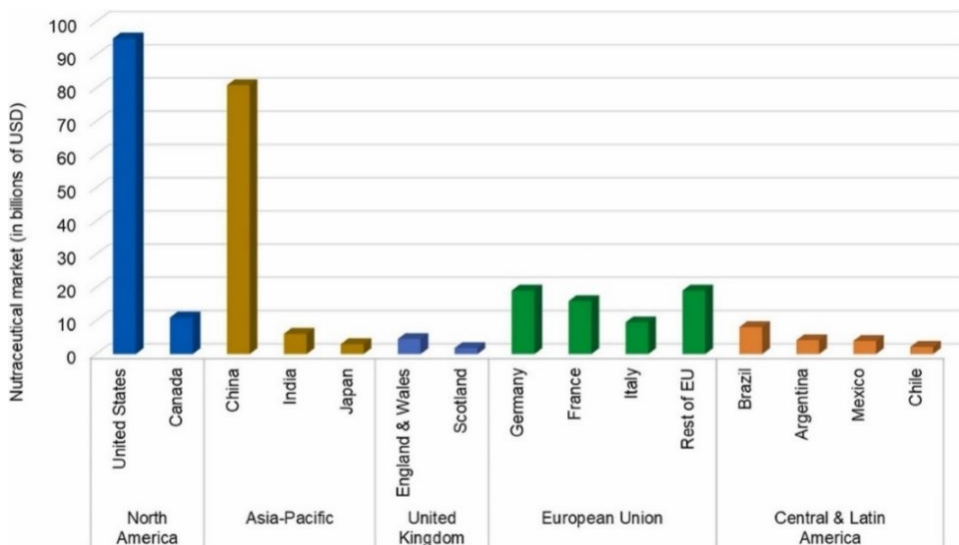


**Figure 1.2.** *The global nutraceutical market and major consumers approximated using 2017 estimates.*

## Chapter 1

Nutraceutical products are not regulated in Europe and in the USA, thus no proof of efficacy and no premarketing approval is required before being placed on the market.<sup>30</sup>

However, the complexity of natural matrices and their chemical composition should be taken into consideration. In fact, nature does not provide products with a standardized composition, as well as the metabolic profile of a given species and the relevant bioactivity can strongly vary according to different factors (e.g. the age of the plant, harvest time, weather conditions, part of the plant used and soil conditions). As a result, the amount of botanical constituents per portion could vary significantly, causing so potential synergistic or antagonistic effects.<sup>31</sup> Therefore, in-depth studies of plant extracts are required in several research areas. From the chemical point of view, the implementation of extraction and purification protocols characterized by high recovery yields and low variability are indispensable to obtain high quality standardized products, as well as the implementation of analytical techniques to investigate the phytochemical profile. On the other hand, the development of in vitro and in vivo assays is required for the evaluation of pharmacokinetic parameters, the interaction between extract constituents and toxicological effects.<sup>32</sup>

For example, a recent study was conducted on Vazguard<sup>®</sup>, a standardized extract from bergamot (*Citrus bergamia* Risso et Poiteau) available at Indena SpA (Milan, Italy) as Phytosome<sup>®</sup> formulation. The Bergamot Polyphenolic Fraction (BPFC) has proved to support health and bring benefits to people affected by disorders due to metabolic syndrome<sup>33-35</sup> (e.g. high blood sugar, fatty liver, abnormal cholesterol or triglyceride levels) commonly

associated with lack of physical activity, overweight, unhealthy diet and irregular lifestyle. Particularly, Indena SpA developed a robust and highly effective procedure to obtain a standardized bergamot extract enriched in bioactive compounds of interest, as well as the protocol for the formulation of the final product. In fact, Vazguard<sup>®</sup> uses the Phytosome<sup>®</sup> formulation strategy, a delivery system that optimizes the biological absorption of polyphenols, which are normally poorly soluble in both water and organic solvents. In order to provide a fingerprint analysis of the constituents of Vazguard<sup>®</sup>, its phytochemical characterization was conducted and reported by Formisano et al. (2019) in collaboration with Indena.<sup>36</sup> The combination of different chromatographic and instrumental techniques (UPLC-DAD-MS and NMR spectroscopy) led to the identification of 39 components in Vazguard<sup>®</sup> including interesting new findings: i) known molecules that had never been found in bergamot extracts, and ii) new secondary metabolites.

Some of the goals fixed in this industrial PhD project fall into this framework: characterization of commercial products obtained from different plant extracts in collaboration with the industrial partner Indena Spa (Milano, Italy), and the development and optimization of the extraction method in the industrial laboratories.

## **1.2 Techniques for natural product analyses**

Since natural products are complex mixtures, multi-technical analytical procedures are required to deconvolute and identify them.

## *Chapter 1*

High-performance liquid chromatography (HPLC) coupled to a variety of detectors (i.e., ultraviolet (UV), Diode-Array (DAD) and refractive index (RI)) are commonly applied for qualitative-quantitative analysis of natural matrices as well as for purification and isolation of their constituents. In addition, advances in the field of technology led to the development of powerful techniques based on Ultra Performance Liquid Chromatography (UPLC) allowing more accurate evaluation due to the improved chromatographic resolution.

The possibility to couple liquid chromatography to mass spectrometry (UPLC-MS) using electrospray ionization (ESI) turned out to be essential for in-depth and high-throughput analyses of extracts and for the detection of metabolites with poor or no UV absorption.

On the other hand, nuclear magnetic resonance (NMR) spectroscopy is probably the crucial technique used for extract characterization since it provides advantages such as: i) identical response factor for different classes of constituents, ii) the opportunity to obtain structural information on the detected compounds (mainly by 2D NMR experiments) and, iii) rapid measurements of constituents without the need for the reference compounds.<sup>37</sup>

### **1.2.1 Mass spectrometry**

Mass spectrometry is an analytical technique applied both to the trace analyses of molecules, and the identification of unknown substances, and it is commonly used coupled to separation

techniques such as gas chromatography and liquid chromatography. Contrary to spectroscopic techniques, mass spectrometry is a destructive method of analysis because the molecule does not remain intact, and it is not based on the interaction between radiation and matter.

The principle is to separate a mixture of ions based on their mass/charge ( $m/z$ ) ratio, generally through a static or oscillating magnet field. Particularly, the experiment includes the ionization of molecules in the gas phase, the separation of the different ions produced and their detection. The result of the experiment is the mass spectrum, a diagram representing the ion relative abundance, in the function of their  $m/z$  ratio. Thus, the mass spectrum is typical of each compound as it is directly correlated to its chemical structure and to the ionization conditions to which it has been subjected. This technique allows to measure the molecular masses, both nominal and exact, and obtain specific fragmentation profiles for each compound.

The experiment takes place in different parts of the mass spectrometer, and the core parts are the *ionization source*, the *analyzer*, and the *detector*. Most of the samples described in the following chapters were analyzed by an Electrospray Ionization (ESI) mass spectrometry through an LTQ Orbitrap XL analyzer.

Electrospray ionization (**Figure 1.3**) is widely used since it is a soft ionization source and can efficiently be coupled to HPLC or UPLC to easily perform MS analysis of complex mixtures. In addition, ESI mass spectrometry allows to analyze non-volatile molecules directly from the liquid phase, dissolving them in a polar solvent. The solution is dispersed into fine droplets and subjected to further

## Chapter 1

solvent evaporation forming smaller and stabilized droplets, through a heated capillary carrying a potential difference. As a result of the capillary electric potential, each droplet of the spray delivers an excess of positive or negative charges which are all the analytes ionized into the capillary. The ions displayed in the mass spectrum derive from the addition of a proton, denoted as  $[M+H]^+$ , or by other cations, as for example, sodium, denoted as  $[M+Na]^+$ . On the other hand, the expulsion of a proton can produce the  $[M-H]^-$  anion. Multiply charged ions,  $[M+nH]^{n+}$  can be also observed. An inert gas, such as nitrogen is often used as a 'vehicle' to facilitate the liquid nebulization and solvent evaporation inside the droplets.

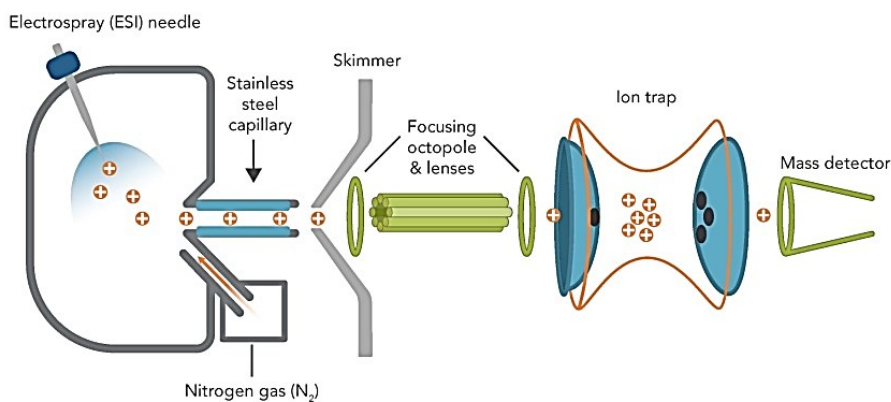


**Figure 1.3.** General components of an ESI-ion trap MS instrument.

High-resolution mass spectrometry (HRMS) is an excellent technique since it ensures the calculation of accurate masses of analyzed ions. The instrumental systems comprise Fourier-transform ion cyclotron resonance (FT-ICR), time-of-flight (TOF), and Orbitrap mass spectrometry.

Orbitrap is an ion trap mass analyzer consisting of a central electrode and two outer electrodes, which enable it to act as both an analyzer and detector. Ions entering the analyzer are captured and oscillate around the central electrode and in between the two outer electrodes (**Figure 1.4**). Different ions oscillate at different frequencies, resulting in their separation. The oscillations frequency is not based on the ion velocity and is inversely proportional to the square root of the mass-to-charge ratio ( $m/z$ ). By measuring the oscillation frequencies induced by ions on the outer electrodes, the mass spectra of the ions are acquired using image current detection.

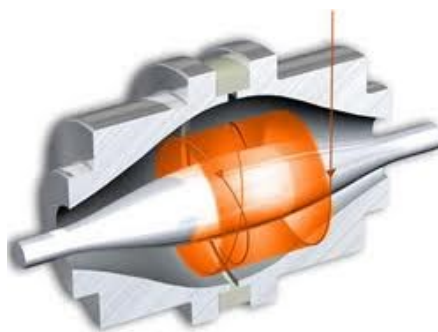


**Figure 1.4.** *Ion trajectories in an Orbitrap mass spectrometer.*

Orbitrap analyzer has a high mass accuracy (1-2 ppm), and a high resolving power (up to 200,000).<sup>38,39</sup>

#### *1.2.1.1 Molecular Networking*

Molecular networking is a computational strategy based on tandem mass spectrometry (MS/MS), recently introduced in drug discovery, metabolomics, and medical fields.

## Chapter 1

Untargeted MS is a key metabolite discovery and annotation strategies in metabolomics, and molecular networking provides a data organizational approach and a visual overview of complex data arising from the analyses.<sup>40</sup>

Molecular networking foundation is a pairwise spectral alignment that uses a modified cosine spectral similarity algorithm.<sup>41</sup> Moreover, molecular networking builds on the important observation that two structurally related molecules share fragment ion patterns when subjected to MS<sup>2</sup> fragmentation methods. Therefore, in the modified spectral similarity search fragmentation, spectra (MS<sup>2</sup>) from ions at identical *m/z* values and MS<sup>2</sup> spectra offset by the same *m/z* difference as the precursor ion, are compared. During a pairwise spectral similarity search/alignment, each MS<sup>2</sup> spectrum in each dataset is compared against every other obtaining a network of MS<sup>2</sup> spectral relations, from which a molecular network is created.

To date, the molecular networking algorithm is accessible to the scientific community and converted to a web-based platform backed by a supercomputer: Global Natural Product Social Molecular Network (GNPS).

It is a crowd-sourced and community-driven analysis infrastructure that facilitates data and knowledge storage, but also enables knowledge capture, dissemination, sharing, and data-driven social networking, meanwhile promoting reproducible data analysis.

To create a molecular network, GNPS aligns each MS<sup>2</sup> spectrum in a dataset to each of the others and then assigns a cosine score to every combination to describe their similarity (**Figure 1.5**). Based on a hierarchical cosine clustering algorithm, identical masses

collapse into a single node or consensus cluster due to the high similarity of their fragment ions.<sup>42</sup> Structurally-related molecules are represented by separate nodes that connect within the network via edges as they provide comparable MS<sup>2</sup> spectra due to similarities in their gas-phase chemistry.<sup>43</sup> All the consensus spectra (node) are then compared with spectral library databases in order to assign them to a putative molecule reported in a network.

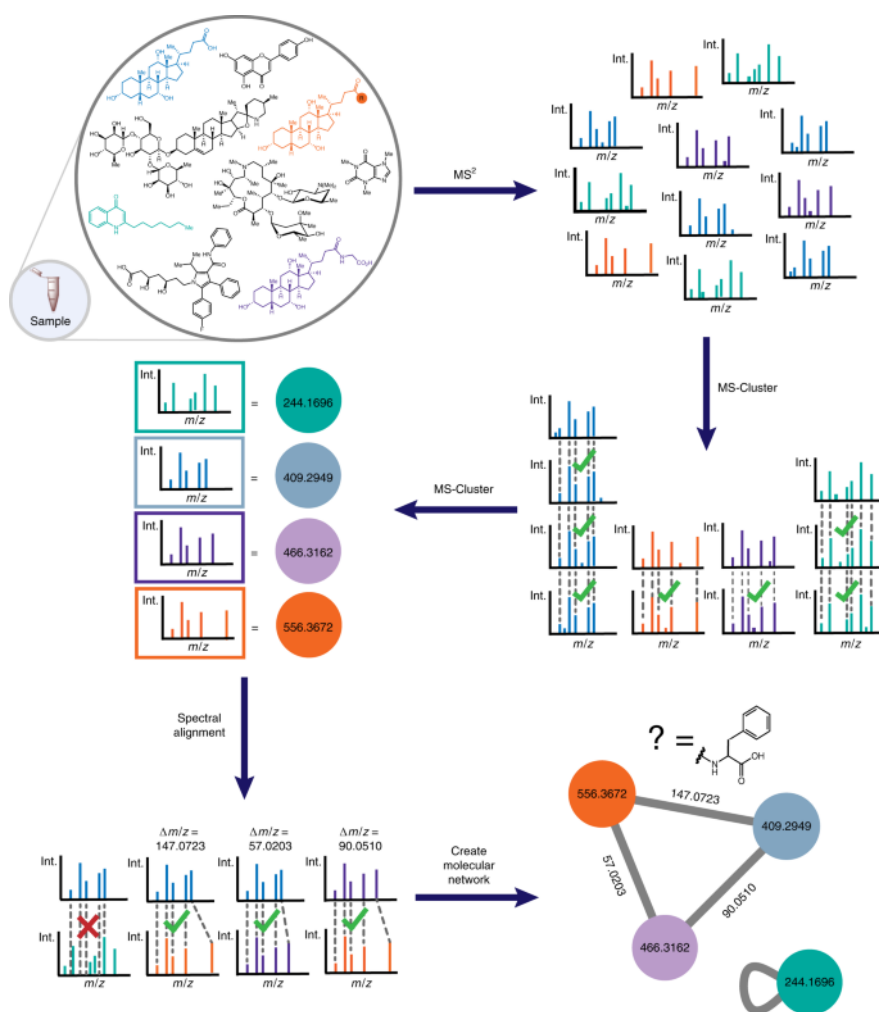


**Figure1.5.** Schematic representation of the process for creating a molecular network for metabolites in complex sample mixtures.

## Chapter 1

Generally, the workflow consists of four main phases: (i) collecting MS<sup>2</sup> spectra, (ii) converting instrument-specific raw data files to an open format (mzXML, .mzML or .mgf), (iii) submitting a job to GNPS, and (iv) visualizing the resulting molecular network.

GNPS molecular networking allows to analyze and compare MS<sup>2</sup> spectra in one or more datasets acquired as part of a specific study, across datasets from multiple studies. In GNPS, the MS<sup>2</sup> spectra are organized in a network according to similarity and compared against a reference database to identify 'molecular families' and putative known molecules in the samples. At last, GNPS-generated molecular networks' visualization and analysis can be performed either in the web browser itself or in Cytoscape, an open-source software for visualizing complex networks.<sup>44,45</sup>

Metabolomics and dereplication analyses (LC-MS and MN) reported in this thesis were carried out under the supervision of Professor Jean-Luc Wolfender, School of pharmaceutical sciences, University of Geneva, Switzerland (by remote due to the covid-19 pandemic situation).

### 1.2.2 Nuclear Magnetic Resonance

Nuclear Magnetic Resonance spectroscopy is a powerful and complex analytical technique used for the structure elucidation of the isolated secondary metabolites in a non-destructive way. Many elemental isotopes have nuclei characterized by a specific number of spin (**I**). Since a spinning charge can generate a magnetic field, a spin-magnet with a magnetic moment (**μ**) proportional to the spin is produced. An external magnetic field (**B<sub>0</sub>**) can be applied,

obtaining various spin states of a nucleus according to the value of  $I$ , with different energy ( $I$  corresponds to  $2I+1$ ); the different energy depends on the applied magnetic field strength. Nuclei with  $I=0$  do not give NMR signals since they do not possess a magnetic property. Hydrogen ( $^1\text{H}$ ), carbon ( $^{13}\text{C}$ ), fluorine ( $^{19}\text{F}$ ) and phosphorus ( $^{31}\text{P}$ ) have nuclei with  $I=1/2$ , therefore, they can be investigated using NMR. Placing nuclei with  $I\neq 0$  in a magnetic field, they will acquire a possible number of various orientations, each corresponding to specific energy levels. Moreover, the number of orientations will depend on the value of  $I$  ( $2I+1$ ).

On the other hand, placing nuclei with  $I= 1/2$  in an external magnetic field, they can assume only two possible orientations: i)  $\alpha$  parallel ( $I = 1/2$ ), corresponding to the lower energy level, or ii)  $\beta$  antiparallel ( $I = - 1/2$ ), corresponding to the higher energy level. The difference in energy is expressed by the equation:

$$\Delta E = \gamma B_0$$

where  $\gamma$  represents the gyromagnetic factor, and it is specific for a certain nucleus. The protons are distributed between the two levels ( $\alpha$  and  $\beta$ ), although with an excess of population in the  $\alpha$  state, having lower energy. Applying energy (a radio frequency pulse), the nuclei migrate from lower to higher levels of energy; once the radiofrequency finishes, the Free Induction Decay (FID) is supplied and converted in the frequency domain, using the Fourier Transform (FT).

One-dimensione (1D) and two-dimensional (2D) NMR experiments have been employed for the structural elucidation of isolated compounds.

## Chapter 1

COSY (CORrelation SpectroscopY) is a homonuclear chemical shift correlation experiment, that determines protons' spin-spin directly J-coupled.

The HSQC (Heteronuclear Single Quantum Correlation) is a heteronuclear correlation experiment, in which the one-bond proton-carbon couplings ( $^1J_{CH}$ ) are provided. This experiment connects the chemical shifts of proton and directly bonded carbon.

The HMBC (Heteronuclear Multiple Bond Correlation) is a heteronuclear experiment which allows to detect correlations from  $^1H$  to  $^{13}C$ , separated by two and three bonds, and, in some cases, the correlations can be detected with a separation of four bonds, such as in conjugated systems. Correlations between protons and carbons directly bonded are not visible.<sup>46,47</sup>

### 1.2.2.1 Determination of relative configuration

In the structure elucidation process, the determination of the relative and absolute configurations of an unprecedented natural, synthetic or semisynthetic compound is a key step. Since there is a strict association between biological activity and the three-dimensional structure, knowing the stereochemistry of a molecule is essential. Generally, the configuration determination starts with establishing the relative configuration of chiral centers by evaluating coupling constants ( $J$ ), chemical shifts ( $\delta$ ), and NOE effects, in NMR experiments.

The relative configuration refers to the organization of a molecule in relation to atoms on the same molecule, in relation to other molecules, or in relation to another form of the same molecule. As

concern the proton chemical shifts of the two diastereomers, they differ since they have diverse chemical milieu. The Karplus equation describes the relationship between  $^3J$  coupling constants and dihedral torsion angles:

$$^3J = A \cos^2 \theta + B \cos \theta + C$$

In this formula,  $^3J$  coupling constant defines the correlation between two vicinal hydrogen atoms; A, B, and C are empirical parameters based on the substituents involved; and  $\theta$  is the dihedral angle. When the value of the coupling constant is large, the angles are between  $0^\circ$  and  $180^\circ$ , whereas when it is small, the angle is close to  $90^\circ$ . The Karplus equation leads to preliminary information about the relative atomic spatial distribution of molecules.<sup>48</sup>

Additional information about the relative configuration can be obtained from the NOE (Nuclear Overhauser Enhancement) and ROE (Rotating-frame Overhauser Enhancement) effects.

NOESY is a NMR-based method to assign the relative configuration of chiral centers. Irradiating a specific NMR signal during the acquisition of the spectra, the NOE effect can be detected. As a result, the relaxation times of all the protons near the irradiated center (distance  $< 2.5 \text{ \AA}$ ) change, along with the protons not belonging to the same spin system. In fact, the NOE effect is obtained through space and not through chemical bonds; therefore, atoms that are in proximity to each other can produce NOE.<sup>49</sup>

ROESY is a NMR-based experiment similar to the previous method. It is based on a homonuclear correlation which can find ROE (Rotating-frame Overhauser Effect). It is used for molecules with a

## Chapter 1

molecular weight of around 1000 daltons, and the NOE is too weak to be observed.

### 1.3 General experimental procedures

In this subsection, general techniques and instruments used for the development of the research described in the thesis are reported. Specific techniques are described in the relevant chapter. Optical rotations (CH<sub>3</sub>OH) were measured at 589 nm on a P2000 JASCO (Dunmow, UK) polarimeter.

1D and 2D NMR experiments were recorded on Bruker Avance 700, Bruker Ascend 600 and Bruker Avance NEO 400 (Bruker, USA) spectrometers. Chemical shifts are referenced to the residual solvent signal (CD<sub>3</sub>OD:  $\delta_{\text{H}}$  3.31,  $\delta_{\text{C}}$  49.0). Homonuclear <sup>1</sup>H connectivities were determined by COSY experiments; one-bond heteronuclear <sup>1</sup>H-<sup>13</sup>C connectivities by the HSQC experiment; and two- and three-bond <sup>1</sup>H-<sup>13</sup>C connectivities by gradient-HMBC experiments optimized for a <sup>2,3</sup>J value of 8 Hz. Through-space <sup>1</sup>H connectivities were obtained using a NOESY experiment with a mixing time of 300 ms.

Low- and high-resolution ESIMS were performed on hybrid linear Ion Trap LTQ Orbitrap XLTL Fourier Transform Mass Spectrometer (FTMS).

Medium-pressure liquid chromatography (MPLC) was performed on a Sepachrom (Italy) instrument; RP-HPLC-UV-vis separations were performed on an Agilent instrument, using, a 1260 Quat Pump VL system, equipped with a 1260 VWD VL UV-vis detector, and a Rheodyne injector; HPLC-RI separations were performed on a

Knauer (Berlin, Germany) 1800 apparatus equipped with a refractive index detector.

Chemical reagents and solvents were purchased from Sigma-Aldrich (Germany) and were used without any further purification. Silica gel 60 (70–230 mesh) was used for gravity column chromatography (CC). Thin-layer chromatography (TLC) was performed on plates coated with silica gel 60 F254 Merck, 0.25 mm.

## References

---

1. Cutler, H. G., & Cutler, S. J. (1999). *Biologically active natural products: agrochemicals*. CRC Press.
2. Samuelsson, G., & Bohlin, L. (2017). *Drugs of natural origin: A treatise of pharmacognosy* (No. Ed. 7). CRC Press Inc.
3. Pang, Z., Chen, J., Wang, T., Gao, C., Li, Z., Guo, L., Xu, J., & Cheng, Y. (2021). Linking plant secondary metabolites and plant microbiomes: a review. *Frontiers in Plant Science*, *12*, 621276.
4. Pant, P., Pandey, S., & Dall'Acqua, S. (2021). The influence of environmental conditions on secondary metabolites in medicinal plants: a literature review. *Chemistry & Biodiversity*, *18*(11), e2100345.
5. Berdigaliyev, N., & Aljofan, M. (2020). An overview of drug discovery and development. *Future medicinal chemistry*, *12*(10), 939-947.
6. Newman, D. J., & Cragg, G. M. (2020). Natural products as sources of new drugs over the nearly four decades from 01/1981 to 09/2019. *Journal of natural products*, *83*(3), 770-803.
7. De la Torre, B. G., & Albericio, F. (2022). The Pharmaceutical Industry in 2021. An Analysis of FDA Drug Approvals from the Perspective of Molecules. *Molecules*, *27*(3), 1075.

8. Atanasov, A. G., Zotchev, S. B., Dirsch, V. M., & Supuran, C. T. (2021). Natural products in drug discovery: advances and opportunities. *Nature reviews Drug discovery*, *20*(3), 200-216.
9. Zhang, L., Song, J., Kong, L., Yuan, T., Li, W., Zhang, W., ... & Du, G. (2020). The strategies and techniques of drug discovery from natural products. *Pharmacology & Therapeutics*, *216*, 107686.
10. Espín, J. C., García-Conesa, M. T., & Tomás-Barberán, F. A. (2007). Nutraceuticals: facts and fiction. *Phytochemistry*, *68*(22-24), 2986-3008.
11. David, B., Wolfender, J. L., & Dias, D. A. (2015). The pharmaceutical industry and natural products: historical status and new trends. *Phytochemistry Reviews*, *14*(2), 299-315.
12. Ditu, L. M., Grigore, M. E., Camen-Comanescu, P., & Holban, A. M. (2018). Introduction in Nutraceutical and Medicinal Foods. In *Therapeutic, Probiotic, and Unconventional Foods* (pp. 1-12). Academic Press.
13. Gul, K., Singh, A. K., & Jabeen, R. (2016). Nutraceuticals and functional foods: the foods for the future world. *Critical reviews in food science and nutrition*, *56*(16), 2617-2627.
14. DeFelice, S. L. (1995). The nutraceutical revolution: its impact on food industry R&D. *Trends in Food Science & Technology*, *6*(2), 59-61.

## Chapter 1

15. Pandey, N., Meena, R. P., Rai, S. K., & Pandey-Rai, S. (2011). Medicinal plants derived nutraceuticals: a re-emerging health aid. *International Journal of Pharma and Bio Sciences*, 2(4), 420-441.
16. Wildman, R. E., Wildman, R., & Wallace, T. C. (2016). *Handbook of nutraceuticals and functional foods*. CRC press.
17. Malik, A., Kumar, P., Kaushik, N., & Singh, A. (2008). The potentials of Nutraceuticals. *Pharmainfo. net*, 6, 151-183.
18. Dureja, H., Kaushik, D., & Kumar, V. (2003). Developments in nutraceuticals. *Indian journal of pharmacology*, 35(6), 363-372.
19. Chauhan, B., Kumar, G., Kalam, N., & Ansari, S. H. (2013). Current concepts and prospects of herbal nutraceutical: A review. *Journal of advanced pharmaceutical technology & research*, 4(1), 4.
20. Das, L., Bhaumik, E., Raychaudhuri, U., & Chakraborty, R. (2012). Role of nutraceuticals in human health. *Journal of food science and technology*, 49(2), 173-183.
21. Dai, J., & Mumper, R. J. (2010). Plant phenolics: extraction, analysis and their antioxidant and anticancer properties. *Molecules*, 15(10), 7313-7352.
22. Chanda, S., & Kaneria, M. (2011). Indian nutraceutical plant leaves as a potential source of natural antimicrobial agents. *Science against microbial pathogens*:

- communicating current research and technological advances*, 2, 1251-1259.
23. Jhansi, D., & Manjula, K. (2016). Functional and nutraceutical properties of herbals and its applications in food. *IJSR*, 5, 196-198.
24. Hoareau, L., & DaSilva, E. J. (1999). Medicinal plants: a re-emerging health aid. *Electronic Journal of biotechnology*, 2(2), 3-4.
25. Cencic, A., & Chingwaru, W. (2010). The role of functional foods, nutraceuticals, and food supplements in intestinal health. *Nutrients*, 2(6), 611-625.
26. Arai, S. (1996). Studies on functional foods in Japan—state of the art. *Bioscience, biotechnology, and biochemistry*, 60(1), 9-15.
27. Williamson, C. (2009). Functional foods: what are the benefits?. *British journal of community nursing*, 14(6), 230-236.
28. Mortazavian, A. M., & Meybodi, N. M. (2016). Medicinal food products; a new approach from ordinary foods to medicine. *Iranian Journal of Pharmaceutical Research: IJPR*, 15(1), 1.
29. Chopra, A. S., Lordan, R., Horbańczuk, O. K., Atanasov, A. G., Chopra, I., Horbańczuk, J. O., ... & Arkells, N. (2022). The current use and evolving landscape of nutraceuticals. *Pharmacological Research*, 175, 106001.

## Chapter 1

30. Wang, J., Guleria, S., Koffas, M. A., & Yan, Y. (2016). Microbial production of value-added nutraceuticals. *Current opinion in biotechnology*, 37, 97-104.
31. Yang, Y., Zhang, Z., Li, S., Ye, X., Li, X., & He, K. (2014). Synergy effects of herb extracts: pharmacokinetics and pharmacodynamic basis. *Fitoterapia*, 92, 133-147.
32. Sut, S., Baldan, V., Faggian, M., Peron, G., & Dall'Acqua, S. (2016). Nutraceuticals, a new challenge for medicinal chemistry. *Current medicinal chemistry*, 23(28), 3198-3223.
33. Risitano, R., Currò, M., Cirimi, S., Ferlazzo, N., Campiglia, P., Caccamo, D., ... & Navarra, M. (2014). Flavonoid fraction of Bergamot juice reduces LPS-induced inflammatory response through SIRT1-mediated NF- $\kappa$ B inhibition in THP-1 monocytes. *PloS one*, 9(9), e107431.
34. Mollace, V., Sacco, I., Janda, E., Malara, C., Ventrice, D., Colica, C., ... & Romeo, F. (2011). Hypolipemic and hypoglycaemic activity of bergamot polyphenols: from animal models to human studies. *Fitoterapia*, 82(3), 309-316.
35. Rondanelli, M., Giacosa, A., Morazzoni, P., Guido, D., Grassi, M., Morandi, G., ... & Perna, S. (2016). MediterrAsian diet products that could raise HDL-cholesterol: a systematic review. *BioMed Research International*, 2016.
36. Formisano, C., Rigano, D., Lopatriello, A., Sirignano, C., Ramaschi, G., Arnoldi, L., ... & Taglialatela-Scafati, O. (2019). Detailed phytochemical characterization of bergamot

- polyphenolic fraction (BPF) by UPLC-DAD-MS and LC-NMR. *Journal of agricultural and food chemistry*, 67(11), 3159-3167.
37. A Farag, M. (2014). Comparative mass spectrometry & nuclear magnetic resonance metabolomic approaches for nutraceuticals quality control analysis: A brief review. *Recent Patents on Biotechnology*, 8(1), 17-24.
38. Makarov, A., Denisov, E., Kholomeev, A., Balschun, W., Lange, O., Strupat, K., & Horning, S. (2006). Performance evaluation of a hybrid linear ion trap/orbitrap mass spectrometer. *Analytical chemistry*, 78(7), 2113-2120.
39. Perry, R. H., Cooks, R. G., & Noll, R. J. (2008). Orbitrap mass spectrometry: instrumentation, ion motion and applications. *Mass spectrometry reviews*, 27(6), 661-699.
40. Quinn, R. A., Nothias, L. F., Vining, O., Meehan, M., Esquenazi, E., & Dorrestein, P. C. (2017). Molecular networking as a drug discovery, drug metabolism, and precision medicine strategy. *Trends in pharmacological sciences*, 38(2), 143-154.
41. Frank, A. M., Bandeira, N., Shen, Z., Tanner, S., Briggs, S. P., Smith, R. D., & Pevzner, P. A. (2008). Clustering millions of tandem mass spectra. *Journal of proteome research*, 7(01), 113-122.
42. Frank, A. M., Monroe, M. E., Shah, A. R., Carver, J. J., Bandeira, N., Moore, R. J., ... & Pevzner, P. A. (2011). Spectral archives: extending spectral libraries to analyze

## Chapter 1

- both identified and unidentified spectra. *Nature methods*, 8(7), 587-591.
43. De Vijlder, T., Valkenburg, D., Lemière, F., Romijn, E. P., Laukens, K., & Cuyckens, F. (2018). A tutorial in small molecule identification via electrospray ionization-mass spectrometry: The practical art of structural elucidation. *Mass spectrometry reviews*, 37(5), 607-629.
44. Shannon, P., Markiel, A., Ozier, O., Baliga, N. S., Wang, J. T., Ramage, D., ... & Ideker, T. (2003). Cytoscape: a software environment for integrated models of biomolecular interaction networks. *Genome research*, 13(11), 2498-2504.
45. Aron, A. T., Gentry, E. C., McPhail, K. L., Nothias, L. F., Nothias-Esposito, M., Bouslimani, A., ... & Dorrestein, P. C. (2020). Reproducible molecular networking of untargeted mass spectrometry data using GNPS. *Nature protocols*, 15(6), 1954-1991.
46. Bax, A., & Summers, M. F. (1986). Proton and carbon-13 assignments from sensitivity-enhanced detection of heteronuclear multiple-bond connectivity by 2D multiple quantum NMR. *Journal of the American Chemical Society*, 108(8), 2093-2094.
47. Palmer III, A. G., Cavanagh, J., Wright, P. E., & Rance, M. (1991). Sensitivity improvement in proton-detected two-dimensional heteronuclear correlation NMR spectroscopy. *Journal of Magnetic Resonance (1969)*, 93(1), 151-170.

48. Karplus, M. (1959). Contact electron-spin coupling of nuclear magnetic moments. *The Journal of chemical physics*, 30(1), 11-15.
49. Sanders, J. K., & Mersh, J. D. (1982). Nuclear magnetic double resonance; the use of difference spectroscopy. *Progress in nuclear magnetic resonance spectroscopy*, 15(4), 353-400.



## **Chapter 2: Phytochemical profile of Centevita® and its madecassoside-enriched fraction**

---

### **2.1 Introduction**

*Centella asiatica* (L.) Urban is a tropical medicinal plant from the *Apiaceae* family native to the warmer regions of both hemispheres; particularly, in Asian countries such as India, Sri Lanka, China, Indonesia, and Malaysia as well as South Africa and Madagascar.<sup>1</sup> The plant is commonly known also as Asiatic Pennywort, Indian Pennywort, and Gotu Kola.

It grows wild in damp and shady places up to 7000 ft. and can be commonly found along banks of rivers, streams, ponds, and irrigated fields. It also grows along rocky areas at an elevation of approximately 2000 ft. in India and Sri Lanka.<sup>2</sup> *C. asiatica* (L.) (**Figure 2.1**) is a prostrate, slightly aromatic, stoloniferous, perennial, usually creeper herb that can attain height up to 25 cm. The stem is glabrous, striated, and rooting at the nodes. Leaves emerge alternately in clusters at stem nodes, with long petioles (2–6 cm), the form is orbicular-reniform with a sheathing leaf base, crenate margins, and glabrous on both sides. Flowers are in fascicled umbels, each of them consisting of three to four white to purple or pink flowers. The flowering occurs in the month of April–June. During the growing season, fruits are borne in approximately 2 in. long, oblong, globular in shape, and strongly thickened pericarp. Seeds have a pendulous embryo, laterally compressed.<sup>3</sup>



**Figure 2.1.** *Centella asiatica*

Available literature reveals that *C. asiatica* has been used as a medicinal herb in China, India, Sri Lanka, Nepal, and Madagascar since ancient time. It is one of the main herbs for treating skin problems, to heal wounds,<sup>4</sup> and for revitalizing the nerves and brain cells, hence primarily known as a " Brain food" in India, and many ailments in the body. In Indian Ayurvedic practice it is well known for promoting longevity. During centuries, its value has further grown, and it has been used in skin treatments, both topically and internally. It is reported to cure leprosy, lupus, and eczema, and as a rejuvenating agent, in China.<sup>2</sup>

To combat nutritional deficiency, the herb is commonly used as porridge for feeding preschool children in Sri Lanka.<sup>5</sup> *C. asiatica* is also a traditional green leafy vegetable (GLV): it is consumed both cooked as a part of a soup or as a main vegetable, and raw as "Gotu kola sambola" or salad, especially in Malaysia and Indonesia.<sup>6,7</sup> It

## *Phytochemical profile of Centevita® and its madecassoside-enriched fraction*

is used as a health tonic and processed into cordial drinks and is available at some markets as a ready-made juice.<sup>8</sup>

*C. asiatica* is a widely used nutraceutical due to its potential antioxidant, antimicrobial, cytotoxic, neuroprotective, and other activities.<sup>3</sup> In addition, many studies have shown that *C. asiatica* is effective against depression,<sup>9</sup> neurologic problems,<sup>10</sup> diabetes mellitus,<sup>11</sup> has wound-healing and antibacterial activities,<sup>12</sup> and can cure many other important ailments in the body.<sup>13</sup>

To date, *C. asiatica* extracts, cell suspensions and centellosides are widely used as constituents in phytotherapeutic remedies, and in cosmetology, and many *C. asiatica*-based products (examples: Madecassol®, Blastoestimulina®, Centellase®, Collaven®, Emdecassol®, CATTf®, TECA®, TTFCA®, Menosan®, Mentat®) in variety of forms (capsules, tablets, tinctures, creams, powders, ointments, injection solutions) are available in the international market, also as dietary supplements.<sup>14</sup>

The biological activities and commercial uses of *C. asiatica* are inherently determined by its secondary metabolites. The main bioactive constituents are the triterpene pentacyclic saponins, collectively known as centelloids and predominantly present in plant leaves. They are synthesized via the isoprenoid pathway producing a hydrophobic cyclic triterpenoid structure (aglycone or sapogenin) conjugated with one or several hydrophilic sugar moieties (saponin).

The basic structure of the sapogenins (**Figure 2.2**) is almost exclusively derived from two pentacyclic triterpenoid subtypes, the ursane and the oleanane series, differing for the methyl substitution pattern at C-19 and C-20. Further diversities derive from the

## Chapter 2

presence and position of double bonds (mainly located at C12-C13, C13-C18 or C20-C21), hydroxylation at various positions, and glycosylation leads to the introduction of mono- or oligosaccharides in different positions of the ring. Some naturally acetylated compounds have been also described. The oligosaccharide moiety could be different but mainly consists in a Rha-(1-4)-Glc-(1-6)-Glc-oligosaccharidic linear chain linked to the triterpene through esterification of the carboxyl group at C-28.

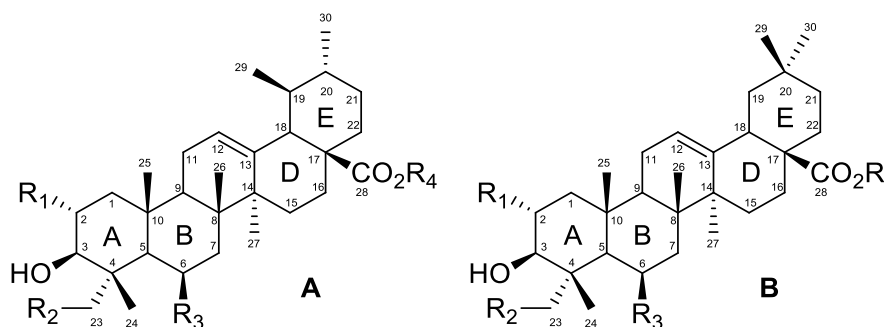


**Figure 2.2.** General substitution patterns of the centelloids of the ursane family (A) and the oleanane family (B):  $R_1$ ,  $R_2$ ,  $R_3$  = H or OH,  $R_4$  = H or oligosaccharide.

From the quantitative point of view, the main saponins include asiaticoside and madecassoside, and, in parallel, the most abundant sapogenins are asiatic and madecassic acids, although the content and relative proportion of triterpene components in *C. asiatica* may considerably vary according to the geographical location and environmental conditions of the plant. *C. asiatica* also contains several other bioactive metabolites, including volatile oils, flavonoids, tannins, phytosterols, mucilages, resins, free amino acids, fatty acids, and sugars.<sup>15</sup>

### 2.1.1 Biosynthesis of centelloids

Triterpenoids are biosynthesized via the isoprenoid pathway resulting from the subsequent condensation of the five-carbon monomers defined as 3-isopentenyl pyrophosphate (IPP) and dimethylallyl pyrophosphate (DMAPP) and derived from the mevalonate pathway (**Figure 2.3**).

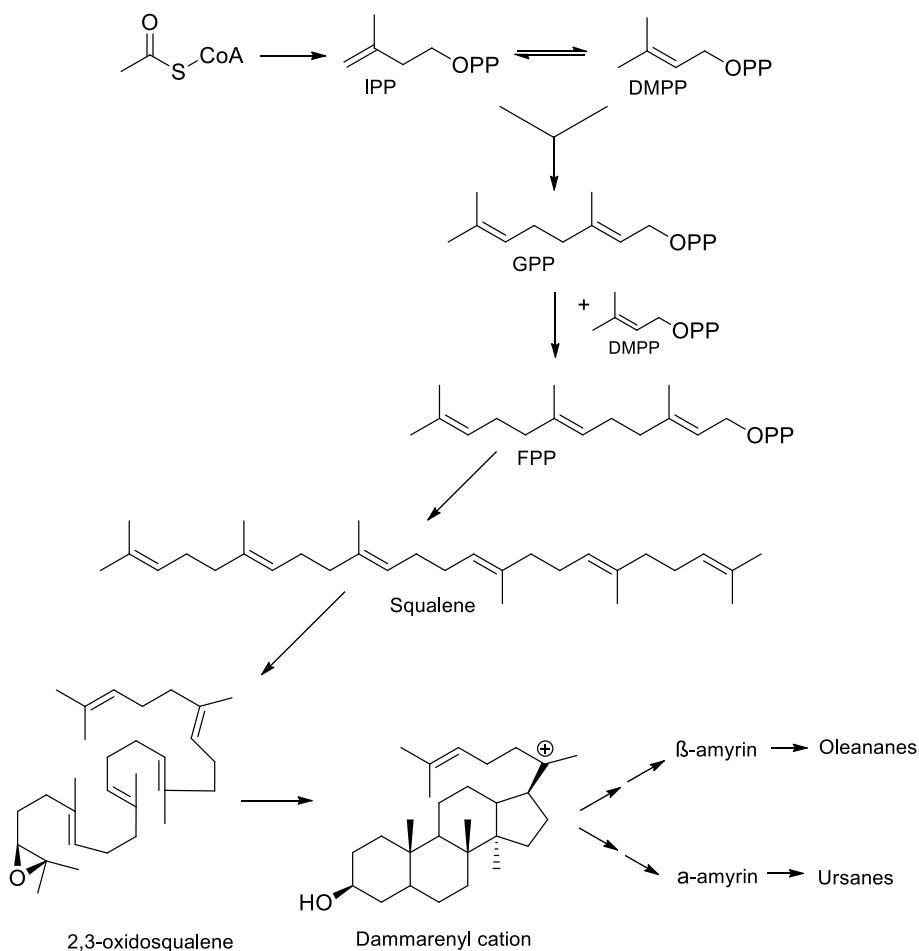


**Figure 2.3.** Initial steps in the biosynthesis of *Centella saponin* aglycones.

## Chapter 2

IPP and DMAPP undergo head-to-tail condensation to give geranyl pyrophosphate (GPP), and addition of another IPP unit, leading to farnesyl pyrophosphate (FPP).

The condensation of two FPP units leads to squalene (C30), subsequently oxidized to 2,3-oxidosqualene (OSQ).

The next step is the enzymic cyclization of OSQ, in which the internal bonds are introduced into the oxidosqualene backbone through double bonds migrations, to form polycyclic structures containing several 5- and 6- membered rings.<sup>16</sup> The formation of different internal linkages during cyclization by oxidosqualene cyclases (OSCs) gives rise to the wide range of naturally occurring triterpenic saponin skeletons.<sup>17,18</sup> In the case of *C. asiatica*, specific OSCs succeed in preventing alternative ways of cyclization into predefined end products.

The functionalization of the different rings is certainly mediated by unknown cytochrome P450-dependent monooxygenases, which confer further diversity mainly by oxidation and hydroxylation(s). On the other hand, little is known about the specific glycosyl transferases probably responsible for triterpenoid glycosylation.<sup>19</sup> The latter is an important step since the introduction of a sugar chain is critical for the biological activity of saponins. The oligosaccharide chains are probably synthesized by the sequential addition of single sugar residues to the aglycone.<sup>20</sup>

### **2.2 *Centella asiatica* as Centevita®**

The *C. asiatica* extract used in the present work is Centevita®, commercially available at Indena SpA (Milan, Italy) as a

## *Phytochemical profile of Centevita® and its madecassoside-enriched fraction*

nutraceutical extract obtained from the leaves of the plant. It is standardized to contain 45% of triterpenes, the main bioactive compounds, but it also contains a polyphenolic fraction claimed to contribute to the biological efficacy of the extract (over 7%).

The main members of the triterpenic fraction (**Figure 2.4**) are asiaticoside (**1**), madecassoside (**2**), asiatic acid (**3**), and madecassic acid (**4**), responsible for the antioxidant activity of the extract and in particular of the promotion collagen type III production in fibroblast cultures.<sup>21</sup> However, this activity has been mainly associated with madecassoside, since asiaticoside, asiatic acid, and madecassic acid are reported to promote the synthesis of collagen type I.<sup>22,23</sup> A recent clinical trial has underlined its properties in the prevention of inflammation and collagen glycation.<sup>24</sup>

In this framework, the research project described in this chapter was focused on a careful analysis of *C. asiatica*. The first purpose of the work was the characterization of an unknown compound emerged from preliminary analyses of a fraction enriched in madecassoside. An in-depth study led to the discovery of a previously unreported ursane saponin that was called isomadecassoside (**6**) (**Figure 2.4**). The new structural analogue turned out to be an accompanying compound of the madecassoside enriched fraction, containing also terminoloside (**5**), obtained during the extract preparation of Centevita®.<sup>25</sup>

Spurred by the first result, the second goal of the work was the in-depth investigation of the full phytochemical profile of Centevita®. Advanced metabolomics and dereplication techniques allowed: i) the characterization of 24 secondary metabolites, including 10

## Chapter 2

polyphenols and 14 triterpenoids in the sapogenin or saponin form and ii) the discovery of isoterminoloside (**7**) (**Figure 2.4**), a new triglycoside saponin of the unprecedented  $2\alpha, 3\beta, 6\beta, 23$ -tetrahydroxyolean-13(18)-en-28-oic acid (isoterminolic acid).<sup>26</sup>

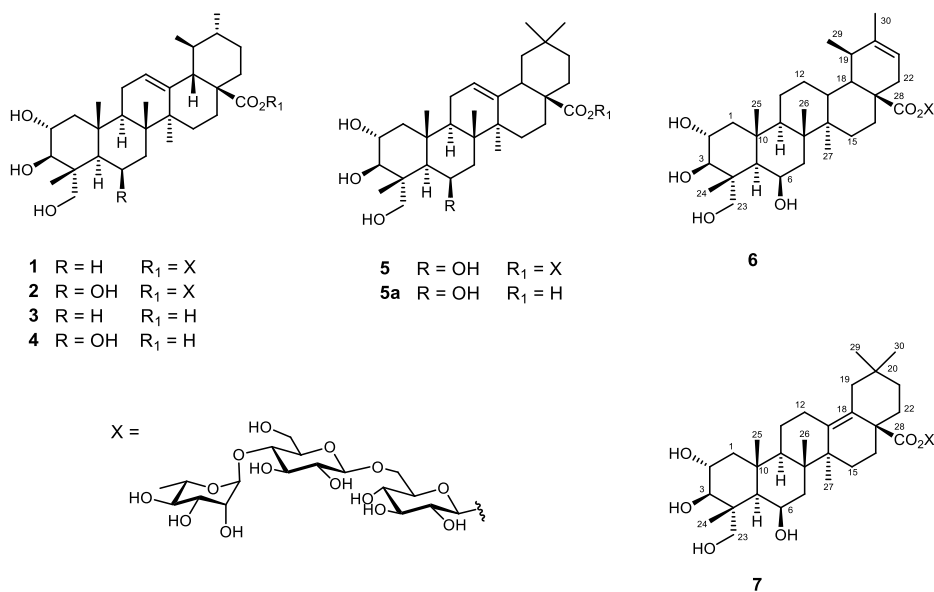


**Figure 2.4.** Chemical structures of the main triterpenoids of *C. asiatica* (**1-5**) and of the new isomadecassoside (**6**) and isoterminoloside (**7**).

### 2.2.1 Phytochemical profile of madecassoside-rich fraction

The madecassoside-rich fraction obtained from the Indena industrial purification of *C. asiatica* extract was subjected to a detailed characterization with the aim of identifying an unknown compound, that preliminary analyses revealed to be present in a mixture along with the expected madecassoside (**2**) and

*Phytochemical profile of Centevita<sup>®</sup> and its madecassoside-enriched fraction*

terminoloside (**5**). The fraction was purified by a reversed-phase HPLC affording the new isomadecassoside (**6**) (**Figure 2.4**).

*Isomadecassoside* (**6**) appears as a white amorphous solid with molecular formula C<sub>48</sub>H<sub>78</sub>O<sub>20</sub>, the same as madecassoside, established by positive HR-ESIMS. The <sup>1</sup>H NMR spectrum of **6** (**Table 2.1**) showed typical resonances of a triterpene glycoside including signals of one methyl doublet ( $\delta_{\text{H}}$  1.04) and five methyl singlets, four of which resonating upfield ( $\delta_{\text{H}}$  1.32, 1.29, 1.05, 1.00), and one at relatively downfields ( $\delta_{\text{H}}$  1.65). An additional methyl doublet at  $\delta_{\text{H}}$  1.28 could be likely ascribable to a rhamnose sugar unit. Moreover, the <sup>1</sup>H NMR spectrum included a series of multiplets located between  $\delta_{\text{H}}$  0.87 and 2.50, all belonging to the aglycone moiety, signals of oxymethines and oxymethylenes located between  $\delta_{\text{H}}$  3.20 and 4.86, and two methines resonating as doublets at  $\delta_{\text{H}}$  5.26 and 5.39. All the proton signals were associated with those of the directly linked carbon atoms through the correlations of the HSQC spectrum, that revealed the presence of only one olefinic proton ( $\delta_{\text{H}}$  5.26,  $\delta_{\text{C}}$  118.0) in the structure of **6**.

**Table 2.1.** <sup>1</sup>H (700 MHz) and <sup>13</sup>C (175 MHz) NMR Data of compound **6** in CD<sub>3</sub>OD.

Pos.	$\delta_{\text{H}}$ , mult., J in Hz	$\delta_{\text{C}}$ , mult.
1a	2.00, dd, 12.5, 5.0	49.9, CH <sub>2</sub>
1b	0.87, dd, 12.5, 11.5	
2	3.76, ddd, 11.5, 8.1, 5.0	69.6, CH
3	3.30 <sup>a</sup>	77.7, CH
4		44.7, C
5	1.23 <sup>a</sup>	48.9, CH
6	4.37, m	68.5, CH
7a	1.65 <sup>a</sup>	42.0, CH <sub>2</sub>
7b	1.61 <sup>a</sup>	

## Chapter 2

8		42.0, C
9	1.50 <sup>a</sup>	52.0, CH
10		38.7, C
11a	1.51 <sup>a</sup>	22.7, CH <sub>2</sub>
11b		
12a	1.47 <sup>a</sup>	28.5, CH <sub>2</sub>
12b		
13	1.80 <sup>a</sup>	39.7, CH
14		42, C
15a	1.59 <sup>a</sup>	30.2, CH <sub>2</sub>
15b	1.15 <sup>a</sup>	
16a	2.06, dt, 12.6, 3.0	33.7, CH <sub>2</sub>
16b	1.45 <sup>a</sup>	
17		50.4, C
18	1.28 <sup>a</sup>	49.4, CH
19a	2.17, m	38.3, CH
19b		
20		144.0, C
21	5.26, d, 7.1	118.0, CH
22a	2.28, dd, 15.2, 7.1	38.3, CH <sub>2</sub>
22b	1.85 <sup>a</sup>	
23a	3.58, d, 11.3	65.5, CH <sub>2</sub>
23b	3.45, d, 11.2	
24	1.05, s	14.7, CH <sub>3</sub>
25	1.32, s	19.7, CH <sub>3</sub>
26	1.29, s	17.2, CH <sub>3</sub>
27	1.00, s	15.2, CH <sub>3</sub>
28		176.4, C
29	1.04, d, 8.0	23.6, CH <sub>3</sub>
30	1.65, brs	21.9, CH <sub>3</sub>
<b>O-β-D-Glc</b>		
1'	5.39, d, 8.2	95.0, CH
2'	3.31 <sup>a</sup>	73.9, CH
3'	3.41 <sup>a</sup>	77.9, CH
4'	3.63, dd, 9.5, 3.4	71.8, CH
5'	3.53 <sup>a</sup>	79.4, CH
6a'	4.09, dd, 12.0, 1.5	69.2, CH <sub>2</sub>
6b'	3.80, dd, 12.0, 5.4	
<b>O-β-D-Glc</b>		
1''	4.42, d, 8.0	104.2, CH
2''	3.24, t, 8.3	75.3, CH
3''	3.47 <sup>a</sup>	76.4, CH
4''	3.54 <sup>a</sup>	79.4, CH
5''	3.35 <sup>a</sup>	76.5, CH

*Phytochemical profile of Centevita® and its madecassoside-enriched fraction*

6a''	3.84 <sup>a</sup>	61.8, CH <sub>2</sub>
6b''	3.67, dd, 12.3, 4.7	
O- $\alpha$ -L-Rha		
1'''	4.86 <sup>a</sup>	102.5, CH
2'''	3.84 <sup>a</sup>	72.1, CH
3'''	3.31 <sup>a</sup>	73.2, CH
4'''	3.42 <sup>a</sup>	73.4, CH
5'''	3.96, m	70.4, CH
6'''	1.28, d, 6.1	17.5, CH <sub>3</sub>

<sup>a</sup> Overlapped with other signals

A careful inspection of COSY, HSQC and HMBC spectra allowed the identification of the aglycone moiety of **6** (**Figure 2.5**) as an ursane-type triterpene including three oxymethine protons ( $\delta_{\text{H}}$  4.37, 3.76, 3.30), one isolated oxymethylene ( $\delta_{\text{H}}$  3.58, 3.45) and an ester carbonyl at C-28 ( $\delta_{\text{C}}$  176.4). In particular, the five spin systems identified from the COSY spectrum, and highlighted in red in **Figure 2.5**, were connected through a network of key HMBC correlations (**Figure 2.5**). The correlations from H<sub>3</sub>-24, H<sub>3</sub>-25, H<sub>3</sub>-26, and H<sub>3</sub>-27 (in black in **Figure 2.5**) were instrumental to build up the architecture of rings A-D, that proved to be nearly identical to that of the structure of madecassoside, with the single exception of a saturated C-12/C-13 bond. As for ring E, the HMBC cross-peaks (in blue in **Figure 2.5**) from H<sub>3</sub>-30 ( $\delta_{\text{H}}$  1.65, s) to C-19 and the  $sp^2$  C-20 ( $\delta_{\text{C}}$  144) and C-21, and those from H<sub>3</sub>-29 ( $\delta_{\text{H}}$  1.04, d, 8.0) to C-18, C-19, and C-20 ( $\delta_{\text{C}}$  144) were diagnostic for the presence of a trisubstituted double bond at  $\Delta^{20,21}$ . Moreover, the key HMBC correlations from H<sub>2</sub>-22 to C-18 ( $\delta_{\text{C}}$  49.4) and C-28 ( $\delta_{\text{C}}$  176.4) placed the ester carbonyl at C-28 and confirmed the planar structure of the aglycone of **6** as an ursane triterpenoid, sharing the same carbon

framework of madecassoside, but showing a different double bond location.

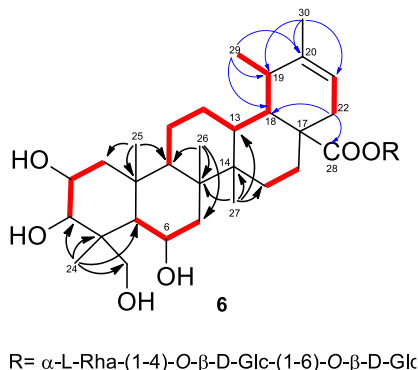


**Figure 2.5.** COSY (in red bold) and key H→C HMBC (black and blue arrows) correlations detected for isomadecassoside (**6**).

The almost complete superimposition of  $^1\text{H}/^{13}\text{C}$  NMR signals and  $J_{\text{H-H}}$  coupling constants of **6** with those of madecassoside, supported by analysis of NOESY cross-peaks, strongly indicated that the two compounds share the relative configuration of the common stereogenic centers, including the three oxymethines at C-2, C-3, and C-6. Moreover, the NOESY cross-peaks from H<sub>3</sub>-29 to H<sub>3</sub>-25 and H<sub>3</sub>-26 were indicative of the  $\beta$ -orientation of CH<sub>3</sub>-29, while the correlation H-13/H<sub>3</sub>-26 indicated the *trans* junction of the C/D rings.

The  $^1\text{H}$  and  $^{13}\text{C}$  NMR spectra, in combination with HSQC spectrum, revealed the presence of three anomeric methines at  $\delta_{\text{H}}$  5.35,  $\delta_{\text{C}}$  95.0;  $\delta_{\text{H}}$  4.42,  $\delta_{\text{C}}$  104.2 and  $\delta_{\text{H}}$  4.86,  $\delta_{\text{C}}$  102.5, of three sugar moieties. The comprehensive and comparative analysis of the  $J_{\text{H-H}}$  coupling constant values and the detailed  $^1\text{H}$ - and  $^{13}\text{C}$ -NMR assignments based on the COSY, HSQC and HMBC spectra

*Phytochemical profile of Centevita<sup>®</sup> and its madecassoside-enriched fraction*

indicated that **6** shares with madecassoside the same sugar portion including two  $\beta$ -glucopyranoses and one  $\alpha$ -rhamnopyranose units linked as  $\alpha$ -L-Rha-(1-4)-O- $\beta$ -D-Glc-(1-6)-O- $\beta$ -D-Glc. The HMBC cross-peak H-1'/C-28 supported the connection of the sugar and aglycone moieties through an ester linkage, thus establishing the structure of the new saponin isomadecassoside (**6**) as the O- $\alpha$ -L-rhamnopyranosyl-(1-4)-O- $\beta$ -D-glucopyranosyl-(1-6)-O- $\beta$ -D-glucopyranosyl ester of 2 $\alpha$ ,3 $\beta$ ,6 $\beta$ ,23-tetrahydroxyurs-20-en-28-oic acid.

The only *C. asiatica* saponin related to **6** is isoasiaticoside (**8**) (**Figure 2.6**), the 2 $\alpha$ ,3 $\beta$ ,23-trihydroxyurs-20-en-28-oic acid O- $\alpha$ -L-rhamnopyranosyl-(1 $\rightarrow$ 4)-O- $\beta$ -D-glucopyranosyl-(1 $\rightarrow$ 6)-O- $\beta$ -D-glucopyranosyl ester reported in 2007 by Yu et al.<sup>27</sup> and belonging to the same urs-20-ene subtype, although its structure is dehydroxylated at position C-6.

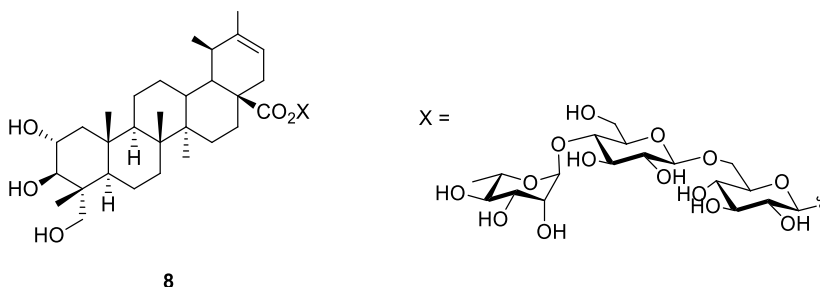


**Figure 2.6.** Chemical structure of isoasiaticoside (**8**).

Thus, compound **6** is a triglycoside of the unprecedented pentacyclic triterpenoid 2 $\alpha$ ,3 $\beta$ ,6 $\beta$ ,23-tetrahydroxyurs-20-en-28-oic acid, for which we propose the trivial name isomadecassic acid.

### 2.2.2 Phytochemical profile of Centevita®

A commercial sample of Centevita® extract was subjected to a metabolomic and dereplication analysis adopting a combination of LC-MS/MS and Molecular networking (MN), allowing the identification of known metabolites as well as structural analogues. The MN acted as a visual approach in the dereplication analysis and from the full network obtained, a cluster containing the saponins derivatives has been found (**Figure 2.7**). The saponins cluster was integrated with the spectral data of a standard consisting of madecassoside and terminoloside, represented by the yellow colour in the node. On the other hand, the green colour represents the masses from Centevita® extract.

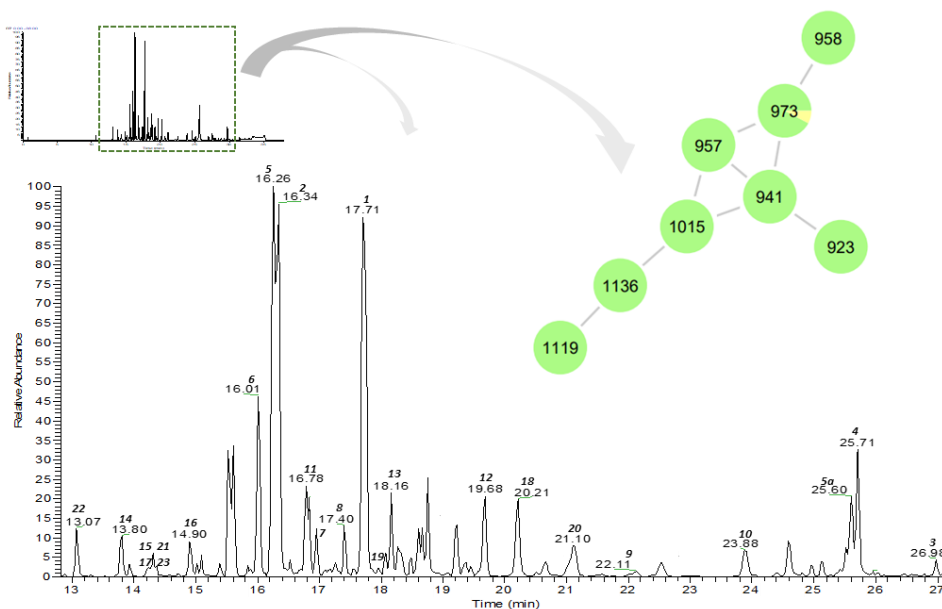


**Figure 2.7.** LC-MS chromatogram and (right) selected saponins cluster from MS/MS-based molecular network (nodes are labelled with the parent  $m/z$  ratio; colours: green for compounds of *C. asiatica*; yellow for standards of madecassoside and terminoloside).

*Phytochemical profile of Centevita<sup>®</sup> and its madecassoside-enriched fraction*

It was observed that saponins with the same molecular mass fit into the same node. In fact, the node  $m/z$  973, represents the sum of all saponins having that base peak, including madecassoside and terminoloside. Although they are two components, they represent only a small slice of the reference node, hence their annotation required further investigation since only three isomers were reported in the literature. The nodes  $m/z$  957 and  $m/z$  941 showed mass values and fragmentation patterns similar to certain structural analogues of the main constituent madecassoside, and they were subsequently identified. This preliminary information guided an accurate manual analysis of the HRMSMS that resulted in the putative identification of several compounds.

In the LC-MS/MS chromatogram (**Figure 2.7**), the main peaks could be associated with the triterpenoid saponins terminoloside ( $t_R$  16.26, **5**), madecassoside ( $t_R$  16.34, **2**), and asiaticoside ( $t_R$  17.71, **1**). This assignment was unambiguously confirmed by injection of standards available in laboratories.

**Table 2.2.** *Metabolites identified in Centevita<sup>®</sup> via LC-MS/MS and Molecular Networking. Compounds are listed in order of LC-MS elution. All mass peaks have been detected as  $[M-H]^-$ .*

Retention time (min)	Measured $m/z$	Molecular formula	Assignment	Identification support
13.07	477.14	C <sub>21</sub> H <sub>18</sub> O <sub>13</sub>	Quercetin 3-O-glucuronide ( <b>22</b> )	Isolation - NMR
13.80	515.23	C <sub>25</sub> H <sub>24</sub> O <sub>12</sub>	3,4-Dicaffeoylquinic acid ( <b>14</b> )	Isolation - NMR
14.10	515.30	C <sub>25</sub> H <sub>24</sub> O <sub>12</sub>	1,3-Dicaffeoylquinic acid ( <b>17</b> )	Isolation - NMR
14.21	515.13	C <sub>25</sub> H <sub>24</sub> O <sub>12</sub>	3,5-Dicaffeoylquinic acid ( <b>15</b> )	Isolation - NMR

## Chapter 2

14.31	461.19	C <sub>21</sub> H <sub>18</sub> O <sub>12</sub>	Kaempferol 3-O-glucuronide ( <b>21</b> )	Isolation - NMR
14.73	491.21	C <sub>22</sub> H <sub>20</sub> O <sub>13</sub>	Isorhamnetin 3-O-glucuronide ( <b>23</b> )	Isolation - NMR
14.90	515.21	C <sub>25</sub> H <sub>24</sub> O <sub>12</sub>	4,5-Dicaffeoylquinic acid ( <b>16</b> )	Isolation - NMR
16.01	973.49	C <sub>48</sub> H <sub>78</sub> O <sub>20</sub>	<i>Isomadecassoside</i> ( <b>6</b> )	Standard
16.26	973.51	C <sub>48</sub> H <sub>78</sub> O <sub>20</sub>	Terminoloside ( <b>5</b> )	Standard
16.34	973.56	C <sub>48</sub> H <sub>78</sub> O <sub>20</sub>	Madecassoside ( <b>2</b> )	Standard
16.78	827.46	C <sub>42</sub> H <sub>68</sub> O <sub>16</sub>	Centellasaponin B ( <b>11</b> )	Isolation - NMR
16.95	973.60	C <sub>48</sub> H <sub>78</sub> O <sub>20</sub>	<i>Isoterminoloside</i> ( <b>7</b> )	Isolation - NMR
17.40	957.61	C <sub>48</sub> H <sub>78</sub> O <sub>19</sub>	Isoasiaticoside ( <b>8</b> )	Isolation - NMR
17.71	957.55	C <sub>48</sub> H <sub>78</sub> O <sub>19</sub>	Asiaticoside ( <b>1</b> )	Standard
17.85	301.18	C <sub>15</sub> H <sub>10</sub> O <sub>7</sub>	Quercetin ( <b>19</b> )	Standard
18.16	957.56	C <sub>48</sub> H <sub>78</sub> O <sub>19</sub>	2 $\alpha$ ,3 $\beta$ ,6 $\beta$ -trihydroxyolean-12-en-28-oic acid triglycoside ( <b>13</b> )	Isolation - NMR
19.68	957.58	C <sub>48</sub> H <sub>78</sub> O <sub>19</sub>	Centellasaponin C ( <b>12</b> )	Isolation - NMR
20.21	185.15	C <sub>15</sub> H <sub>10</sub> O <sub>6</sub>	Kaempferol ( <b>18</b> )	Standard
21.10	315.17	C <sub>16</sub> H <sub>12</sub> O <sub>7</sub>	Isorhamnetin ( <b>20</b> )	Isolation - NMR
22.11	999.41	C <sub>50</sub> H <sub>80</sub> O <sub>20</sub>	Asiaticoside C ( <b>9</b> )	Isolation - NMR
23.88	941.94	C <sub>48</sub> H <sub>78</sub> O <sub>18</sub>	Asiaticoside F ( <b>10</b> )	Isolation - NMR
25.60	503.53	C <sub>30</sub> H <sub>48</sub> O <sub>6</sub>	Terminolic acid ( <b>5a</b> )	Standard
25.71	503.50	C <sub>30</sub> H <sub>48</sub> O <sub>6</sub>	Madecassic acid ( <b>4</b> )	Standard

*Phytochemical profile of Centevita<sup>®</sup> and its madecassoside-enriched fraction*

26.98	487.46	C <sub>30</sub> H <sub>48</sub> O <sub>5</sub>	Asiatic acid ( <b>3</b> )	Standard
-------	--------	--	---------------------------	----------

---

Terminoloside and madecassoside are the ursane/oleanane pair and, given the very similar structures, they possess practically identical retention times and overlapping fragmentation patterns. Thus, not surprisingly, the presence of terminoloside has been frequently overlooked and, as already verified with the previously reported (*par.* 2.2.1) analysis of the madecassoside-rich fraction, that referred as madecassoside is, most likely, a nearly equimolar pair of madecassoside and terminoloside.

As reported in **Table 2.2**, using standards available from previous studies, isomadecassoside (**6**) and the triterpenoid aglycones asiatic (**3**), madecassic (**4**), and terminolic (**5a**) acids have also been identified. The LC/MS profile confirmed at least seven additional peaks attributable to triterpenoid saponins, one of which isomeric to terminoloside/madecassoside (C<sub>48</sub>H<sub>78</sub>O<sub>20</sub>) and three isomeric to asiaticoside (C<sub>48</sub>H<sub>78</sub>O<sub>19</sub>). In addition, peaks attributable to dicaffeoylquinic acids, flavonoid and their glycosides have been detected. The structures of these compounds cannot be unambiguously assigned on the basis of LC/MS and MN, therefore, isolation and detailed NMR spectroscopic investigation were deemed necessary.

To this purpose, a sample of Centevita<sup>®</sup> extract was subjected to MPLC-DAD and then repeated HPLC purifications, guided by the preliminary LC profile. In this way, several pure compounds were obtained (**Table 2.2**), and their structures were assigned based on the comparison of their chromatographic (LC-MS), NMR spectral data. Thus, the triterpenoid saponin profile was completed by

## Chapter 2

characterization of isoasiaticoside (**8**),<sup>27</sup> asiaticoside C (**9**) and F (**10**),<sup>28</sup> centellasaponins B (**11**) and C (**12**),<sup>29</sup> and **13**, the oleanane analogue of centellasaponin C (**Figure 2.8**).<sup>30</sup> Since NMR literature data for centellasaponin C (**12**) are only available in DMSO-*d*<sub>6</sub>, a full NMR assignment in CD<sub>3</sub>OD in the experimental section has been compiled.

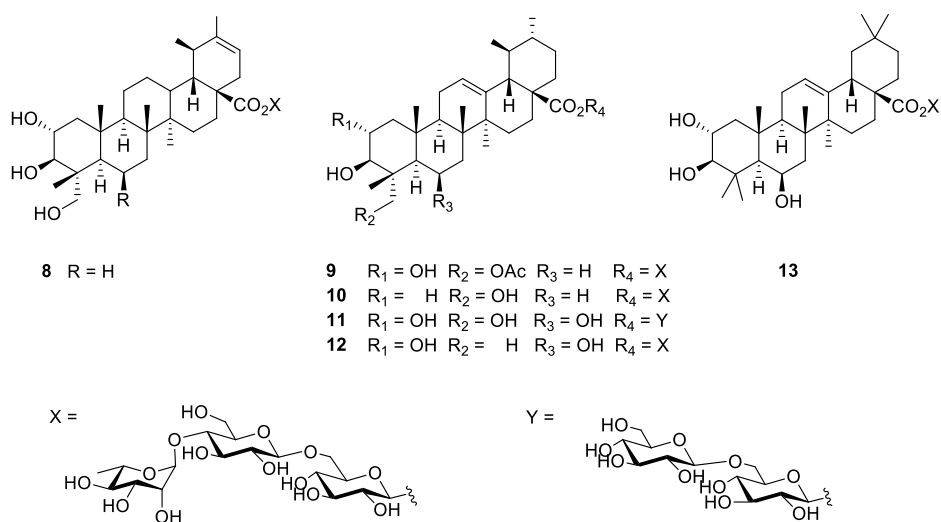


**Figure 2.8.** The structures of the minor triterpenoid saponins characterized from *Centevita*<sup>®</sup>.

Four dicaffeoylquinic acids (**14-17**)<sup>31</sup> and the flavonoids kaempferol (**18**), quercetin (**19**), isorhamnetin (**20**) and their 3-glucuronides (**21-23**)<sup>32</sup> (**Figure 2.9**) were also isolated and characterized. Compound **23** had never been previously reported from *C. asiatica*.

*Phytochemical profile of Centevita<sup>®</sup> and its madecassoside-enriched fraction*

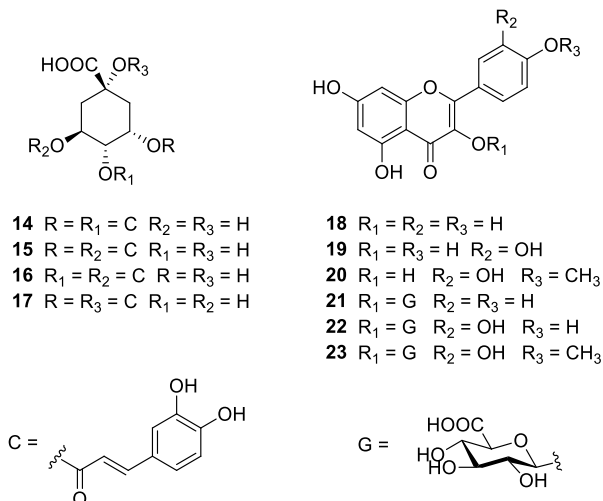


**Figure 2.9.** The structures of dicaffeoylquinic acids (**14-17**), flavonoids (**18-20**) and flavonoid glucuronides (**21-23**) characterized from Centevita<sup>®</sup>.

The isolation of Centevita<sup>®</sup> secondary metabolites in the pure form allowed their quantitative evaluation. **Table 2.3** reports the amount obtained for each metabolite (or class of metabolites) after the different chromatographic steps, that inevitably resulted in some loss of compound. As expected, the triterpenoid fraction (about 42.5% w/w) is dominated by asiaticoside (**1**), followed by the terminoloside/madecassoside pair, while the polyphenolic fraction (about 6% w/w) is almost equally represented by dicaffeoylquinic acids, free flavonoids, and flavonoid glucuronides.

Therefore, the above-mentioned data are in accordance with the specifications of Centevita<sup>®</sup> nutraceutical extract.

**Table 2.3.** Amount obtained for the metabolites (or class of metabolites) of Centevita®.

Compounds	Amount (mg)	Percentage (referred to 1.5 g of extract)
Asiaticoside (1)	358	23.8
Terminoloside (5)	123	8.2
Madecassoside (2)	80	5.3
Other saponins	21	1.4
Asiatic acid (3)	46	3.1
Terminolic acid (5a)	5	0.3
Madecassic acid (4)	5	0.3
<i>Total triterpenoid fraction</i>	638	42.5
Dicaffeoylquinic acids	32.5	2.2
Free flavonoids	27	1.8
Flavonoid glucuronides	30	2.0
<i>Total polyphenolic fraction</i>	89.5	6.0

### 2.2.2.1 Structural elucidation of isoterminoloside

*Isoterminoloside* (7) was isolated during the phytochemical investigation of Centevita® extract. It is an amorphous solid with  $[\alpha]_D - 3.0$  and molecular formula  $C_{48}H_{78}O_{20}$  (HRESIMS found  $m/z$  973.4999  $[M - H]^-$ , required  $m/z$  973.5014), the same as madecassoside/terminoloside. The  $^1H$  NMR spectrum of 7 (Table 2.4) showed typical resonances of an oleanane triterpene glycoside including signals of six methyl singlets, all resonating in the upfield region of the spectrum ( $\delta_H$  1.36, 1.22, 1.20, 1.06, 0.95, 0.79), whereas a methyl doublet at  $\delta_H$  1.28 could be assigned to a

*Phytochemical profile of Centevita® and its madecassoside-enriched fraction*

rhamnose sugar unit. In addition, the  $^1\text{H}$  NMR spectrum included a series of overlapped multiplets located between  $\delta_{\text{H}}$  0.92 and 2.86, all belonging to the aglycone moiety, signals of oxymethines and oxymethylenes located between  $\delta_{\text{H}}$  3.32 and 4.86, and a single deshielded methine resonating as doublets at  $\delta_{\text{H}}$  5.45.

Having associated all the proton signals to those of the directly attached carbon atoms through the correlations of the HSQC spectrum, it was excluded the presence of  $sp^2$  methines in the structure of **7**.

**Table 2.4.**  $^1\text{H}$  (700 MHz) and  $^{13}\text{C}$  (175 MHz) NMR Data of compound **7** in  $\text{CD}_3\text{OD}$ .

Pos.	$\delta_{\text{H}}$ , mult., J in Hz	$\delta_{\text{C}}$ , mult.
1a	2.04, dd, 12.6, 4.86	48.9, CH <sub>2</sub>
1b	0.92 <sup>a</sup>	
2	3.77 <sup>a</sup>	68.4, CH
3	3.32 <sup>a</sup>	76.6, CH
4		43.7, C
5	1.29 <sup>a</sup>	47.6, CH
6	4.39 <sup>a</sup>	67.3, CH
7a	1.74 <sup>a</sup>	41.3, CH <sub>2</sub>
7b	1.61, dd, 14.4, 2.6	
8		40.7, C
9	1.69 <sup>a</sup>	51.0, CH
10		37.5, C
11a	1.65 <sup>a</sup>	21.5, CH <sub>2</sub>
11b	1.55 <sup>a</sup>	
12a	2.86 <sup>a</sup>	25.2, CH <sub>2</sub>
12b	1.94 <sup>a</sup>	
13		138.4, C
14		44.5, C
15a	1.90 <sup>a</sup>	26.8, CH <sub>2</sub>
15b	1.14 <sup>a</sup>	
16a	1.62 <sup>a</sup>	25.5, CH <sub>2</sub>
16b	1.60 <sup>a</sup>	
17		48.3, C
18		127.5, C

## Chapter 2

19a	2.50, d, 14.4	40.4, CH <sub>2</sub>
19b	1.82, d, 14.4	
20		31.9, C
21a	2.23 <sup>a</sup>	35.9, CH <sub>2</sub>
21b	1.35 <sup>a</sup>	
22a	2.22 <sup>a</sup>	35.1, CH <sub>2</sub>
22b	1.36 <sup>a</sup>	
23a	3.60 <sup>a</sup>	64.5, CH <sub>2</sub>
23b	3.47 <sup>a</sup>	
24	1.06, s	13.7, CH <sub>3</sub>
25	1.36, s	18.6, CH <sub>3</sub>
26	1.22, s	18.7, CH <sub>3</sub>
27	1.20, s	20.4, CH <sub>3</sub>
28		176.0, C
29	0.79, s	23.2 CH <sub>3</sub>
30	0.95, s	31.7, CH <sub>3</sub>
<u>O-β-D-Glc</u>		
1'	5.45, d, 8.14	94.5, CH
2'	3.34 <sup>a</sup>	72.4, CH
3'	3.41 <sup>a</sup>	76.8, CH
4'	3.60 <sup>a</sup>	76.9, CH
5'	3.52 <sup>a</sup>	76.6, CH
6a'	4.12, dd, 12.0, 1.7	68.1, CH <sub>2</sub>
6b'	3.81 <sup>a</sup>	
<u>O-β-D-Glc</u>		
1''	4.47, d, 7.85	103.6, CH
2''	3.26 <sup>a</sup>	73.9, CH
3''	3.35 <sup>a</sup>	75.5, CH
4''	3.54 <sup>a</sup>	78.3, CH
5''	3.48 <sup>a</sup>	75.4, CH
6a''	3.84 <sup>a</sup>	60.5, CH <sub>2</sub>
6b''	3.67, dd, 12.0, 4.5	
<u>O-α-L-Rha</u>		
1'''	4.86 <sup>a</sup>	101.0, CH
2'''	3.85 <sup>a</sup>	71.1, CH
3'''	3.65, m	71.0, CH
4'''	3.42 <sup>a</sup>	72.3, CH
5'''	3.98, m	69.5, CH
6'''	1.28, d, 6.3	16.4, CH <sub>3</sub>

<sup>a</sup> Overlapped with other signals

*Phytochemical profile of Centevita® and its madecassoside-enriched fraction*

A careful inspection of COSY, HSQC and HMBC spectra allowed the identification of the aglycone moiety of **7** (**Figure 2.10**) as an oleanane-type triterpene including three oxymethine protons ( $\delta_{\text{H}}$  4.39, 3.77, 3.32), one uncoupled oxymethylene ( $\delta_{\text{H}}$  3.60, 3.47) and an ester carbonyl at C-28 ( $\delta_{\text{C}}$  176.0). The COSY spectrum allowed identification of five spin systems, highlighted in red (**Figure 2.10**), that could be connected through the network of HMBC correlations (**Figure 2.10**). The correlations exhibited by the six methyl singlets were instrumental to build up the architecture of rings A-E (in black in **Figure 2.10**), that proved to be nearly identical to that of the structure of terminoloside (**5**), with the single exception of a tetrasubstituted C-12/C-13 double bond. The HMBC cross-peaks from H<sub>2</sub>-12 and H<sub>3</sub>-27 to the *sp*<sup>2</sup> carbon at  $\delta_{\text{C}}$  138.4 (C-13) and those from H<sub>2</sub>-12 and H<sub>2</sub>-16 to the *sp*<sup>2</sup> carbon at  $\delta_{\text{C}}$  127.5 (C-18) were diagnostic for the presence of a tetrasubstituted double bond at  $\Delta^{13,18}$  (in blue in **Figure 2.10**). Accordingly, the protons at C-12 and C-19 resonated in the allylic region (H<sub>2</sub>-12 =  $\delta_{\text{H}}$  2.86 and 1.94; H<sub>2</sub>-19 =  $\delta_{\text{H}}$  2.50 and 1.82). Finally, the key HMBC correlations from H<sub>2</sub>-22 and H<sub>2</sub>-16 to the signal at  $\delta_{\text{C}}$  176.0 placed a carbonyl ester at C-28 and confirmed the planar structure of the aglycone of **7** as an oleanane triterpenoid, sharing the same carbon framework with terminoloside (**5**), but with a different double bond location.

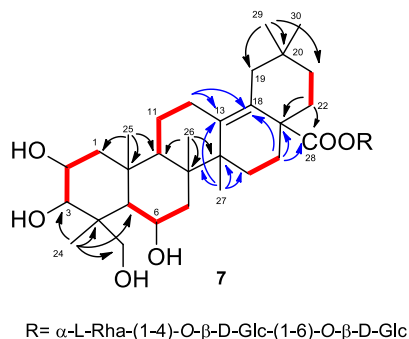


**Figure 2.10.** COSY (in red bold) and key H→C HMBC (black and blue arrows) correlations detected for isoterminoloside (**7**).

The almost complete superimposition of  $^1\text{H}/^{13}\text{C}$  NMR signals and of **7** with those of terminoloside strongly indicated that the two compounds share the relative configurations of the common stereogenic centers, including the three oxymethines at C-2, C-3, and C-6 and the configuration at the unprotonated C-4.

The  $^1\text{H}$  and  $^{13}\text{C}$  NMR resonances of three anomeric methines at  $\delta_{\text{H}}$  5.45,  $\delta_{\text{C}}$  94.5;  $\delta_{\text{H}}$  4.47,  $\delta_{\text{C}}$  103.6 and  $\delta_{\text{H}}$  4.86,  $\delta_{\text{C}}$  101.0, coupled through the HSQC spectrum, supported the presence of three sugar units. The detailed  $^1\text{H}$ - and  $^{13}\text{C}$ -NMR assignments based on COSY, HSQC and HMBC spectra indicated that **7** shares with terminoloside the same sugar portion including two  $\beta$ -D-glucopyranoses and one  $\alpha$ -L-rhamnopyranose units linked as  $\alpha$ -L-Rha-(1-4)-O- $\beta$ -D-Glc-(1-6)-O- $\beta$ -D-Glc. The HMBC cross-peak H-1'/C-28 supported the connection of the sugar and aglycone moieties through an ester linkage, thus establishing the structure of the new saponin isoterminoloside (**7**) as the  $\alpha$ -L-rhamnopyranosyl-(1-4)-O- $\beta$ -D-glucopyranosyl-(1-6)-O- $\beta$ -D-glucopyranosyl ester of 2 $\alpha$ ,3 $\beta$ ,6 $\beta$ ,23-tetrahydroxyolean-13(18)-en-28-oic acid.

## *Phytochemical profile of Centevita<sup>®</sup> and its madecassoside-enriched fraction*

Isoterminoloside (**7**) seems to be a triglycoside of an unprecedented pentacyclic triterpenoid for which we propose the trivial name isoterminolic acid.

### **2.3 Conclusions**

*Centella asiatica* is a very popular medicinal plant with several phytotherapeutic products on the market that include its extracts, enriched fractions, or pure compounds as active constituents.

The fraction enriched in madecassoside of the *C. asiatica* extract contains significant amounts of the new saponin isomadecassoside (**6**), in addition to the main madecassoside (**2**) and terminoloside (**5**). The new compound is a triglycoside ester of an unprecedented ursane triterpene acid, namely 2 $\alpha$ , 3 $\beta$ , 6 $\beta$ , 23-tetrahydroxyurs-20-en-28-oic acid (isomadecassic acid). Since isomadecassoside (**6**) shares the same molecular formula and a closely similar chromatographic behavior to madecassoside (**2**) and terminoloside (**5**), it had been overlooked in the dozens of phytochemical analyzes on *C. asiatica* carried out to date.

From an LC-MS guided phytochemical investigation on the commercial *C. asiatica* leaves extract named Centevita<sup>®</sup>, 24 secondary metabolites have been identified and quantified, belonging to two structural classes, triterpenoids (and their glycosides) and polyphenol derivatives. The total amounts found for these components (ab. 43% for triterpenoids and 6% for polyphenols) well correspond to the values reported for the standardized extract. The metabolomic characterization also resulted in the discovery of isoterminoloside (**7**), a new triglycoside

## Chapter 2

saponin of the unprecedented  $2\alpha,3\beta,6\beta,23$ -tetrahydroxyolean-13(18)-en-28-oic acid (isoterminolic acid).

The pharmacological potential of the incredible chemodiversity disclosed for *C. asiatica* saponins still awaits a systematic investigation, aimed at highlighting the biological impact of even punctual changes. In this regard, a recent manuscript reporting the synthesis and anti-inflammatory activity of oleanolic acid saponins<sup>33</sup> has revealed that olean-13(18)-en-28-oic acid derivatives were significantly more potent than their olean-12-en-28-oic acid counterparts in activating AMP-activated protein kinase, a central regulator of energy homeostasis.

## 2.4 Experimental section

### 2.4.1 Plant material and extraction of Centevita®

The *C. asiatica* extract named Centevita® is commercially available at Indena SpA (Milan, Italy) and was obtained as a free sample from the manufacturing company. To prepare this extract, *C. asiatica* leaves were collected in Madagascar, dried, ground, and then extracted with ethanol. The concentrated ethanol extract was diluted with water, centrifuged, purified on a resin column, and finally filtrated, concentrated, and dried.

### 2.4.2 Extraction and isolation of madecassoside-enriched fraction

Industrial purification of *C. asiatica* leaves afforded a madecassoside- and terminoloside-rich fraction (7.5 Kg) that was

*Phytochemical profile of Centevita® and its madecassoside-enriched fraction*

loaded onto a reverse phase C18 Zeoprep column (500 Kg). The elution was performed with water/acetone 78:22, collecting fractions of 200 kg each (flow rate 100 Kg/h, column head pressure: 2.5-3 bar). The obtained fractions were combined as follows: head fractions up to the appearance of madecassoside, heart fractions (sum of madecassoside and terminoloside), tails fraction. The head fractions were combined and concentrated to dryness, yielding 2.5 kg of an intermediate solid product. A part of this product (400 g) was dissolved in methanol at reflux (3200 mL), the solution was cooled to 25°C, and crystallized under stirring for two days. The suspension was filtered, washed with methanol and dried under vacuum for 18 hours to yield a white solid product (170 g). A small part of this fraction (50 mg) was subjected to repeated chromatographic purifications by analytical HPLC-UV-vis (Shimadzu instrument, pump LC-10AD, SPD-10A Detector) on a Phenomenex Synergi 4 $\mu$  Polar-RP 80Å 250  $\times$  4.60 mm column. The mobile phase was a mixture of acetonitrile and water with 50 ppm (v/v) of formic acid added to both solvents with the following elution gradient: 0-5 min = H<sub>2</sub>O:CH<sub>3</sub>CN 85:15 isocratic; from 6-22 min = from H<sub>2</sub>O:CH<sub>3</sub>CN 85:15 to H<sub>2</sub>O:CH<sub>3</sub>CN 70:30; 22-27 min = H<sub>2</sub>O:CH<sub>3</sub>CN 70:30 isocratic. Other parameters: injected volume 20  $\mu$ L; flow rate 1.0 mL/min; UV detection  $\lambda$  200 nm. Isomadecassoside (**6**,  $t_R$  24.5 min, 2.1 mg), asiaticoside B/terminoloside (**5**,  $t_R$  25.1 min, 3.8 mg) and madecassoside (**2**,  $t_R$  25.5 min, 25.9 mg) were obtained in pure state.

*Isomadecassoside (6)*. White amorphous solid;  $[\alpha]^{22}_D - 7.05$  (c 12, CH<sub>3</sub>OH); <sup>1</sup>H NMR (CD<sub>3</sub>OD, 700 MHz) and <sup>13</sup>C NMR (CD<sub>3</sub>OD, 175

## Chapter 2

MHz): Table 2.1; HR-ESIMS found  $m/z$  997.4978  $[M + Na]^+$ ;  $C_{48}H_{78}O_{20}Na$  requires 997.4984.

### 2.4.3 LC-MS/MS and Molecular Networking

All LC-MS and LC-MS/MS experiments were performed using hybrid linear Ion Trap LTQ Orbitrap XLTL Fourier Transform Mass Spectrometer (FTMS), equipped with an Ultimate 3000 HPLC system. Chromatographic separation was achieved using a Kinetex Polar C18 column (100 x 3.0 mm, 100Å, 2.6  $\mu$ m). The injection volume was 5  $\mu$ L. Gradient elution was performed using a mobile phase consisting of water (solvent A) and acetonitrile (solvent B), both containing 0.1% v/v formic acid. Flow rate was 0.5 mL/min. The chromatographic method lasted 33 min, and the gradient design was as follows: an initial 2 min at 5% B, from 2 to 16 min B, reached 30%, hold at 30% B from 16 to 21, then from 21 to 31 min B reached 95% and hold at 95% B from 31 to 33 min. The analysis was carried out in negative (ESI-) and positive (ESI+) ionization modes. Source conditions were: Spray voltage: 3.5 kV (positive mode) and 2.9 kV (negative mode); Capillary voltage: 23 V (positive mode) and -48 V (negative mode); Source temperature: 320 °C. The acquisition range was  $m/z$  150–1500. Although the spectra were recorded in positive and negative modes, only the data obtained in negative modes have been analyzed, due to their more complex profiles.

A molecular network was created on GNPS (<https://gnps.ucsd.edu>). The ESI- raw data file was converted in mzXML file using MSconvert software and then exported to GNPS (<https://gnps.ucsd.edu>) for

### *Phytochemical profile of Centevita<sup>®</sup> and its madecassoside-enriched fraction*

analysis. The data was filtered by removing all MS/MS fragment ions within +/- 17 Da of the precursor. *m/z* MS/MS spectra were window filtered by choosing only the top 6 fragment ions in the +/- 50 Da window throughout the spectrum. The precursor ion mass tolerance was set to 2 Da and the MS/MS fragment ion tolerance to 0.5 Da. A molecular network was then created where edges were filtered to have a cosine score above 0.6 and more than 6 matched peaks. Further, edges between two nodes were kept in the network if and only if each of the nodes appeared in each other's respective top 10 most similar nodes. Finally, the maximum size of a molecular family was set to 100, and the lowest scoring edges were removed from molecular families until the molecular family size was below this threshold. The spectra in the network were then searched against GNPS spectral libraries.<sup>34,35</sup> The library spectra were filtered in the same manner as the input data. All matches kept between network spectra and library spectra were required to have a score above 0.7 and at least 6 matched peaks. The DEREPLICATOR was used to annotate MS/MS spectra.<sup>36</sup> The molecular networks were visualized using Cytoscape\_v3.7.2 software.<sup>37</sup>

#### **2.4.4 Chromatographic separation of Centevita<sup>®</sup>**

A sample of Centevita<sup>®</sup> (1.5 g) was subjected to a first chromatographic purification by MPLC-DAD (Sepachrom instrument) on a Cartridge C18 60Å 50µm - Size 40 g – Column Volume (CV) 50 mL. The mobile phase was a mixture of water with 0.1% formic acid (solvent A) acetonitrile (solvent B); and methanol

## Chapter 2

(solvent C) with a gradient method as follows: starting conditions: 95% A – 5%B for two CV; from CV<sub>12</sub> to CV<sub>23</sub>: 75%A – 30%B; from CV<sub>31</sub> to CV<sub>33</sub>: 5%A – 95%B; from CV<sub>34</sub> to CV<sub>39</sub>: 5%A – 95%C. The injected volume was 10 mL and flow rate was 20.0 mL/min. The UV detection wavelength was set at 200 nm. This separation led to isolation of asiaticoside (**1**, 358.5 mg, CV 12) in a pure state. The remaining fractions needed a subsequent HPLC purification (Agilent instrument, using 1260 Quat Pump VL system, equipped with a 1260 VWD VL UV-vis detector) using Luna 10µm C18 100Å 250 x 10 mm columns. Fraction F (eluted with a mixture of A:B 75:25) was re-chromatographed by RP-18 HPLC-UV using H<sub>2</sub>O:CH<sub>3</sub>CN (80:20, flow rate 3.0 mL/min) to afford quercetin-3-O-glucuronide (**22**, 8.8 mg, *t<sub>R</sub>* 15.1 min), 3,4-dicaffeoylquinic acid (**14**, 8.0 mg, *t<sub>R</sub>* 18.4 min), 1,3-dicaffeoylquinic acid (**17**, 7.7 mg, *t<sub>R</sub>* 21 min), 3,5-dicaffeoylquinic acid (**15**, 9.0 mg, *t<sub>R</sub>* 21.5 min), kaempferol 3-O-glucuronide (**21**, 16.2 mg, *t<sub>R</sub>* 22.3 min), isorhamnetin 3-O-glucuronide (**23**, 5.0 mg, *t<sub>R</sub>* 25.7 min) and 4,5-dicaffeoylquinic acid (**16**, 7.8 mg, *t<sub>R</sub>* 27.8 min). Fraction H (eluted with a mixture of A:B 7:3) was re-chromatographed by RP-18 HPLC-UV using the following elution gradient: 0-5 min = A:B 75:25; 15-22 min = A:B 70:30 (flow rate 3.0 mL/min) affording isomadecassoside (**6**, 2.5 mg, *t<sub>R</sub>* 13.7 min), terminoloside (**5**, 123.2 mg, *R<sub>t</sub>* 16 min), madecassoside (**2**, 80.0 mg, *t<sub>R</sub>* 16.2 min), isoasiaticoside (**8**, 2.0 mg, *t<sub>R</sub>* 16.9 min), centellasaponin B (**11**, 3.6 mg, *t<sub>R</sub>* 18.1 min) and isoterminoloside (**7**, 2.2 mg, *t<sub>R</sub>* 18.4 min) in a pure state. Fraction L (eluted with a mixture of A:B 65:35) was separated by RP-18 HPLC-UV using the following elution gradient: 0-5 min = A:B 80:20 isocratic; 10-40 min = A:B 70:30 isocratic, flow rate 3.0 mL/min

*Phytochemical profile of Centevita® and its madecassoside-enriched fraction*

affording 2 $\alpha$ ,3 $\beta$ ,6 $\beta$ -trihydroxyolean-12-en-28-oic acid triglycoside (**13**, 2.1 mg,  $t_R$  26 min), quercetin (**19**, 12.6 mg,  $t_R$  26.8 min) and centellasaponin C (**12**, 3.7 mg,  $t_R$  28.5 min) in a pure state. The fraction M (eluted with a mixture of A:B 62:38) was separated by RP-18 HPLC-UV using A:B 70:30 isocratic, flow rate 3.0 mL/min, to yield asiaticoside C (**9**, 2.1 mg,  $t_R$  32.1 min), kaempferol (**18**, 8.9 mg,  $t_R$  35.6 min), isorhamnetin (**20**, 5.5 mg,  $t_R$  38.2 min) and asiaticoside F (**10**, 2.8 mg,  $t_R$  41.4 min). Fraction P (eluted with a mixture of A:B 4:6) was separated by normal-phase MPLC using the following elution gradient: 0-2 CV = *n*-hexane:EtOAc 100:0; 2-77 CV = *n*-hexane:EtOAc 0:100, flow rate 15.0 mL/min obtaining asiatic acid (**3**, 46.0 mg, CV 75) madecassic and terminolic acids (**4** and **5a**, 9.7 mg).

*Centellasaponin C (12)*. White amorphous solid.  $^1\text{H}$  NMR ( $\text{CD}_3\text{OD}$ , 700 MHz,  $J$  in Hz): *aglycone moiety*:  $\delta$ : 5.31 (1H, overlapped, H-12); 4.48 (1H, br, H-6); 3.70 (1H, overlapped, H-2); 2.86 (1H, d,  $J = 9.6$  Hz, H-3); 2.28 (1H, d,  $J = 11.5$  Hz, H-18); 2.30 (1H, overlapped, H-22a); 2.09 (1H, overlapped, H-11a); 2.00 (2H, overlapped, H-11b); 1.98 (2H, overlapped, H-15b); 1.95 (2H, dd,  $J_1 = 12.2$  Hz,  $J_2 = 4.4$  Hz, H-1a); 1.80 (m, H-22b) 1.72 (1H, overlapped, H-7a); 1.64 (1H, overlapped, H-9); 1.60-1.57 (2H, overlapped, H-16a and H-16b); 1.56 (1H, overlapped, H-7b); 1.54 (2H, overlapped, H-21a); 1.42 (1H, overlapped, H-19); 1.41 (3H, s,  $\text{CH}_3$ -25); 1.37 (1H, overlapped, H-21b); 1.20 (3H, s,  $\text{CH}_3$ -23); 1.13 (1H, overlapped, H-15b); 1.11 (3H, s,  $\text{CH}_3$ -26); 1.10 (3H, s,  $\text{CH}_3$ -27); 1.09 (3H, s,  $\text{CH}_3$ -24); 0.99 (3H, br s,  $\text{CH}_3$ -30); 0.92 (3H, d,  $J = 6.4$  Hz,  $\text{CH}_3$ -29); 0.90 (1H, overlapped, H-1b); 0.83 (1H, br, H-5). *Sugar moiety*:  $\delta$ : 5.31 (1H,

## Chapter 2

overlapped, H-1'); 4.87 (1H, overlapped, H-1'''); 4.39 (1H, d,  $J = 7.9$  Hz, H-1''); 4.10 (2H, dd,  $J_1 = 11.9$  Hz,  $J_2 = 1.7$  Hz, H-6'a); 3.99 (1H, overlapped, H-5'''); 3.84 (2H, overlapped, H-6''a); 3.84 (1H, overlapped, H-2'''); 3.77 (1H, dd,  $J = 11.9$  Hz,  $J_2 = 5.2$  Hz, H-6'b); 3.67 (1H, overlapped, H-6''b); 3.65 (1H, dd,  $J_1 = 9.9$  Hz,  $J_2 = 3.4$  Hz, H-4'); 3.56 (1H, overlapped, H-4''); 3.51 (1H, overlapped, H-3'''); 3.42 (1H, overlapped, H-4'''); 3.41 (1H, overlapped, H-3'); 3.35 (1H, overlapped, H-5'); 3.35 (1H, overlapped, H-5'''); 3.32 (1H, overlapped, H-2'); 3.31 (1H, overlapped, H-3'''); 3.25 (1H, d,  $J = 8.4$  Hz H-2''); 1.29 (3H, d,  $J = 6.2$  Hz, CH<sub>3</sub>-6'''). <sup>13</sup>C-NMR (CD<sub>3</sub>OD, 175 MHz): *aglycone moiety*:  $\delta$ : 176.5 (C-28); 137.3 (C-13); 125.7 (C-12); 83.3 (C-3); 68.2 (C-2); 67.2 (C-6); 55.6 (C-5); 52.8 (C-18); 49.3 (C-1); 48.5 (C-17); 48.0 (C-9); 42.6 (C-14); 40.4 (C-7); 39.9 (C-4); 39.3 (C-8); 39.1 (C-19); 38.9 (C-20); 38.5 (C-10); 38.3 (C-22); 30.3 (C-21); 27.9 (C-15); 27.7 (C-24); 25.3 (C-16); 23.3 (C-11); 22.7 (C-27); 20.2 (C-30); 18.1 (C-26); 17.7 (C-25); 17.5 (C-23); 16.2 (C-29). *Sugar moiety*:  $\delta$ : 103.1 (C-1''); 101.6 (C-1'''); 94.5 (C-1'); 78.4 (C-4''); 78.0 (C-5'); 76.7 (C-3'); 76.5 (C-3'' and C-5''); 75.5 (C-2'); 74.0 (C-2''); 73.4 (C-4'''); 73.2 (C-3'''); 72.1 (C-2'''); 70.9 (C-4'); 69.3 (C-5'''); 68.3 (C-6'); 60.6 (C-6''); 16.5 (C-6'''). (-)-ESIMS  $m/z$  957 [M - H]<sup>-</sup>. HR-ESIMS found  $m/z$  957.5060; C<sub>48</sub>H<sub>77</sub>O<sub>19</sub> requires  $m/z$  957.5065.

*Isoterminaloside (7)*. White amorphous solid.  $[\alpha]_D = -3.0$  (c 0.1, CH<sub>3</sub>OH); <sup>1</sup>H NMR (CD<sub>3</sub>OD, 700 MHz) and <sup>13</sup>C NMR (CD<sub>3</sub>OD, 175 MHz): Table 2.4; HR-ESIMS found  $m/z$  973.4999 [M - H]<sup>-</sup>. C<sub>48</sub>H<sub>77</sub>O<sub>20</sub> requires  $m/z$  973.5014.

## References

---

1. Jamil, S. S., Nizami, Q., & Salam, M. (2007). *Centella asiatica* (Linn.) Urban—a review.
2. Sayasinha, P., Warnasuriya, D., & Dissanayake, H. (1999). History, medicinal and aromatic plant series: Vol. 1 (p. 1). Colombo: Information Services Centre Industrial Technology Institute.
3. Seevaratnam, V., Banumathi, P., Premalatha, M. R., Sundaram, S. P., & Arumugam, T. (2012). Functional properties of *Centella asiatica* (L.): a review. *Int J Pharm Pharm Sci*, 4(5), 8-14.
4. Shukla, A., Rasik, A. M., Jain, G. K., Shankar, R., Kulshrestha, D. K., & Dhawan, B. N. (1999). In vitro and in vivo wound healing activity of asiaticoside isolated from *Centella asiatica*. *Journal of ethnopharmacology*, 65(1), 1-11.
5. Cox, D. N., Rajasuriya, S. V., Soysa, P. E., Gladwin, J., & Ashworth, A. (1993). Problems encountered in the community-based production of leaf concentrate as a supplement for pre-school children in Sri Lanka. *International journal of food sciences and nutrition*, 44(2), 123-132.
6. Huda-Faujan, N., Noriham, A., Norrakiah, A., & Babji, A. S. (2007). Antioxidative activities of water extracts of some Malaysian herbs. *ASEAN Food Journal*.

## Chapter 2

7. Brinkhaus, B., Lindner, M., Schuppan, D., & Hahn, E. G. (2000). Chemical, pharmacological and clinical profile of the East Asian medical plant *Centella asiatica*. *Phytomedicine*, 7(5), 427-448.
8. Adenan, M. I. (1998). Opportunities on the planting of medicinal and herbal plants in Malaysia. *Planter (Malaysia)*.
9. Chen, Y., Han, T., Qin, L., Rui, Y., & Zheng, H. (2003). Effect of total triterpenes from *Centella asiatica* on the depression behavior and concentration of amino acid in forced swimming mice. *Zhong yao cai= Zhongyaocai= Journal of Chinese medicinal materials*, 26(12), 870-873.
10. Lee, M. K., Kim, S. R., Sung, S. H., Lim, D., Kim, H., Choi, H., ... & Ki, Y. C. (2000). Asiatic acid derivatives protect cultured cortical neurons from glutamate-induced excitotoxicity. *Research communications in molecular pathology and pharmacology*, 108(1-2), 75-86.
11. Chauhan, P. K., Pandey, I. P., Dhatwalia, V. K., & Singh, V. (2010). Extract of *Centella asiatica* on alloxan induced diabetic rats. *International Journal of Pharma and Bio Sciences*, 1, 2.
12. Das, A. J. (2011). Review on nutritional, medicinal and pharmacological properties of *Centella asiatica* (Indian pennywort). *Journal of Biologically Active Products from Nature*, 1(4), 216-228.
13. Chandrika, U. G., & Kumara, P. A. P. (2015). Gotu Kola (*Centella asiatica*): nutritional properties and plausible health

- benefits. *Advances in food and nutrition research*, 76, 125-157.
14. Kunjumon, R., Johnson, A. J., & Baby, S. (2022). *Centella asiatica*: Secondary metabolites, biological activities and biomass sources. *Phytomedicine Plus*, 2(1), 100176.
  15. Azerad, R. (2016). Chemical structures, production and enzymatic transformations of sapogenins and saponins from *Centella asiatica* (L.) Urban. *Fitoterapia*, 114, 168-187.
  16. Haralampidis, K., Trojanowska, M., & Osbourn, A. E. (2002). Biosynthesis of triterpenoid saponins in plants. *History and Trends in Bioprocessing and Biotransformation*, 31-49.
  17. Xu, R., Fazio, G. C., & Matsuda, S. P. (2004). On the origins of triterpenoid skeletal diversity. *Phytochemistry*, 65(3), 261-291.
  18. Augustin, J. M., Kuzina, V., Andersen, S. B., & Bak, S. (2011). Molecular activities, biosynthesis and evolution of triterpenoid saponins. *Phytochemistry*, 72(6), 435-457.
  19. Costa, F. D., Barber, C. J., Reed, D. W., & Covello, P. S. (2016). From plant extract to a cDNA encoding a glucosyltransferase candidate: proteomics and transcriptomics as tools to help elucidate saponin biosynthesis in *Centella asiatica*. In *Biotechnology of Plant Secondary Metabolism* (pp. 43-48). Humana Press, New York, NY.

## Chapter 2

20. Kim, O. T., Um, Y., Jin, M. L., Kim, Y. C., Bang, K. H., Hyun, D. Y., ... & Lee, Y. (2014). Analysis of expressed sequence tags from *Centella asiatica* (L.) Urban hairy roots elicited by methyl jasmonate to discover genes related to cytochrome P450s and glucosyltransferases. *Plant biotechnology reports*, 8(2), 211-220.
21. Maquart, F. X., Bellon, G., Gillery, P., Wegrowski, Y., & Borel, J. P. (1990). Stimulation of collagen synthesis in fibroblast cultures by a triterpene extracted from *Centella asiatica*. *Connective tissue research*, 24(2), 107-120.
22. Bonté, F., Dumas, M., Chaudagne, C., & Meybeck, A. (1995, January). Comparative activity of asiaticoside and madecassoside on type I and III collagen synthesis by cultured human fibroblasts. In *Annales pharmaceutiques francaises* (Vol. 53, No. 1, pp. 38-42).
23. Wu, F., Bian, D., Xia, Y., Gong, Z., Tan, Q., Chen, J., & Dai, Y. (2012). Identification of major active ingredients responsible for burn wound healing of *Centella asiatica* herbs. *Evidence-Based Complementary and Alternative Medicine*, 2012.
24. Maramaldi, G., Togni, S., Franceschi, F., & Lati, E. (2014). Anti-inflammaging and antiglycation activity of a novel botanical ingredient from African biodiversity (Centevita™). *Clinical, Cosmetic and Investigational Dermatology*, 7, 1.

25. Chianese, G., Masi, F., Cicia, D., Ciceri, D., Arpini, S., Falzoni, M., ... & Tagliatela-Scafati, O. (2021). Isomadecassoside, a new ursane-type triterpene glycoside from *Centella asiatica* leaves, reduces nitrite levels in LPS-stimulated macrophages. *Biomolecules*, 11(4), 494.
26. Masi, F., Chianese, G., Peterlongo, F., Riva, A., & Tagliatela-Scafati, O. (2022). Phytochemical profile of Centevita<sup>®</sup>, a *Centella asiatica* leaves extract, and isolation of a new oleanane-type saponin. *Fitoterapia*, 158, 105163.
27. Yu, Q. L., Duan, H. Q., Gao, W. Y., & Takaishi, Y. (2007). A new triterpene and a saponin from *Centella asiatica*. *Chinese Chemical Letters*, 18(1), 62-64.
28. Jiang, Z. Y., Zhang, X. M., Zhou, J., & Chen, J. J. (2005). New triterpenoid glycosides from *Centella asiatica*. *Helvetica chimica acta*, 88(2), 297-303.
29. Matsuda, H., Morikawa, T., Ueda, H., & Yoshikawa, M. (2001). Medicinal foodstuffs. XXVII. Saponin constituents of gotu kola (2): structures of new ursane-and oleanane-type triterpene oligoglycosides, centellasaponins B, C, and D, from *Centella asiatica* cultivated in Sri Lanka. *Chemical and Pharmaceutical Bulletin*, 49(10), 1368-1371.
30. Nhiem, N. X., Tai, B. H., Quang, T. H., Van Kiem, P., Van Minh, C., Nam, N. H., ... & Kim, Y. H. (2011). A new ursane-type triterpenoid glycoside from *Centella asiatica* leaves modulates the production of nitric oxide and secretion of

## Chapter 2

- TNF- $\alpha$  in activated RAW 264.7 cells. *Bioorganic & Medicinal Chemistry Letters*, 21(6), 1777-1781.
31. Wu, C., Chen, F., Wang, X., Wu, Y., Dong, M., He, G., ... & Huang, G. (2007). Identification of antioxidant phenolic compounds in feverfew (*Tanacetum parthenium*) by HPLC-ESI-MS/MS and NMR. *Phytochemical Analysis: An International Journal of Plant Chemical and Biochemical Techniques*, 18(5), 401-410.
32. Satake, T., Kamiya, K., An, Y., Oishi, T., & Yamamoto, J. (2007). The anti-thrombotic active constituents from *Centella asiatica*. *Biological and Pharmaceutical Bulletin*, 30(5), 935-940.
33. Liu, L., Li, H., Hu, K., Xu, Q., Wen, X., Cheng, K., ... & Sun, H. (2021). Synthesis and anti-inflammatory activity of saponin derivatives of  $\delta$ -oleanolic acid. *European Journal of Medicinal Chemistry*, 209, 112932.
34. Wang, M., Carver, J. J., Phelan, V. V., Sanchez, L. M., Garg, N., Peng, Y., ... & Bandeira, N. (2016). Sharing and community curation of mass spectrometry data with Global Natural Products Social Molecular Networking. *Nature biotechnology*, 34(8), 828-837.
35. Horai, H., Arita, M., Kanaya, S., Nihei, Y., Ikeda, T., Suwa, K., ... & Nishioka, T. (2010). MassBank: a public repository for sharing mass spectral data for life sciences. *Journal of mass spectrometry*, 45(7), 703-714.

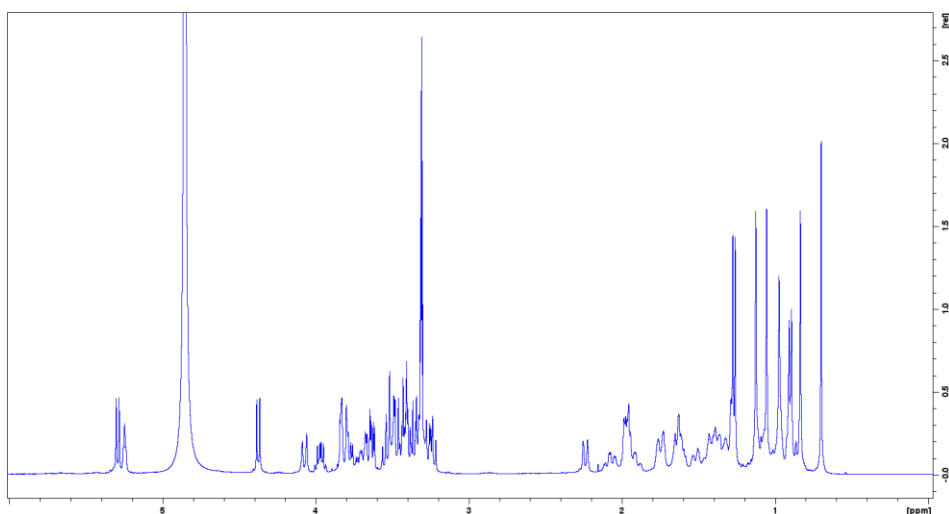
36. Mohimani, H., Gurevich, A., Shlemov, A., Mikheenko, A., Korobeynikov, A., Cao, L., ... & Pevzner, P. A. (2018). Dereplication of microbial metabolites through database search of mass spectra. *Nature communications*, 9(1), 1-12.
37. Paul Shannon, 1 *et al.* Cytoscape: A Software Environment for Integrated Models. *Genome Res.* 13, 426 (1971).

## Appendix A: Spectral data of chapter 2

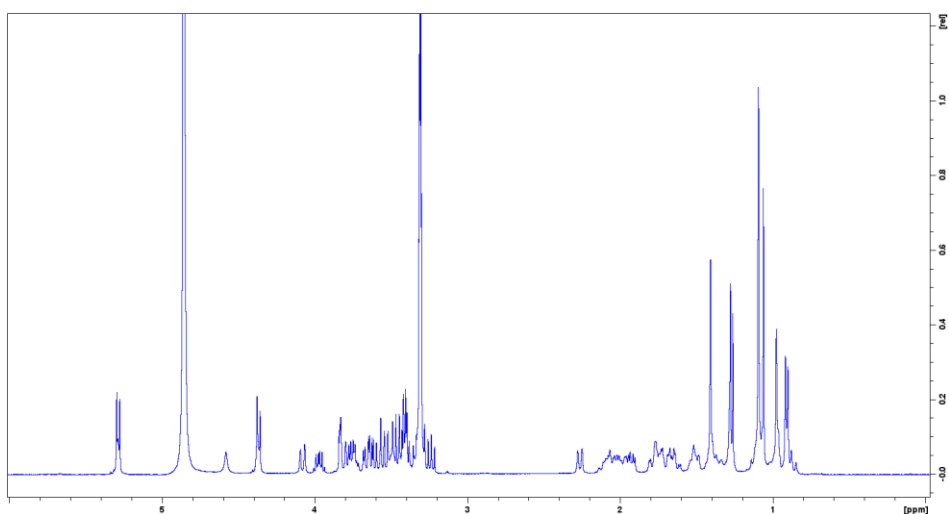
---

Herein are reported the NMR spectra of the main constituent of Centevita®.

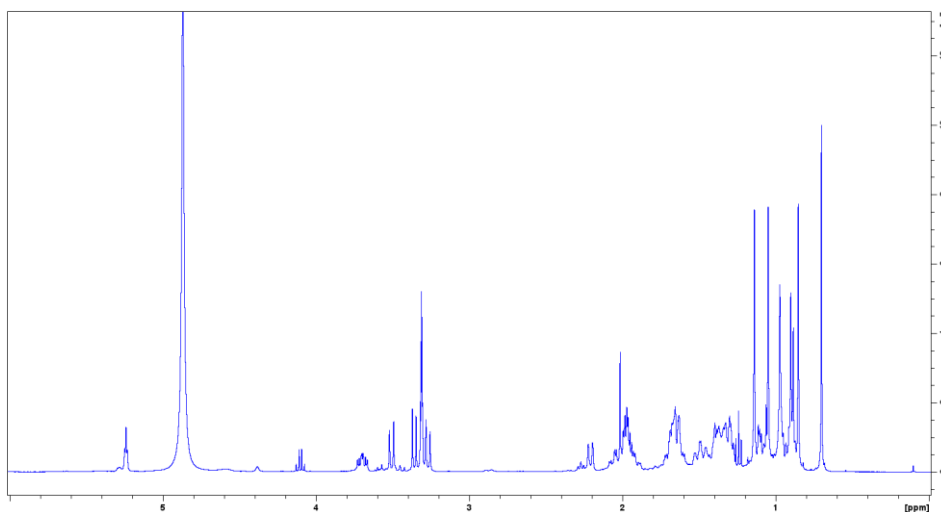
$^1\text{H}$  NMR spectrum (400 MHz) of asiaticoside (**1**) in  $\text{CD}_3\text{OD}$



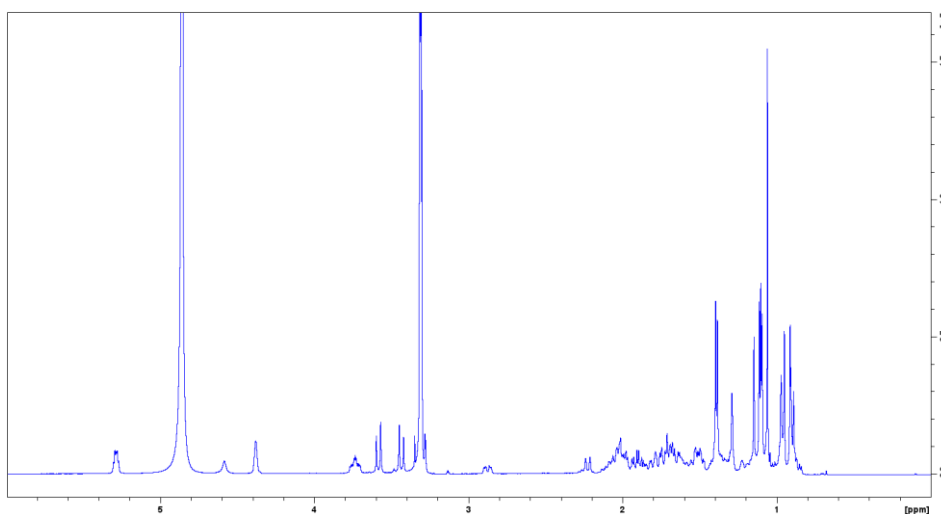
$^1\text{H}$  NMR spectrum (400 MHz) of madecassoside (**2**) in  $(\text{CD}_3\text{OD})$



$^1\text{H}$  NMR spectrum (400 MHz) of asiatic acid (**3**) in ( $\text{CD}_3\text{OD}$ )

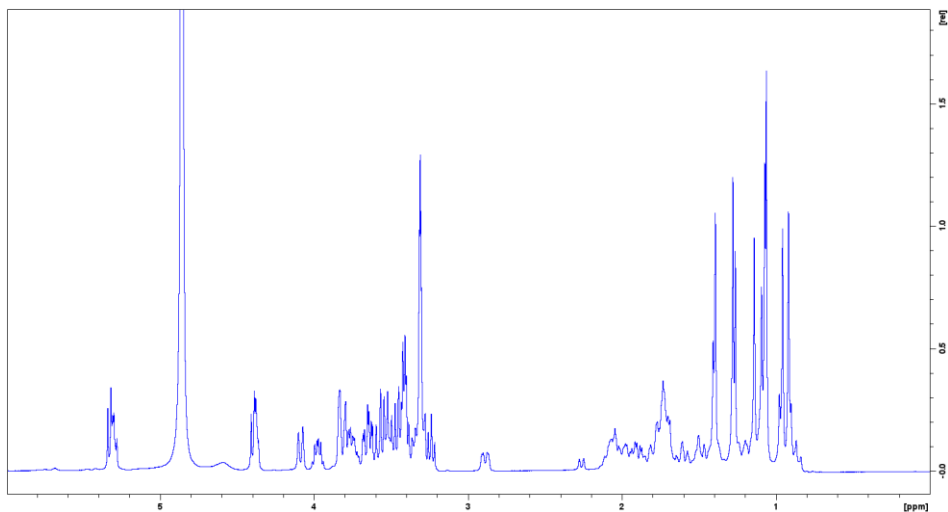


$^1\text{H}$  NMR spectrum (400 MHz) of madecassic acid (**4**) in ( $\text{CD}_3\text{OD}$ )

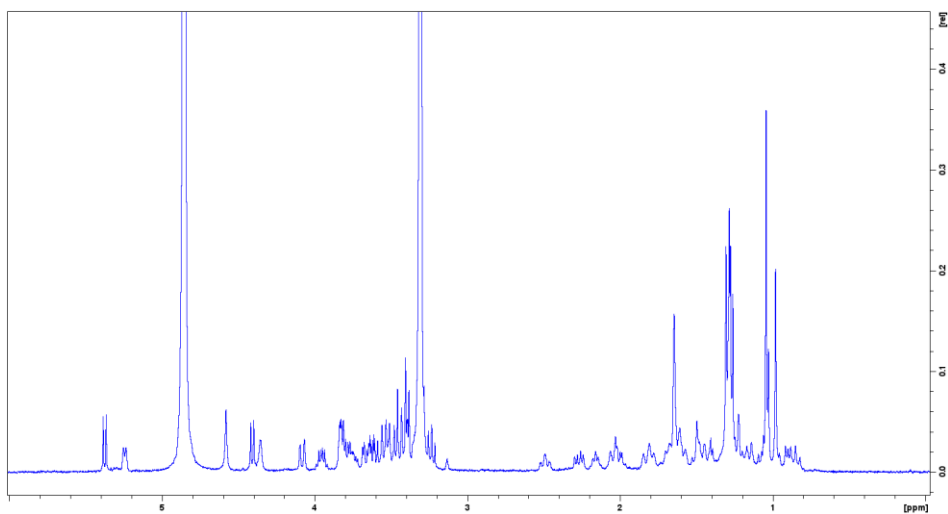


## Appendix A

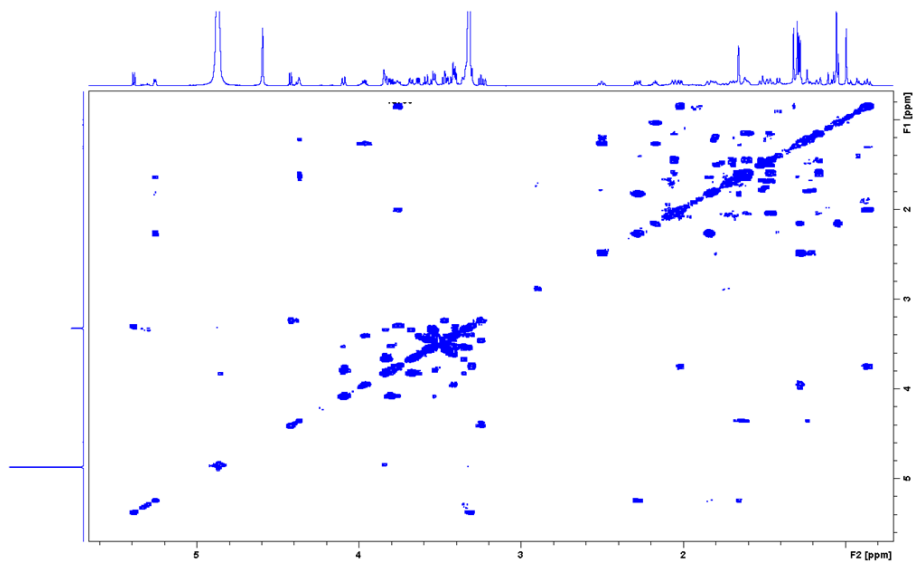
$^1\text{H}$  NMR spectrum (400 MHz) of terminoloside (**5**) in ( $\text{CD}_3\text{OD}$ )



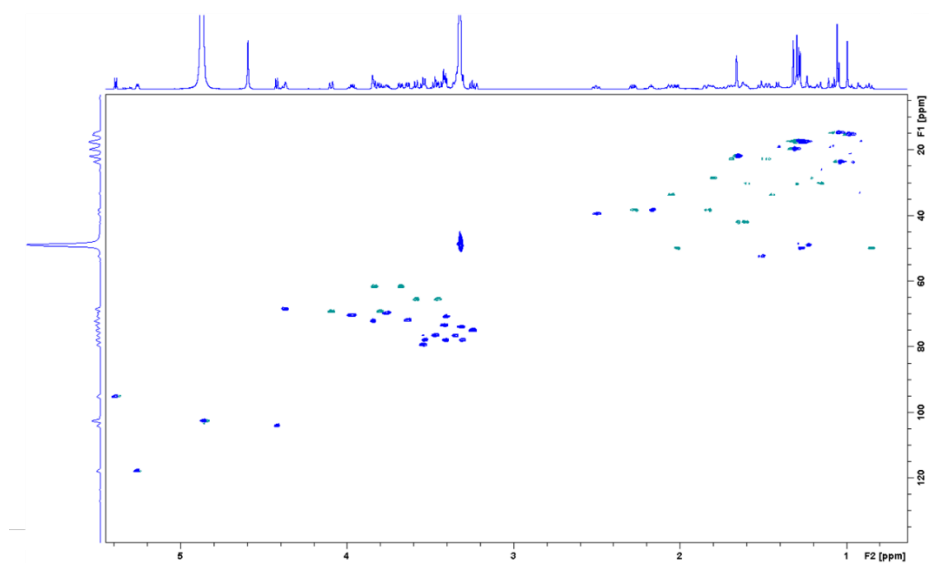
$^1\text{H}$  NMR spectrum (700 MHz) of isomadecassoside (**6**) in ( $\text{CD}_3\text{OD}$ )



COSY NMR spectrum (700 MHz) of isomadecassoside (**6**) in (CD<sub>3</sub>OD)

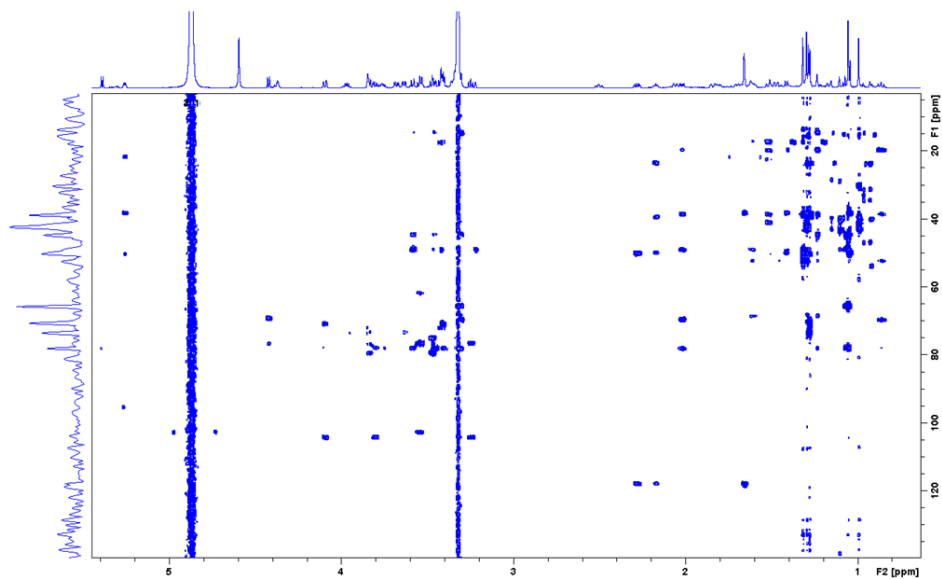


HSQC NMR spectrum (700 MHz) of isomadecassoside (**6**) in (CD<sub>3</sub>OD)

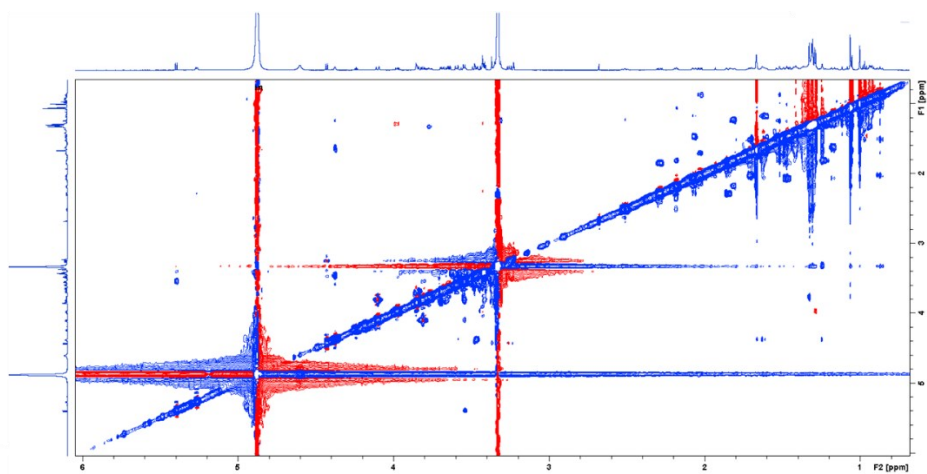


## Appendix A

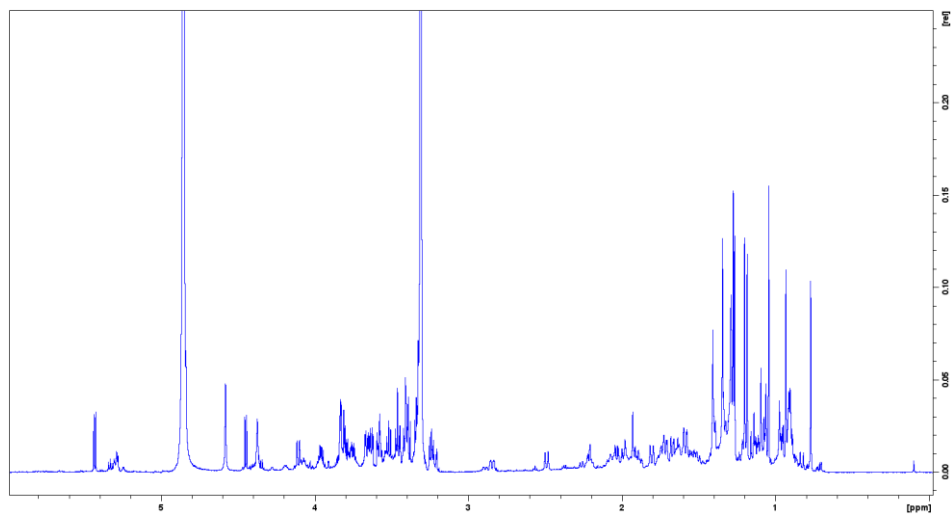
HMBC NMR spectrum (700 MHz) of isomadecassoside (**6**) in (CD<sub>3</sub>OD)



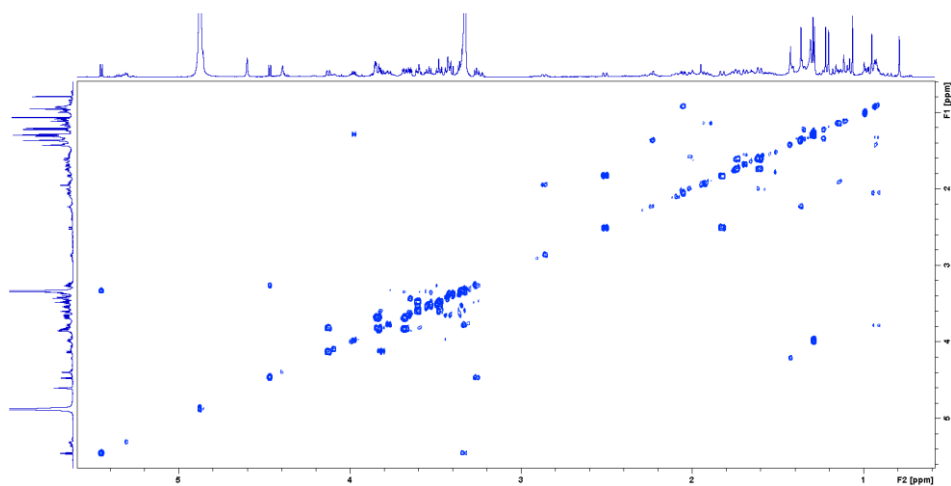
NOESY NMR spectrum (700 MHz) of isomadecassoside (**6**) in (CD<sub>3</sub>OD)



$^1\text{H}$  NMR spectrum (700 MHz) of isoterminoloside (**7**) in ( $\text{CD}_3\text{OD}$ )

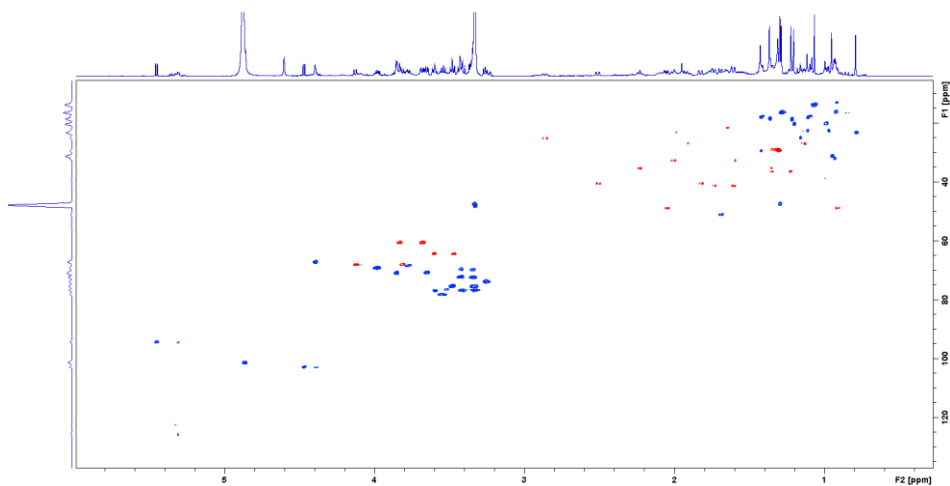


COSY NMR spectrum (700 MHz) of isoterminoloside (**7**) in ( $\text{CD}_3\text{OD}$ )

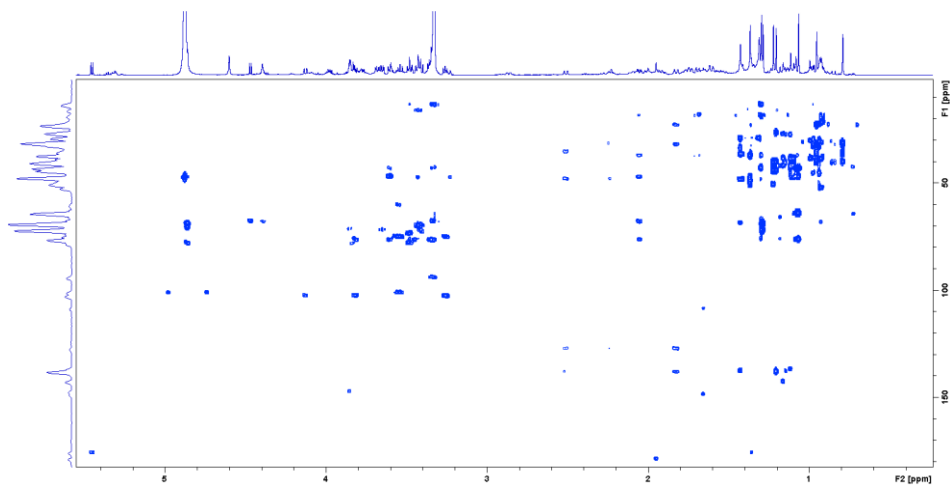


## Appendix A

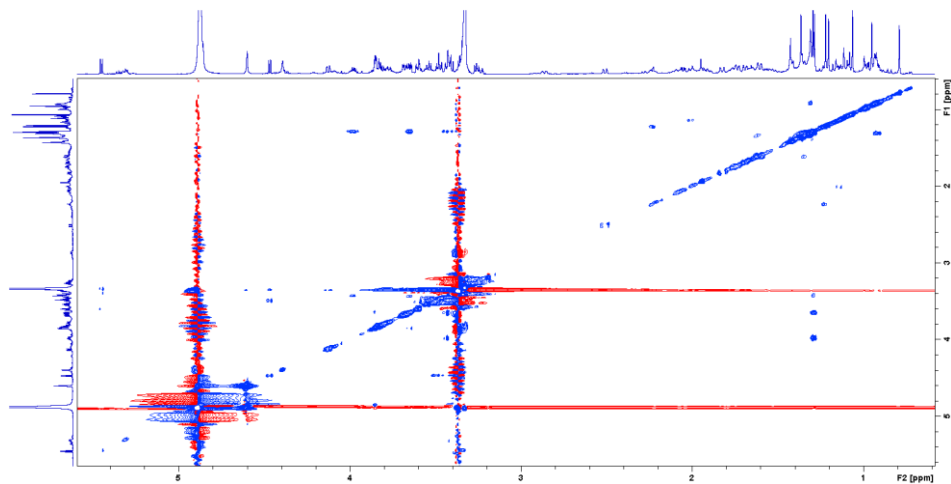
HSQC NMR spectrum (700 MHz) of isoterminoloside (**7**) in (CD<sub>3</sub>OD)



HMBC NMR spectrum (700 MHz) of isoterminoloside (**7**) in (CD<sub>3</sub>OD)



TOCSY NMR spectrum (700 MHz) of isoterminoloside (**6**) in (CD<sub>3</sub>OD)





## **Chapter 3: Phytochemical profile of an industrial *Rhodiola rosea* extract**

---

### **3.1 Introduction**

The genus *Rhodiola* belongs to the plant family *Crassulaceae* and includes nearly 200 species. One of them, is *Rhodiola rosea* L., known by the common names Rosen root, Golden Root, Arctic Root, Orpin Rose, among others, and has a long history as a valuable medicinal plant in several European countries.<sup>1</sup> The name “golden root” refers to the “*exquisite pharmacological properties of the root compounds*” and “rose root” to the rose scent that comes from freshly sliced roots; while “arctic root” refers to the geographic distribution of this species.<sup>2</sup> In fact, the plant grows on sea cliffs and in crevices of mountain rocks of Arctic regions of Europe, Asia (mainly in Siberia) and North America.<sup>3</sup>

*R. rosea* (**Figure 3.1**) is a long-lived perennial, with a life expectancy of over 80 years. The plants grow 5–50 cm tall and have deciduous (vs. marcescent) flowering stems. The rootstocks are 1–2 cm in diameter, cylindrical to long obconical in shape and branched when mature and well developed. Plants can have multiple flowering stems of 1–6 mm in diameter, are smooth, glabrous, and generally pale green, but can be glaucous. *R. rosea* inflorescences can include between 25 and 70 flowers and measure up to 5 cm in diameter. Depending on the region, the flowering period occurs from April to August and the fruiting period from July to September. There are records of *R. rosea* with monoecious or hermaphroditic flowers, but the species is effectively dioecious.<sup>4,5</sup>



**Figure 3.1.** *Rhodiola rosea*

For centuries, *R. rosea* rhizomes have been an important raw material in the folk medicine of Russia, Scandinavia, Mongolia, and China as a health supplement for stimulating the nervous system, enhancing physical and mental performance, psychological stress, depression, alleviating fatigue, impotence, and preventing high altitude sickness.<sup>6-8</sup> Furthermore, the rhizomes and roots show anti-stress, antioxidative, cardioprotective, hepatoprotective, immunomodulatory and anticancer properties; they can stimulate the central nervous system increasing cognitive functions such as attention, memory, and learning.<sup>1,7-9</sup>

Nowadays, *R. rosea* extracts constitute the active ingredient in many important commercial preparations such as food additives, dietary supplements, commercial pharmaceutical preparations, and drinks sold worldwide.<sup>10,11</sup>

Analysis of chemical compositions carried out on different parts of the plant, has led to the identification of approximately 150 bioactive compounds, belonging to several classes. However, the most

interesting compounds from the most relevant pharmacological point of view are certain phenylpropanoids, namely the cinnamyl alcohol glycosides, collectively referred to as rosavins, and the phenylethanoid compound salidroside with its aglycone tyrosol (**Figure 3.2**).<sup>2,12,13</sup>

Other compounds are glycosylated monoterpene derivatives, flavonoids, aryl glycosides, proanthocyanidins and gallic acid derivatives.<sup>1</sup>

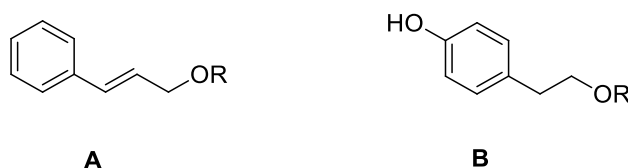


**Figure 3.2.** Main active compounds of *R. rosea*: cinnamyl alcohol (**A**) and phenylethanoids (**B**) derivatives. *R* = *H* or glycosides.

### **3.1.1 Biosynthesis of rosavins**

Cinnamyl alcohol glycosides (CAGs) (rosin, rosavin and rosarin) and salidroside are the valuable bioactive compounds of roseroot, and both derive from the basic phenylpropanoid metabolism via the shikimate pathway (**Figure 3.3**).<sup>14</sup> Different hypothetical pathways for salidroside biosynthesis are found in the literature, although none of them has been completely supported by molecular experimental results.

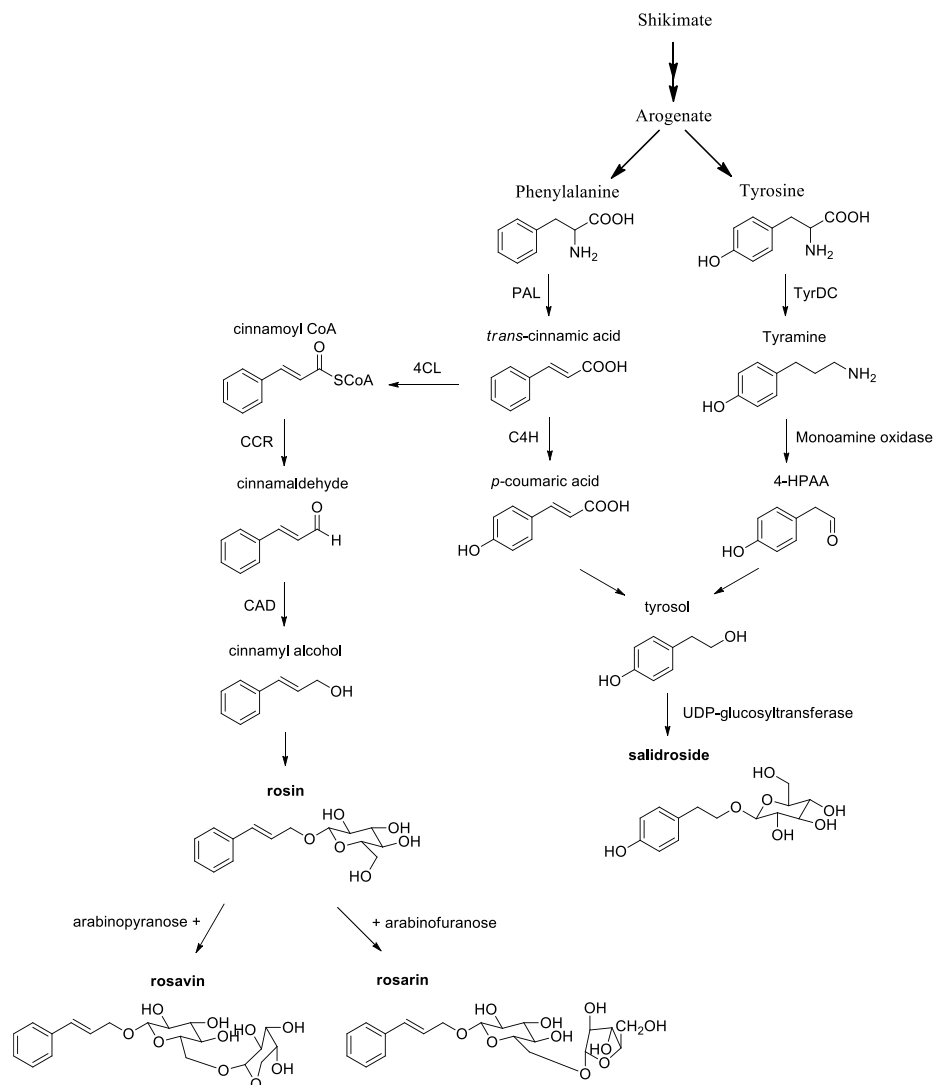


**Figure 3.3.** Schematic of the biosynthesis of key marker phytochemicals salidroside, tyrosol and the rosavins.

Phenylalanine and tyrosine are the important precursors of a large and diverse group of phenylpropanoids. Phenylalanine ammonia-lyase (PAL) is the first enzyme that catalyzes the phenylalanine deamination with the consequent production of *trans*-cinnamic acid

production,<sup>15</sup> the common precursor for the synthesis of both CAGs and salidroside.

The further steps depend on the downstream enzymatic activities involved in the pathway leading to the formation of either cinnamoyl-CoA in CAGs biosynthesis or *p*-coumaric acid (*trans-p*-hydroxycinnamic acid) in salidroside (4-hydroxyphenethyl *O*- $\beta$ -D-glucopyranoside) biosynthesis.

In the CAGs biosynthesis pathway,<sup>14</sup> *trans*-cinnamic acid is converted to cinnamoyl-CoA ester by the activity of 4-coumarate-CoA ligase (4CL), which is reduced to cinnamaldehyde by cinnamoyl-CoA oxidoreductase (CCR).<sup>16,17</sup> Subsequently, the cinnamaldehyde is further reduced by cinnamyl alcohol dehydrogenase (CAD) to cinnamyl alcohol.

The enzyme(s) involved in the formation of the glycosides of cinnamyl alcohol are not yet described. Rosin is the simplest glycoside of roseroot because it includes one molecule of glucose attached to the cinnamyl alcohol. Arabinosylation of rosin affords rosavin or rosarin according to the cyclic form of this pentose sugar, pyranose in the first and furanose in the latter. Depending on the sugar type and the site it is attached to, further glycosides may be formed.<sup>14</sup>

### **3.2 *Rhodiola rosea* as Rhodiola 5%**

Rhodiola 5% is a nutraceutical extract of Indena SpA (Milan, Italy) obtained from the roots of *Rhodiola rosea*. Its name derives from the fact that it is standardized and purified to 5% of rosavins, although a similar product with a different rosavin content is present

### Chapter 3

among the products of Indena (Rhodiola 3%). Rosavins are the main bioactive compounds of the extract, which include rosarin (**1**), rosavin (**2**), and rosin (**3**) that differ by the mono- or disaccharides substituents.<sup>18</sup> In addition, salidroside (**4**)<sup>18</sup> is a minor compound standardized to 1.8% in the extract.

Rhodiola 5% bio-pharmacological indication is as an adaptogen and tonic, probably via the hypothalamic-pituitary-adrenal (HPA) axis, as proved for *R. rosea* extract.<sup>19</sup> As a result, various products (dietary supplements or nutraceuticals), in different formulations (tablets and capsules) alone or in combination with other active ingredients or excipients, have been prepared from this extract. The most frequently proposed biological activity is related to the regulation of the nervous system activity, decreasing stress levels and relieving depression.

In this scenario, there is growing interest in an in-depth investigation of this extract, to also discover the minor compounds and characterize them both from the chemical and pharmacological point of view. The phytochemical investigation carried out in this doctoral project resulted in: i) the characterization of 18 secondary metabolites including 13 polyphenols and 6 terpenoids, and ii) the discovery of rhodiosidin (**5**) (**Figure 3.4**), a new compound, the first glycosylated derivative with both terpenoid and phenolic portions.

## Phytochemical profile of an industrial *Rhodiola rosea* extract

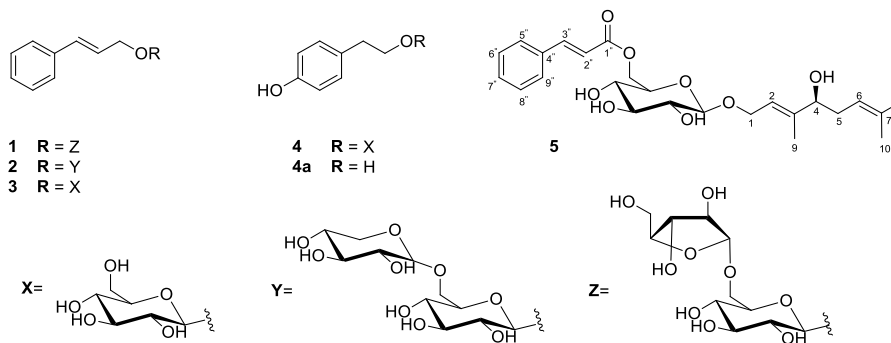


**Figure 3.4.** Chemical structures of the main compounds of *Rhodiola* 5% (1-4) and of the new rhodiosidin (5).

### 3.2.1 Dereplication of the extract

The extract was dereplicated by adopting the LC-MS/MS approach, obtaining the chromatogram shown in **Figure 3.5**.

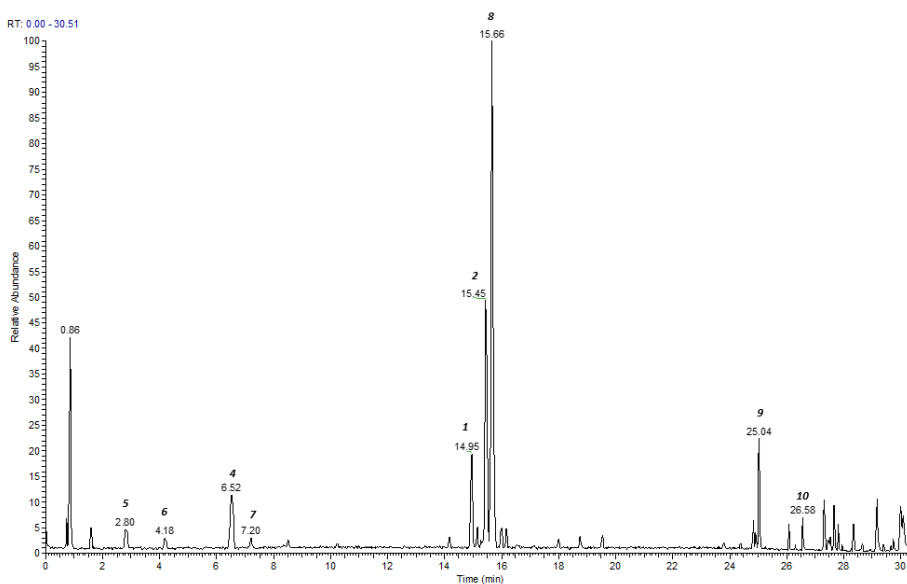


**Figure 3.5.** LC-MS chromatogram of *Rhodiola* 5% in positive ionization mode.

### Chapter 3

This preliminary analysis resulted in a putative identification of the main compounds, based on their measured mass and fragmentation patterns (**Table 3.1**). As a result, the phenylethanoid salidroside ( $t_R$  6.52, **4**), and rosarin ( $t_R$  14.95, **1**) and rosavin ( $t_R$  15.45, **2**) are among the rosavins that have been putatively identified (**Figure 3.4**).

**Table 3.1.** Metabolites identified in *Rhodiola* 5% via LC-MS/MS. Compounds are listed in order of LC-MS elution. All mass peaks have been detected as  $[M+Na]^+$ .

Retention time (min)	Measured $m/z$	Molecular formula	Assignment
2.80	282.12	C <sub>11</sub> H <sub>17</sub> NO <sub>6</sub>	Rhodiocyanoside A ( <b>6</b> )
4.18	284.07	C <sub>11</sub> H <sub>19</sub> NO <sub>6</sub>	Lotaustralin ( <b>7</b> )
6.52	323.12	C <sub>14</sub> H <sub>20</sub> O <sub>7</sub>	Salidroside ( <b>4</b> )
7.20	350.40	C <sub>16</sub> H <sub>18</sub> O <sub>3</sub>	Rhodioloside D ( <b>8</b> )
14.95	451.27	C <sub>20</sub> H <sub>28</sub> O <sub>10</sub>	Rosarin ( <b>1</b> )
15.45	451.29	C <sub>20</sub> H <sub>28</sub> O <sub>10</sub>	Rosavin ( <b>2</b> )
15.66	355.27	C <sub>16</sub> H <sub>28</sub> O <sub>7</sub>	Rosiridin ( <b>9</b> )
25.04	471.27	C <sub>21</sub> H <sub>20</sub> O <sub>11</sub>	Rhodionin ( <b>10</b> )
26.58	331.13	C <sub>17</sub> H <sub>14</sub> O <sub>7</sub>	Tricin ( <b>11</b> )

In addition, in the more polar region, the two cyanogenic glycosides rhodyocyanoside A ( $t_R$  2.80, **6**)<sup>20</sup> and lotaustralin ( $t_R$  4.18, **7**)<sup>21</sup> and the glycosylated terpenoid rhodioloside D ( $t_R$  7.20, **8**)<sup>22</sup> were recognized (**Figure 3.6**). In the more apolar region, after the elution of rosavins, the glycosylated terpenoid rosiridin ( $t_R$  15.66, **9**)<sup>18</sup> and some flavonoids such as rhodionin ( $t_R$  25.04, **10**)<sup>23</sup> and tricrin ( $t_R$  26.58, **11**) (**Figure 3.6**) have been putatively identified. The final

assignment was confirmed upon isolation and detailed NMR spectroscopic investigation.

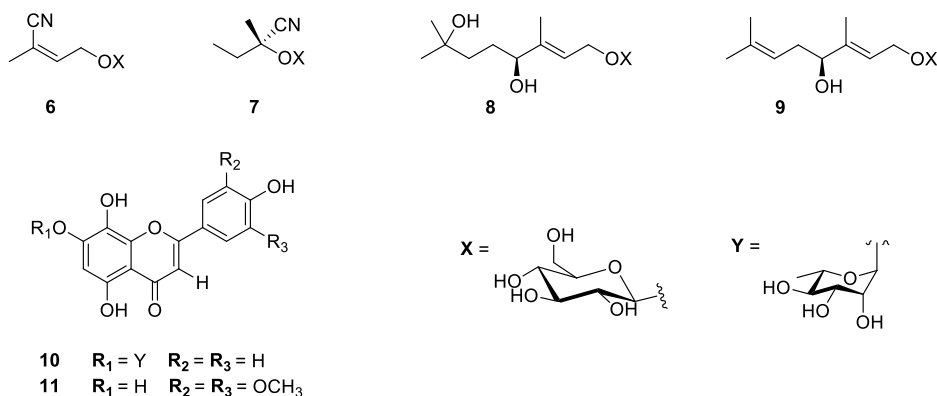


**Figure 3.6.** Chemical structure of the main compounds putatively identified by preliminary LC-MS analysis.

To this aim, Rhodiola 5% extract was subjected to MPLC-DAD on a C<sub>18</sub> column followed by repeated HPLC purifications, guided by the preliminary LC profile. Thus, the putative assignments could be supported by the chromatographic and spectroscopic analyses. Moreover, several compounds previously undetected in the preliminary untargeted LC-MS analysis, were also characterized. In particular, the LC-MS approach did not allow the identification of such compounds due to their low relative abundance (some of them were minor components present at trace levels in the extract) associated with a matrix effect on the ionization behaviour (ion suppression).

Therefore, one of the main constituents of the rosavins, rosin (**3**) was identified in the extract, only after its isolation (**Figure 3.4**).

### Chapter 3

Similarly, the free phenylethanoid aglycone of salidroside, tyrosol (**4a**) was also isolated and characterized (**Figure 3.4**).<sup>24</sup>

The terpenoid profile was completed by the characterization of rosiridol (**12**),<sup>25</sup> the free monoterpene of rosiridin (**9**) and of kenposide A (**13**),<sup>23</sup> a monoterpene disaccharide (**Figure 3.7**).

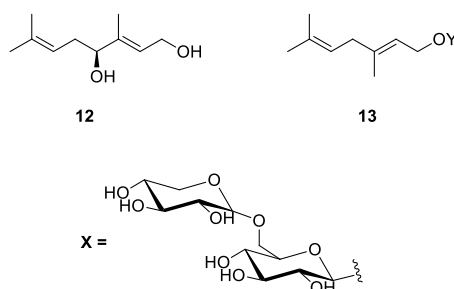


**Figure 3.7.** Structures of monoterpenoids (**11,12**) isolated and characterized in *Rhodiola* 5%.

The phenylmethanoid benzyl-O- $\beta$ -D-glucopyranoside (**14**),<sup>26</sup> the cinnamyl alcohol (**15**)<sup>27</sup> and epigallocatechin gallate (**16**)<sup>28</sup> were also isolated and characterized (**Figure 3.8**). Moreover, two additional flavonoids, rhodiolinin (**17**) and rhodiosin (**18**), have been characterized (**Figure 3.8**).<sup>23</sup>

## Phytochemical profile of an industrial *Rhodiola rosea* extract

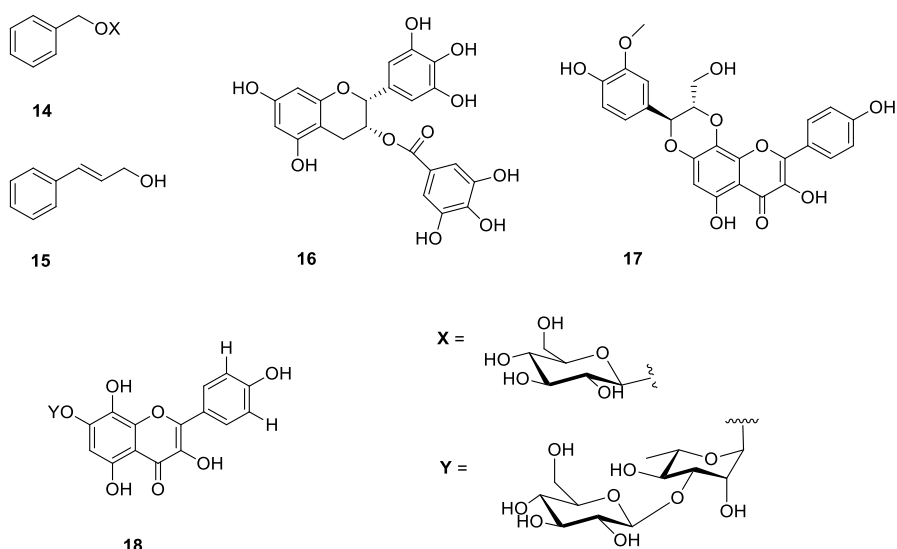


**Figure 3.8.** Structures of benzyl-*O*- $\beta$ -D-glucopyranoside (**14**), cinnamyl alcohol (**15**), epigallocatechin gallate (**16**) and flavonoids (**17,18**) characterized from *Rhodiola* 5%.

The phytochemical composition of *Rhodiola* plants is highly species-specific, even though salidroside (**4**) production in other species has also been reported. Several literature reports have established that the twenty-one species of the *Rhodiola* genus, yet morphologically similar to *R. rosea*, do not show the same phytochemical profile.<sup>1,3,29-33</sup> Thus, the presence of cinnamyl alcohol glycosides and of a relatively high content of phenylpropanoids of the rosavin family are a hallmark of *R. rosea*.

The isolation of *R. rosea* secondary metabolites in the pure form allowed to confirm that the main constituents of the extract are rosavins, although their distribution is not symmetrical, since rosavin and rosarin are more abundant than rosin. Thereafter, the most abundant compounds are salidroside (**4**), rosiridin (**8**) and the epigallocatechin gallate (**16**).

### 3.2.2 Structural elucidation of rhodiosidin

The chromatographic purification of *R. rosea* extract afforded also, in the pure form, a new rosiridin derivative, named rhodiosidin (**5**). It (**5**) was isolated as an amorphous brown solid with  $[\alpha]_D + 24.6$  and molecular formula  $C_{25}H_{34}O_8$  (HRESIMS found 485.2125  $[M+Na]^+$ , required  $m/z$  485.2151). The  $^1H$  NMR and  $^{13}C$  spectra of **5** (Table 3.2) showed typical resonances of rosiridin (**9**), including signals of the three methyl singlets, all resonating in the allylic region ( $\delta_H$  1.58, 1.63, 1.67), two olefinic protons resonating at  $\delta_H$  5.05 (t,  $J = 6.84$  Hz, H-6) and 5.55 (t,  $J = 6.55$  Hz, H-2), one oxymethine located at  $\delta_H$  3.96 (t,  $J = 6.55$  Hz, H-4), and one oxymethylene at  $\delta_H$  4.31 (overlapped, H-1). These observations in addition to the resonances of the  $\beta$ -glucopyranosyl moiety, [ $\delta_H$  4.33 (d,  $J = 7.6$  Hz, H-1');  $\delta_C$  101.1 (C-1')], confirmed the assignment of **5** of a rosiridin derivative.

On the other hand, the  $^1H$  NMR spectrum also included the typical resonances of a cinnamic group. In particular, the overlapped aromatic signals at  $\delta_H$  7.41 and 7.61, integrating for five protons and the two mutually coupled olefinic protons at  $\delta_H$  6.56 and 7.73 (d,  $J = 16$  Hz, H-2'' and H-3'', respectively) were attributable to a *trans*-cinnamic acid residue.

**Table 3.2.**  $^1H$  (700 MHz) and  $^{13}C$  (175 MHz) NMR Data of rhodiosidin (**5**) in  $CD_3OD$ .

Pos.	$\delta_H$ , mult., $J$ in Hz	$\delta_C$ , mult.
1	4.31 <sup>a</sup>	64.4, CH <sub>2</sub>
2	5.55, t, 6.55	121.2, CH
3		142.3, C
4	3.96, t, 6.55	76.6, CH
5a	2.22 <sup>a</sup>	33.5, CH <sub>2</sub>

*Phytochemical profile of an industrial Rhodiola rosea extract*

5b	2.34 <sup>a</sup>	
6	5.05, t, 6.84	119.8, CH
7		132.6, C
8	1.67, s	24.6, CH <sub>3</sub>
9	1.63, s	10.6, CH <sub>3</sub>
10	1.58, s	16.7, CH <sub>3</sub>
1'	4.33, d, 7.63	101.1, CH
2'	3.21, d, 7.63	73.7, CH
3'	3.38 <sup>a</sup>	76.5, CH
4'	3.51 <sup>a</sup>	73.9, CH
5'	3.35 <sup>a</sup>	70.4, CH
6a'	4.36 <sup>a</sup>	63.5, CH <sub>2</sub>
6b'	4.54, d, 11.8	
1''		167.0, C
2''	6.56, d, 16.00	117.3, CH
3''	7.73, d, 16.00	145.0, CH
4''		134.5, C
5''	7.61, 4.02	127.9, CH
6''	7.41 <sup>a</sup>	130.2, CH
7''	7.41 <sup>a</sup>	128.7, CH
8''	7.41 <sup>a</sup>	130.2, CH
9''	7.61, 4.02	127.9, CH

All the proton signals were associated with those of the directly linked carbon atoms through the correlations in the HSQC spectrum. The 2D NMR COSY spectrum allowed the identification of five spin system, highlighted in **Figure 3.8**, including the hexopyranose spin system and the remaining four spin systems spanning from H<sub>2</sub>-1 to H-2, H-4 to H-6, H-2'' to H-3'' and the aromatic ring system from H-5'' to H-9''.

The 2D NMR HMBC cross-peaks from H-1 to C-1' and from H-6' to C-1'' provided evidence to join together the above subunits, locating the cinnamoyl group at C-6' of glucose, whose protons, accordingly, have unusually high chemical shifts in the <sup>1</sup>H NMR spectrum. The absolute configuration of the stereogenic centers in **5** were assigned as those of the co-occurring rosiridin (**9**). Thus, compound

### Chapter 3

**5** was determined to be (2*E*,4*S*)-4-hydroxy-3,7-dimethyl-2,6-octadienyl-(6'-*O*-cinnamoyl)- $\beta$ -D-glucopyranoside.

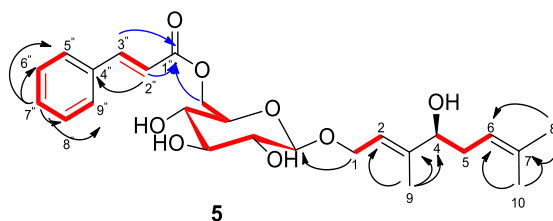


**Figure 3.9.** COSY (in red bold) and key H $\rightarrow$ C HMBC (black and blue arrows) correlations detected for **5**.

Interestingly, rhodiosidin (**5**) is unique among the components of *R. rosea* extract in possessing terpene, sugar and phenolic portions. The most similar compound of this class to be present in the literature is glehnoside (**Figure 3.10**), isolated from Son M. J. (2015) from the aerial parts of *Aster glehni* (family Asteraceae), including a caffeoyl residue in place of the cinnamoyl one and a hemiterpene in place of the monoterpene residue.<sup>34</sup>

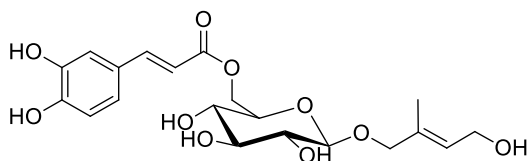


**Figure 3.10.** Chemical structure of glehnoside isolated from *A. glehni*.

### **3.2.3 Pharmacological evaluation**

*R. rosea* is considered a versatile phyto-adaptogen possessing antioxidant,<sup>35</sup> antistress<sup>36</sup> and antibacterial properties,<sup>37</sup> among others. It has been postulated that inflammation, and the related generation of reactive oxygen species (ROS) that can damage cellular biomolecules, constitute the common trait in the etiology of the disorders treated with *R. rosea*.<sup>38</sup> Accordingly, it was demonstrated that *R. rosea* root extract significantly inhibited the oedema formation induced by carrageenan and caused significant inhibition of the enzyme phospholipase A<sub>2</sub>, involved in the liberation of arachidonic acid from cell membranes, and of the isoform COX-2 of cyclooxygenase, the enzyme that catalyses the conversion of arachidonic acid to prostaglandins.<sup>38</sup> In another study, *R. rosea* extract was proved to be able to exert anti-neuroinflammatory effects by inhibiting NF- $\kappa$ B nuclear translocation.<sup>39</sup> However, to our knowledge, an investigation on the anti-inflammatory activity of the main constituents of this plant is still lacking, with exception of salidroside (**4**), which has been found to inhibit ROS production and pro-inflammatory cytokines in LPS stimulated murine macrophages.<sup>40</sup> Very recently, salidroside has been also demonstrated to act as chemosensitization agent for the treatment of multi-drug-resistant tumors.<sup>41</sup>

To start filling the gap in our knowledge about the *R. rosea* anti-inflammatory potential against lipid mediator producing enzymes, the extract Rhodiola 5% and its main constituents were evaluated for inhibitory activity against 5-lipoxygenase (5-LO), the enzyme that catalyzes two steps in the biosynthesis of leukotrienes (LTs), lipid mediators of inflammation derived from arachidonic acid. The

tests were carried out in human polymorphonuclear leukocytes (PMNL) and in a cell-free assay. While no inhibition was detected for extract and isolated compounds against 5-LO in PMNL (data not shown), probably due to low permeability, significant activity was observed against isolated 5-LO in cell-free assays (**Figure 3.11**). The potent 5-LO inhibiting activity shown by the total extract could not be ascribed to salidroside (**4**), but mostly to the monoterpene glycosides rosiridin (**9**) and kenposide A (**13**) and to the cinnamyl alcohol glycosides (rosavins) rosarin (**1**) and rosavin (**2**). In particular, at 10  $\mu\text{M}$ , rosiridin and the two rosavins caused almost 50% enzyme inhibition while, at the same concentration, kenposide A (**13**) almost completely abolished the enzymatic activity.

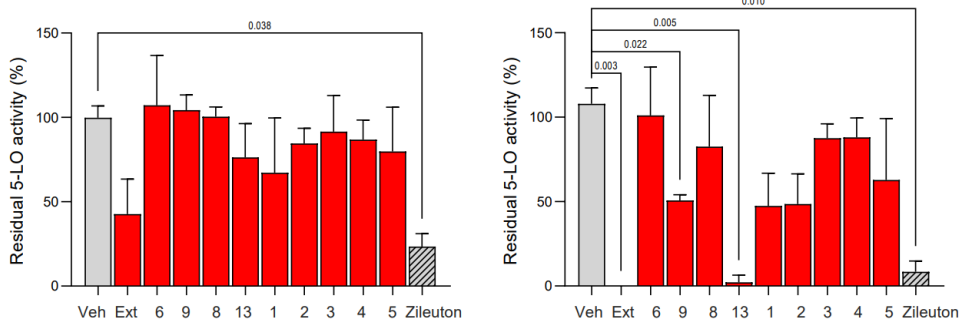


**Figure 3.11.** Biological activity against isolated 5-LO. Residual enzyme activity presented as arithmetic means (bars) after 10 min incubation with 1  $\mu\text{M}$  (left) or 10  $\mu\text{M}$  (right) of test compounds ( $n = 3-4$ ) or 3  $\mu\text{M}$  of the control inhibitor zileuton ( $n = 6$ ). Statistical significance was assigned by mixed effects analysis with Geisser-Greenhouse correction and Dunnett's multiple comparisons test. Veh = Vehicle.

Further investigations are needed to support these results and evaluate the *R. rosea* components against other isolated enzymes

involved in lipid mediator synthesis (mPGES-1, COX-1 and COX-2).

### **3.3 Conclusion**

*Rhodiola rosea* is a very popular medicinal plant and several phytotherapeutic products on the market include its extracts.

An LC-MS guided phytochemical investigation on the commercial *R. rosea* root Indena extract named Rhodiola 5%, allowed the putative identification of some of the main components. Thus, a chromatographic analysis was required, affording 18 secondary metabolites. These belong to two main structural classes, monoterpenoids (and their glycosylated derivatives) and phenolic derivatives. From the analysis, the ratio between these classes of components seems to follow the industrial specifications, confirming the title of 5% of rosavins and 1.8% of salidroside. Furthermore, among the main compounds rosavins, rosarin (**1**) and rosavin (**2**) appear to be more abundant than rosin (**3**), while salidroside (**4**) is the second most abundant compound in the extract after the rosavins.

The metabolomic characterization also resulted in the discovery of rhodiosidin (**5**), a new rosiridin (**9**) derivative with *trans*-cinnamyl alcohol as substituent at the hydroxyl group of 6'- of glucose.

Considering the high anti-inflammatory potential of *R. rosea* extract against lipid mediator producing enzymes, the 5-lipoxygenase inhibition activity of the main components was characterized, revealing rosiridin (**9**), kenposide A (**13**) and rosavins (**1** and **2**) mainly responsible for the activity of the extract.

## 3.4 Experimental section

### 2.4.1 Plant material and extraction of *Rhodiola* 5%

The *Rhodiola rosea* extract named Rhodiola 5% is commercially available at Indena SpA (Milan, Italy) and was obtained as a free sample from the manufacturing company. To prepare this extract, *R.rosea* roots were collected in Siberia, dried, ground, and then heat extracted with 70% ethanol. The solutions were filtered, pooled and concentrated to small volume under vacuum. The dry product was ground to yield Rhodiola dry extract 5%.

### 2.4.2 LC-MS/MS analysis

All LC-MS and LC-MS/MS experiments were performed using hybrid linear Ion Trap LTQ Orbitrap XLTL Fouries Transform Mass Spectrometer (FTMS), (Thermo Fisher Scientific Spa, Rodano, Italy) equipped with an Ultimate 3000 HPLC system (Agilent Technology, Cernusco sul Naviglio, Italy). Chromatographic separation was achieved using a Kinetex Polar C18 column (100 x 3.0 mm, 100Å, 2.6 µm) (Phenomenex, Torrance, CA, USA). The injection volume was 5 µL. Gradient elution was performed using a mobile phase consisting of water (solvent A) and acetonitrile (solvent B), both containing 0.1% v/v formic acid. Flow rate was 0.5 mL/min. The chromatographic procedure lasted 33 min, and the gradient design was as follows: an initial 2 min at 5% B, from 2 to 16 min B, reached 200%, hold at 20% B from 16 to 21, then from 21 to 31 min B reached 95% and hold at 95% B from 31 to 33 min. The analysis was carried out in positive (ESI+) ionization modes. Source conditions were: Spray voltage: 4.8 kV; Capillary voltage: 9

V; Source temperature: 285 °C. The acquisition range was m/z 150–1500.

### **2.4.3 Chromatographic separation of Rhodiola 5%**

A sample of *Rhodiola rosea* extract (6g) was subjected to a first chromatographic purification by MPLC-DAD on a Cartridge C18 60Å 50µm - Size 120g – Column Volume (CV) 155 mL. The mobile phase was a mixture of (A) water with a 0.1% formic acid, (B) acetonitrile and (C) methanol with a gradient method as follows: starting conditions: 95%A – 5%B for two CV; from CV<sub>7</sub> to CV<sub>10</sub>: 80%A – 20%B; from CV<sub>20</sub> to CV<sub>25</sub>: 5%A – 95%B; from CV<sub>26</sub> to CV<sub>30</sub>: 5%A – 95%C. The flow rate was 40.0 mL/min. The UV detection wavelength was set at 275 nm. A total of 19 fractions (A–U) were obtained and further purified by HPLC. Fraction F (eluted with a mixture of A: B 95: 5) was first separated by RP-18 HPLC-UV using the following elution gradient: 0-10 min = 90% A -5% B – 5% C isocratic; 15-20 min = 70% A – 25% B – 5% C isocratic (flow rate 3.0 mL/min) affording rhodiocyanoside A (**6**, 5.3 mg, *t<sub>R</sub>* 13.0 min). Then fraction F11 (*R<sub>t</sub>* 19.5 min of fraction F) was further purified by RP-HPLC-UV using an isocratic eluent of 80% A – 20% B, Kinetex 5µm Biphenyl column, flow rate 1.0 mL/min, to yield rhodiocyanoside A (**6**, 29.3 mg, *t<sub>R</sub>* 5.6 min) and lotaustralin (**7**, 2.4 mg, *t<sub>R</sub>* 6.4 min). Fraction H (eluted with a mixture of A:B (90:10) was rechromatographed by RP-18 HPLC-UV using A:B:C (80:15:5, flow rate 3.0 mL/min) to yield rhodioloside D (**8**, 6.5 mg, *t<sub>R</sub>* 5.5 min), salidroside (**4**, 80.4 mg, *t<sub>R</sub>* 6.3 min) and tyrosol (**4a**, 5.8 mg, *t<sub>R</sub>* 10.7 min). Fraction I (eluted with a mixture of A:B 90:10) was separated

### Chapter 3

by RP-18 HPLC-UV using the following elution gradient: 0-25 min = 85% A - 10% B - 5% C isocratic; 30-40 min = 70% A - 25% B - 5% C isocratic (flow rate 3.0 mL/min) affording tyrosol (**4a**, 43.9 mg,  $t_R$  16.1 min), benzyl-O- $\beta$ -D-glucopyranoside (**14**, 13.3 mg,  $t_R$  21.9 min) and epigallocatechin gallate (**16**, 63.5 mg,  $t_R$  29.5 min). Fraction L (eluted with a mixture of A:B 80:20) was rechromatographed by HPLC-RI using an isocratic eluent of 80% A - 15% B - 5% C, a Kinetex biphenyl column and a flow rate of 1.0 mL/min, to yield rosiridin (**9**, 50.8 mg,  $t_R$  10.0 min), rosarin (**1**, 72.4 mg,  $t_R$  14.8 min) and rosavin (**2**, 72.4 mg,  $t_R$  15.2 min). Fraction N (eluted with a mixture of A:B 80:20) was rechromatographed on RP-18 HPLC-UV using an isocratic eluent of 70% A - 25% B - 5% C, flow rate 3.0 mL/min, to obtain rosin (**3**, 29.7 mg,  $t_R$  10.2 min). Fraction Q (eluted with a mixture of A:B 70:30) was separated by RP-18 HPLC-UV using the following elution gradient: 0-20 min = 70% A - 25% B - 5% C isocratic; 25-30 min = 50% A - 45% B - 5% C isocratic (flow rate 3.0 mL/min) affording rhodiosin (**18**, 14.3 mg,  $t_R$  13.8 min), rhodionin (**10**, 1.4 mg,  $t_R$  16.7 min), rosiridol (**12**, 11.4 mg,  $t_R$  18.1 min) and kenposide A (**13**, 71.7 mg,  $R_t$  27.4 min). Fraction R (eluted with a mixture of A:B 50:50) was rechromatographed on RP-18 HPLC-UV using the following elution gradient: 0-10 min = 60% A - 35% B - 5% C isocratic; 20-25 min = 50% A - 45% B - 5% C isocratic (flow rate 3.0 mL/min) to yield cinnamic alcohol (**15**, 2.7 mg,  $t_R$  13.5 min). Fraction S (eluted with a mixture of A:B 45:55) was rechromatographed by RP-18 HPLC-UV using the following elution gradient: 0-7 min = 60% A - 35% B - 5% C isocratic; 22-25 min = 55% A - 40% B - 5% C isocratic; 28-35 min = 50% A - 45% B - 5% C isocratic (flow rate 3.0 mL/min) to yield tricrin (**11**, 7.0 mg,  $R_t$

## *Phytochemical profile of an industrial Rhodiola rosea extract*

14.8 min), rhodiolinin (**17**, 1.6 mg,  $R_t$  25.2 min) and rhodiosidin (**5**, 1.6 mg,  $R_t$  29.5 min).

*Rhodiosidin (5)*. Brown amorphous solid.  $[\alpha]_D = + 24.6$  (c 0.1, CH<sub>3</sub>OH); <sup>1</sup>H NMR (CD<sub>3</sub>OD, 700 MHz) and <sup>13</sup>C NMR (CD<sub>3</sub>OD, 175 MHz): Table 3.2; HR-ESIMS found  $m/z$  485.2125 [M + Na]<sup>+</sup>; C<sub>25</sub>H<sub>34</sub>O<sub>8</sub>Na requires  $m/z$  485.2151.

### **2.4.4 Cell-free 5-LO assay**

Human recombinant 5-LO was expressed in E. coli BL21 (DE3) transformed with the plasmid pT3-5-LO and purified by affinity chromatography on an ATP-agarose column.<sup>42</sup> The isolated enzyme was immediately used for activity studies as described before.<sup>43</sup> Briefly, 0.5 µg of 5-LO in PBS (pH 7.4) containing EDTA (1 mM) were pre-incubated with vehicle (0.1% MeOH) or test compounds for 10 min before adding 2 mM CaCl<sub>2</sub> and 20 µM AA to start 5-LO product formation. After 10 min at 37°C, an equal volume of ice-cold methanol was added to stop the reaction. 5-LO products were extracted after adding 500 µL acidified PBS and 200 ng of internal standard (PGB1) by solid-phase extraction (SPE). Eluates were analyzed for 5-LO products (trans-LTB<sub>4</sub>, epi-trans-LTB<sub>4</sub>, and 5-HETE) by RP-HPLC using a C-18 Radial-PAK column (Waters, Eschborn, Germany).

### **2.4.5 Cell-based 5-LO assay in PMNL**

Human PMNL were freshly isolated from peripheral blood obtained at the Institute for Transfusion Medicine of the University

### *Chapter 3*

Hospital Jena (Germany) as described before.<sup>44</sup> In brief, leukocyte concentrates were obtained from venous blood by centrifugation and PMNL were isolated by dextran sedimentation and centrifugation on Histopaque-1077 cushions (SigmaAldrich, Deisenhofen, Germany). Erythrocytes were lysed under hypotonic conditions, while PMNL were recovered by centrifugation and re-suspended in PBS (pH 7.4) containing 1 mg/ml glucose and 1 mM CaCl<sub>2</sub>. For evaluation of 5-LO product formation,  $5 \times 10^7$  PMNL were incubated with test compounds for 10 min at 37 °C before stimulation with 2.5  $\mu$ M Ca<sup>2+</sup> ionophore A23187 (Cayman, Ann Arbor, USA) for 10 min. The incubation was stopped with an equal volume of ice-cold methanol and analyzed for 5-LO products (LTB<sub>4</sub>, trans-LTB<sub>4</sub>, epi-trans-LTB<sub>4</sub>, and 5-HETE) as described above.

## References

---

1. Panossian, A., Wikman, G., & Sarris, J. (2010). Rosenroot (*Rhodiola rosea*): traditional use, chemical composition, pharmacology and clinical efficacy. *Phytomedicine*, 17(7), 481-493.
2. Ghiorghita, G., Maftai, D. I., & Maftai, D. E. (2015). *Rhodiola rosea* L.-a valuable plant for traditional and for the modern medicine. *Analele Stiintifice ale Universitatii "Al. I. Cuza" din Iasi*, 61(1/2), 5.
3. Saratikov, A.S., Krasnov, E.A. (2004). *Rhodiola rosea* (Golden root) Fourth edition, Revised and Enlarged. Tomsk State University Publishing House, pp. 22–41.
4. Small, E., & Catling, P. M. (2000). *Les cultures médicinales canadiennes*. NRC Research Press.
5. Brinckmann, J. A., Cunningham, A. B., & Harter, D. E. (2021). Running out of time to smell the roseroots: Reviewing threats and trade in wild *Rhodiola rosea* L. *Journal of Ethnopharmacology*, 269, 113710.
6. Galambosi, B., Galambosi, Z., Hethelyi, E., Szöke, E., Volodin, V., Poletaeva, I., & Iljina, I. (2010). Importance and quality of roseroot (*Rhodiola rosea* L.) growing in the European North. *Zeitschrift für Arznei- & Gewürzpflanzen*, 15(4), 160-169.
7. Bykov, V. A., Zapesochnaya, G. G., & Kurkin, V. A. (1999). Traditional and biotechnological aspects of obtaining

### Chapter 3

- medicinal preparations from *Rhodiola rosea* L. (A review). *Pharmaceutical Chemistry Journal*, 33(1), 29-40.
8. Limanaqi, F., Biagioni, F., Busceti, C. L., Polzella, M., Fabrizi, C., & Fornai, F. (2020). Potential antidepressant effects of *Scutellaria baicalensis*, *Hericium erinaceus* and *Rhodiola rosea*. *Antioxidants*, 9(3), 234.
  9. Edwards, D., Heufelder, A., & Zimmermann, A. (2012). Therapeutic Effects and Safety of *Rhodiola rosea* Extract WS® 1375 in Subjects with Life-stress Symptoms—Results of an Open-label Study. *Phytotherapy Research*, 26(8), 1220-1225.
  10. Chiang, H. M., Chen, H. C., Wu, C. S., Wu, P. Y., & Wen, K. C. (2015). *Rhodiola* plants: Chemistry and biological activity. *Journal of Food and Drug Analysis*, 23(3), 359-369.
  11. Polumackanycz, M., Konieczynski, P., Orhan, I. E., Abaci, N., & Viapiana, A. (2022). Chemical Composition, Antioxidant and Anti-Enzymatic Activity of Golden Root (*Rhodiola rosea* L.) Commercial Samples. *Antioxidants*, 11(5), 919.
  12. Alperth, F., Turek, I., Weiss, S., Vogt, D., & Bucar, F. (2019). Qualitative and quantitative analysis of different *Rhodiola rosea* rhizome extracts by UHPLC-DAD-ESI-MSn. *Scientia Pharmaceutica*, 87(2), 8.
  13. Elameen, A., Kosman, V. M., Thomsen, M., Pozharitskaya, O. N., & Shikov, A. N. (2020). Variability of major

- phenyletanes and phenylpropanoids in 16-year-old *Rhodiola rosea* L. clones in Norway. *Molecules*, 25(15), 3463.
14. György, Z. (2006). *Glycoside production by in vitro Rhodiola rosea cultures*. University of Oulu.
15. Hahlbrock, K., & Scheel, D. (1989). Physiology and molecular biology of phenylpropanoid metabolism. *Annual review of plant physiology and plant molecular biology*, 40(1), 347-369.
16. Gross, G. G., & Zenk, M. H. (1974). Isolation and properties of hydroxycinnamate: CoA ligase from lignifying tissue of *Forstia*. *European Journal of Biochemistry*, 42(2), 453-459.
17. Kumar, A., & Ellis, B. E. (2003). 4-Coumarate: CoA ligase gene family in *Rubus idaeus*: cDNA structures, evolution, and expression. *Plant molecular biology*, 51(3), 327-340.
18. Wiedenfeld, H., Dumaa, M., Malinowski, M., Furmanowa, M., & Narantuya, S. (2007). Phytochemical and analytical studies of extracts from *Rhodiola rosea* and *Rhodiola quadrifida*. *Die Pharmazie-An International Journal of Pharmaceutical Sciences*, 62(4), 308-311.
19. Li, Y., Pham, V., Bui, M., Song, L., Wu, C., Walia, A., ... & Zi, X. (2017). *Rhodiola rosea* L.: an herb with anti-stress, anti-aging, and immunostimulating properties for cancer chemoprevention. *Current pharmacology reports*, 3(6), 384-395.

### Chapter 3

20. Yoshikawa, M., Shimada, H., Shimoda, H., MURAKAMI, N., YAMAHARA, J., & MATSUDA, H. (1996). Bioactive constituents of Chinese natural medicines. II. *Rhodiola* radix.(1). Chemical structures and Antiallergic activity of Rhodiocyanosides A and B from the underground Part of *Rhodiola quadrifida* (PALL.) FISCH. et MEY. (Crassulaceae). *Chemical and pharmaceutical bulletin*, 44(11), 2086-2091.
21. Akgul, Y., Ferreira, D., Abourashed, E. A., & Khan, I. A. (2004). from *Rhodiola rosea* roots. *Fitoterapi Lotaustralina*, 75(6), 612-614.
22. Simon, K., Jones, P. G., & Lindel, T. (2011). Total Syntheses of Rhodiolosides A and D and of Sachalinols A–C.
23. Jeong, H. J., Ryu, Y. B., Park, S. J., Kim, J. H., Kwon, H. J., Kim, J. H., ... & Lee, W. S. (2009). Neuraminidase inhibitory activities of flavonols isolated from *Rhodiola rosea* roots and their in vitro anti-influenza viral activities. *Bioorganic & medicinal chemistry*, 17(19), 6816-6823.
24. Gautschi, J. T., Tenney, K., Compton, J., & Crews, P. (2007). Chemical investigations of a deep water marine-derived fungus: Simple amino acid derivatives from an *Arthrinium* sp. *Natural Product Communications*, 2(5), 1934578X0700200506.
25. Yoshikawa, M., Nakamura, S., Li, X., & Matsuda, H. (2008). Reinvestigation of absolute stereostructure of (-)-rosiridol: structures of monoterpene glycosides, rosiridin, rosiridosides

- A, B, and C, from *Rhodiola sachalinensis*. *Chemical and Pharmaceutical Bulletin*, 56(5), 695-700.
26. Tolonen, A., Pakonen, M., Hohtola, A., & Jalonen, J. (2003). Phenylpropanoid glycosides from *Rhodiola rosea*. *Chemical and Pharmaceutical Bulletin*, 51(4), 467-470.
27. Machado, L. L., Monte, F. J. Q., Maria da Conceição, F., de Mattos, M. C., Lemos, T. L., Gotor-Fernández, V., ... & Gotor, V. (2008). Bioreduction of aromatic aldehydes and ketones by fruits' barks of *Passiflora edulis*. *Journal of Molecular Catalysis B: Enzymatic*, 54(3-4), 130-133.
28. Yang, L. L., Chang, C. C., Chen, L. G., & Wang, C. C. (2003). Antitumor principle constituents of *Myrica rubra* var. *acuminata*. *Journal of agricultural and food chemistry*, 51(10), 2974-2979.
29. Kurkin, V. A., & Zapesochnaya, G. G. (1986). The chemical-composition and pharmacological properties of rhodiola plants. *Khimiko-Farmatsevticheskii Zhurnal*, 20(10), 1231-1244.
30. Kurkin, V. A., Zapesochnaya, G. G., Shchavlinskii, A. N., Nukhi-movskii, E. L., & Vandyshev, V. V. (1985). Method of analysis of identity and quality of *Rhodiola rosea* rhizome. *Khim. Farm. Zh*, 19, 185-190.
31. Wu, S., Zu, Y., & Wu, M. (2003). High yield production of salidroside in the suspension culture of *Rhodiola sachalinensis*. *Journal of Biotechnology*, 106(1), 33-43.

### Chapter 3

32. Yousef, G. G., Grace, M. H., Cheng, D. M., Belolipov, I. V., Raskin, I., & Lila, M. A. (2006). Comparative phytochemical characterization of three *Rhodiola* species. *Phytochemistry*, 67(21), 2380-2391.
33. Van Diermen, D., Marston, A., Bravo, J., Reist, M., Carrupt, P. A., & Hostettmann, K. (2009). Monoamine oxidase inhibition by *Rhodiola rosea* L. roots. *Journal of ethnopharmacology*, 122(2), 397-401.
34. Son, M. J., Jin, C., Lee, Y. S., Lee, J. Y., & Kim, H. J. (2015). Characterization of caffeoylglucoside derivatives and hypouricemic activity of the ethyl acetate fraction from *Aster glehni*. *Bulletin of the Korean chemical society*, 36(2), 503-512.
35. Anilakumar, P. K., Khanum, F., & Bawa, A. S. (2006). Phytoconstituents and antioxidant potency of *Rhodiola rosea*—a versatile adaptogen. *Journal of Food Biochemistry*, 30(2), 203-214.
36. Spasov, A. A., Wikman, G. K., Mandrikov, V. B., Mironova, I. A., & Neumoin, V. V. (2000). A double-blind, placebo-controlled pilot study of the stimulating and adaptogenic effect of *Rhodiola rosea* SHR-5 extract on the fatigue of students caused by stress during an examination period with a repeated low-dose regimen. *Phytomedicine*, 7(2), 85-89.
37. Ming, D. S., Hillhouse, B. J., Guns, E. S., Eberding, A., Xie, S., Vimalanathan, S., & Towers, G. N. (2005). Bioactive compounds from *Rhodiola rosea* (Crassulaceae).

- Phytotherapy Research: An International Journal Devoted to Pharmacological and Toxicological Evaluation of Natural Product Derivatives*, 19(9), 740-743.
38. Bawa, A. S., & Khanum, F. (2009). Anti-inflammatory activity of *Rhodiola rosea* – “a second-generation adaptogen”. *Phytotherapy Research: An International Journal Devoted to Pharmacological and Toxicological Evaluation of Natural Product Derivatives*, 23(8), 1099-1102.
39. Borgonetti, V., Governa, P., Biagi, M., Dalia, P., & Corsi, L. (2020). *Rhodiola rosea* L. modulates inflammatory processes in a CRH-activated BV2 cell model. *Phytomedicine*, 68, 153143.
40. Guan, S., Feng, H., Song, B., Guo, W., Xiong, Y., Huang, G., ... & Deng, X. (2011). Salidroside attenuates LPS-induced pro-inflammatory cytokine responses and improves survival in murine endotoxemia. *International immunopharmacology*, 11(12), 2194-2199.
41. Zeng, Q., Nie, X., Li, L., Liu, H. F., Peng, Y. Y., Zhou, W. T., ... & Chen, X. L. (2022). Salidroside Promotes Sensitization to Doxorubicin in Human Cancer Cells by Affecting the PI3K/Akt/HIF Signal Pathway and Inhibiting the Expression of Tumor-Resistance-Related Proteins. *Journal of Natural Products*, 85(1), 196-204.
42. Fischer, L., Szellas, D., Rådmark, O., Steinhilber, D., & Werz, O. (2003). Phosphorylation-and stimulus-dependent

### Chapter 3

inhibition of cellular 5-lipoxygenase activity by nonredox-type inhibitors. *The FASEB journal*, 17(8), 1-24.

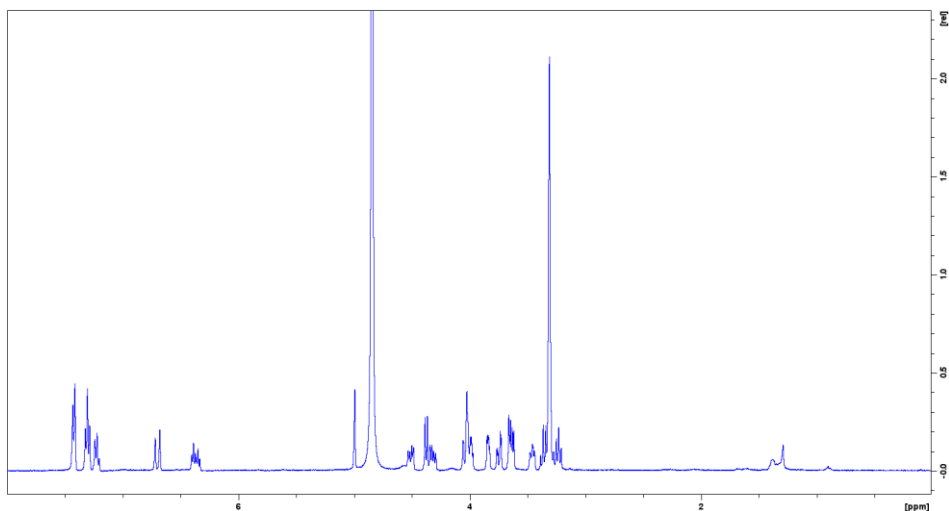
43. Pace, S., Zhang, K., Jordan, P. M., Bilancia, R., Wang, W., Börner, F., ... & Werz, O. (2021). Anti-inflammatory celastrol promotes a switch from leukotriene biosynthesis to formation of specialized pro-resolving lipid mediators. *Pharmacological Research*, 167, 105556.
44. Kretzer, C., Jordan, P. M., Meyer, K. P., Hoff, D., Werner, M., Hofstetter, R. K., ... & Werz, O. (2022). Natural chalcones elicit formation of specialized pro-resolving mediators and related 15-lipoxygenase products in human macrophages. *Biochemical Pharmacology*, 195, 114825.

## Appendix B: Spectral data of chapter 3

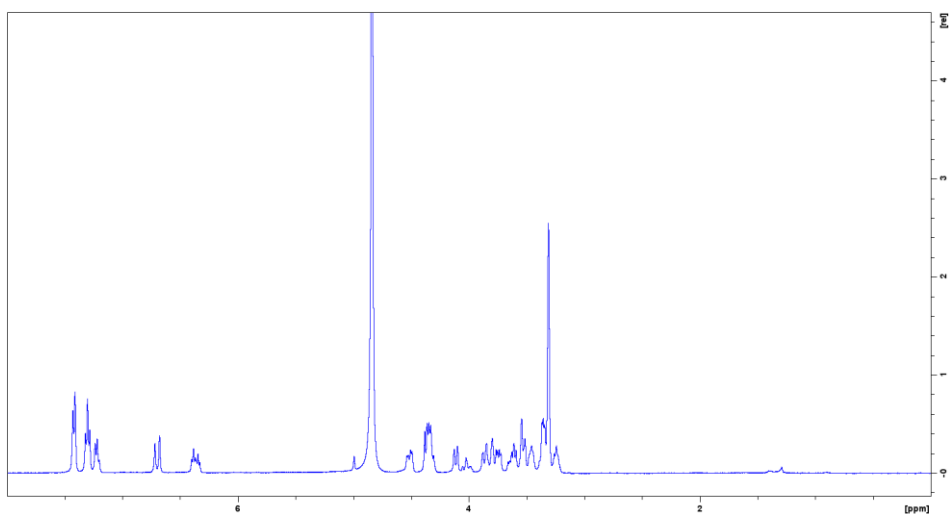
---

Herein are reported the NMR spectra of the main constituent of *Rhodiola* 5%.

$^1\text{H}$  NMR spectrum (400 MHz) of rosarin (**1**) in  $\text{CD}_3\text{OD}$

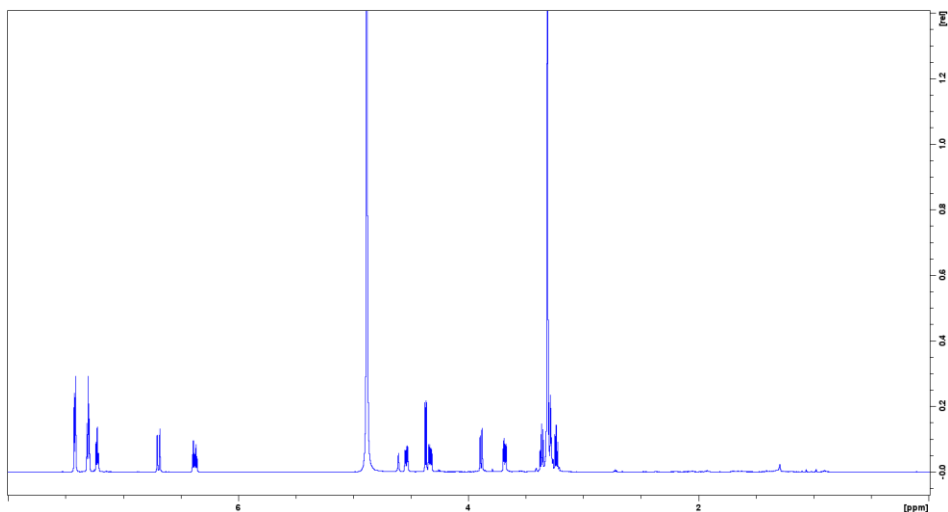


$^1\text{H}$  NMR spectrum (400 MHz) of rosavin (**2**) in  $\text{CD}_3\text{OD}$

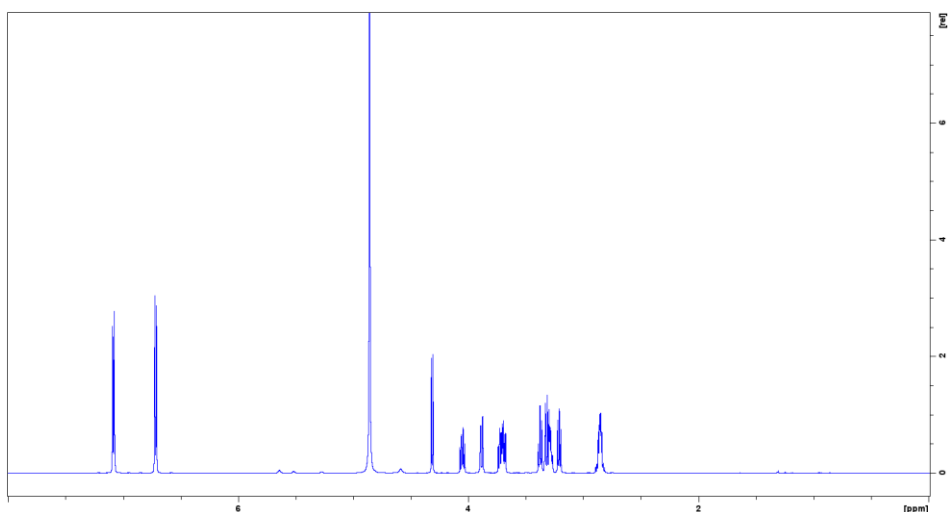


## Appendix B

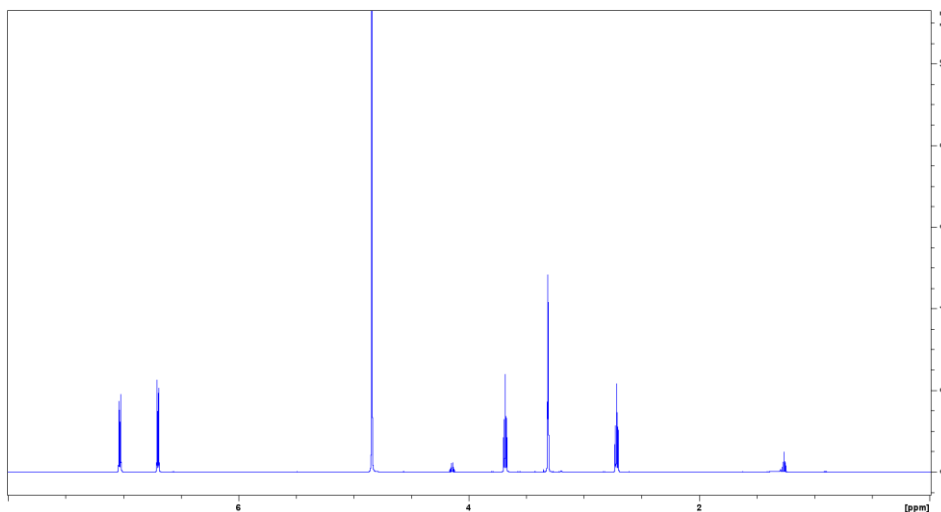
$^1\text{H}$  NMR spectrum (400 MHz) of rosin (**3**) in  $\text{CD}_3\text{OD}$



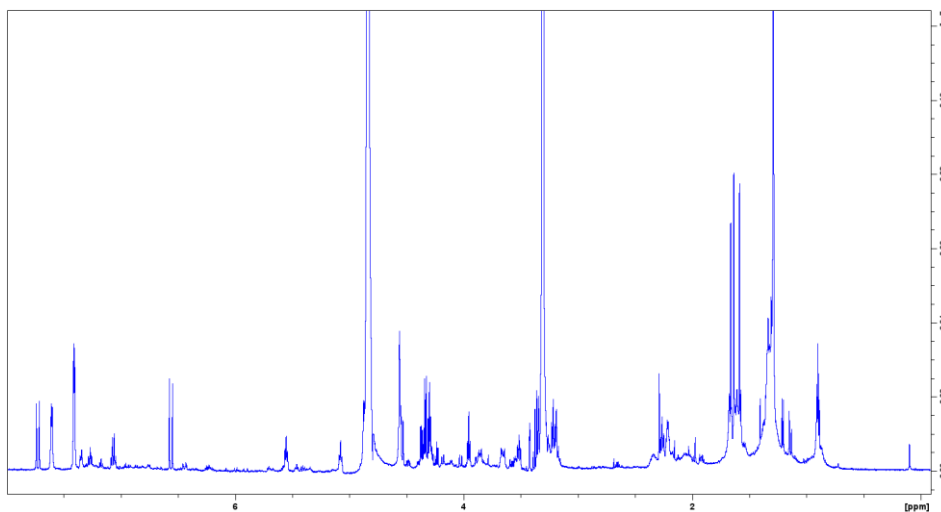
$^1\text{H}$  NMR spectrum (600 MHz) of salidroside (**4**) in  $\text{CD}_3\text{OD}$



$^1\text{H}$  NMR spectrum (600 MHz) of tyrosol (**4a**) in  $\text{CD}_3\text{OD}$

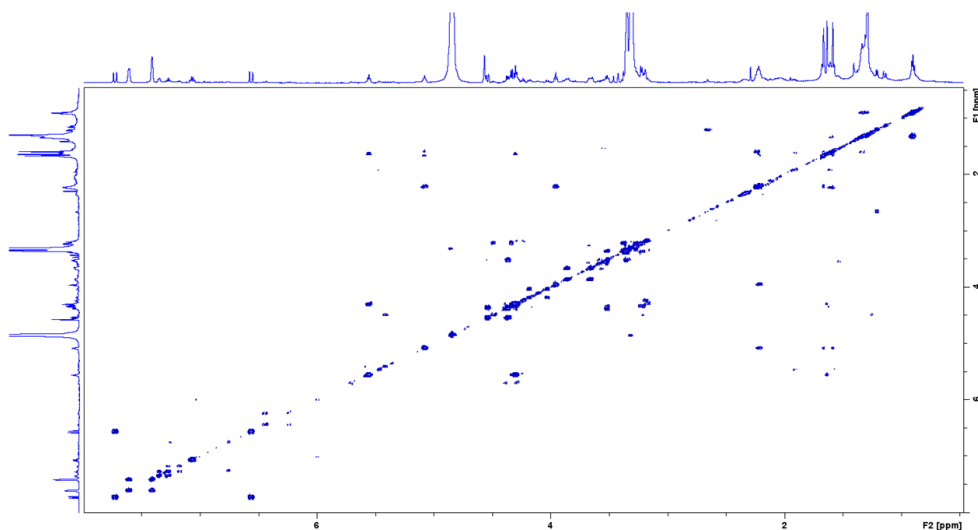


$^1\text{H}$  NMR spectrum (700 MHz) of rhodiosidin (**5**) in  $\text{CD}_3\text{OD}$

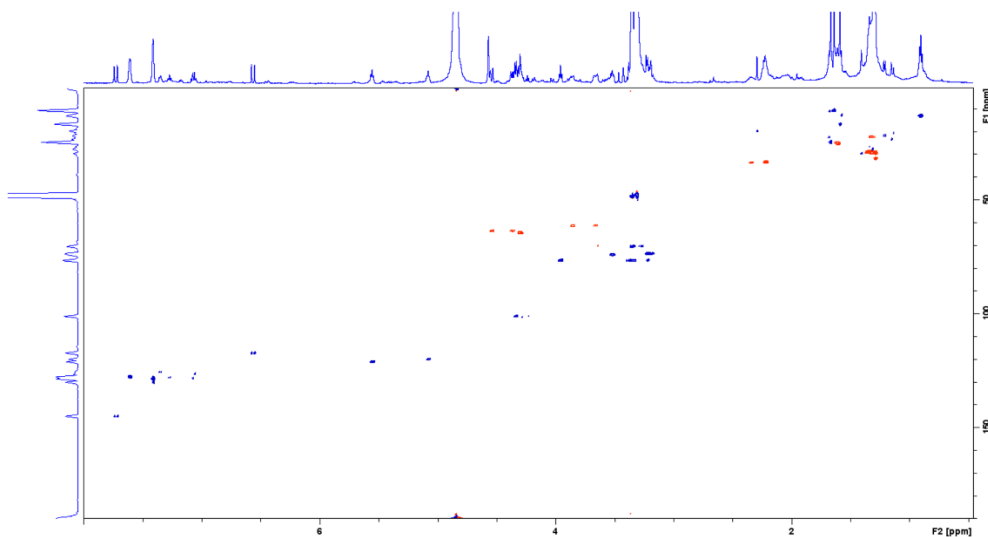


## Appendix B

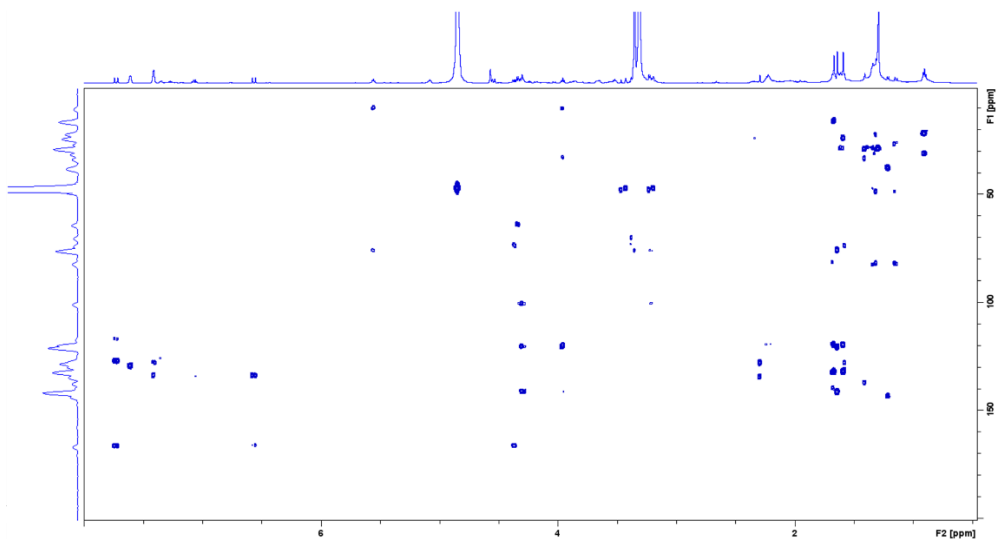
COSY NMR spectrum (700 MHz) of rhodiosidin (**5**) in CD<sub>3</sub>OD



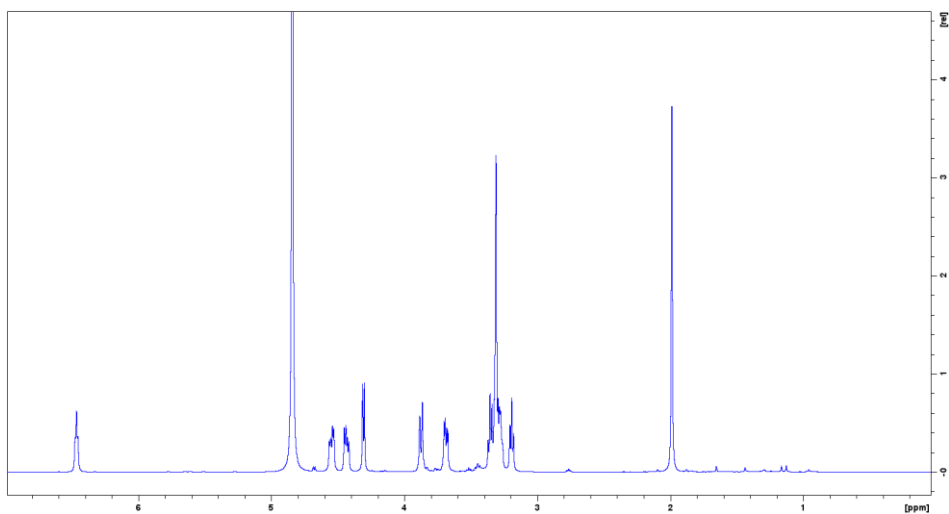
HSQC NMR spectrum (700 MHz) of rhodiosidin (**5**) in CD<sub>3</sub>OD



HMBC NMR spectrum (700 MHz) of rhodiosidin (**5**) in CD<sub>3</sub>OD

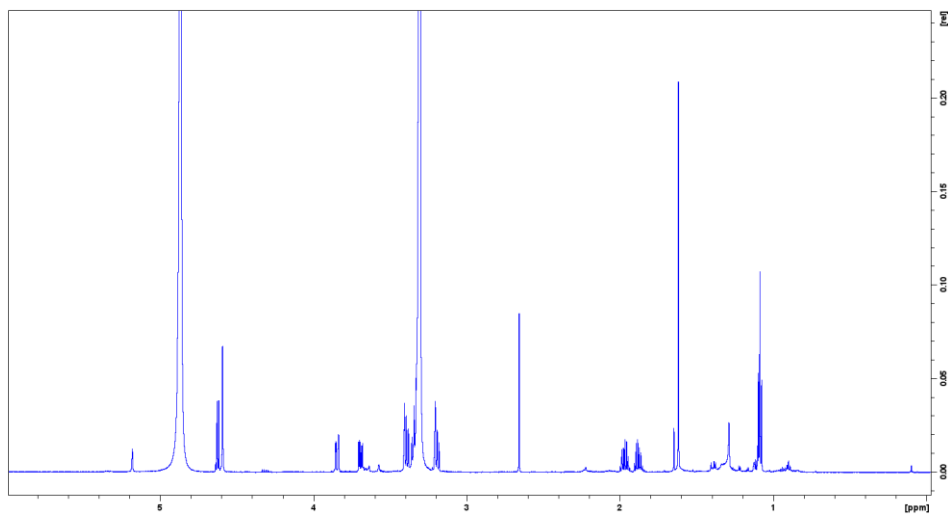


<sup>1</sup>H NMR spectrum (600 MHz) of rhodiocyanoside A (**6**) in CD<sub>3</sub>OD

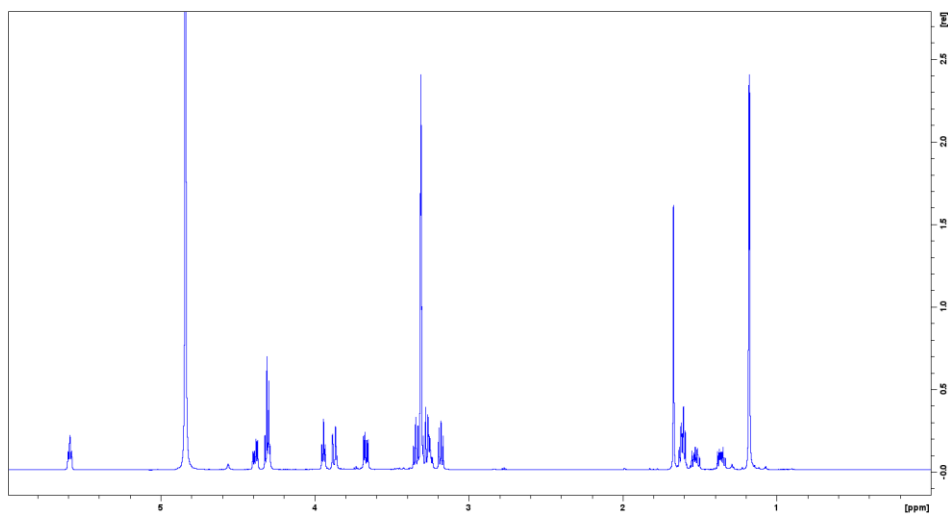


## Appendix B

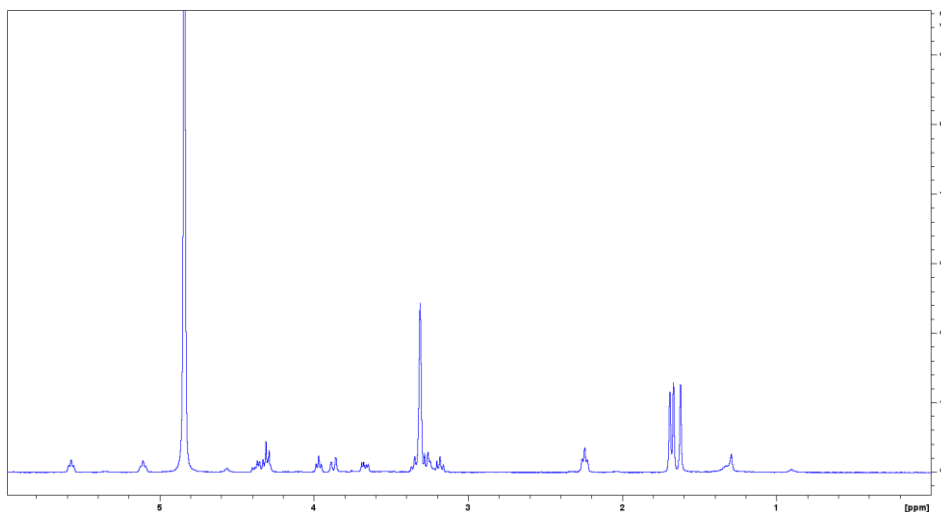
$^1\text{H}$  NMR spectrum (600 MHz) of lotaustralin (**7**) in  $\text{CD}_3\text{OD}$



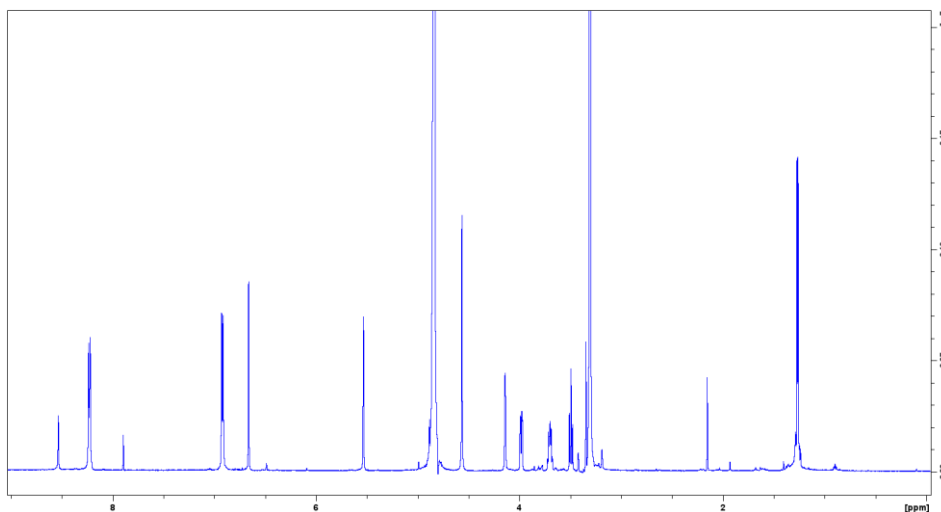
$^1\text{H}$  NMR spectrum (400 MHz) of rhodioloside D (**8**) in  $\text{CD}_3\text{OD}$



$^1\text{H}$  NMR spectrum (600 MHz) of rosiridin (**9**) in  $\text{CD}_3\text{OD}$

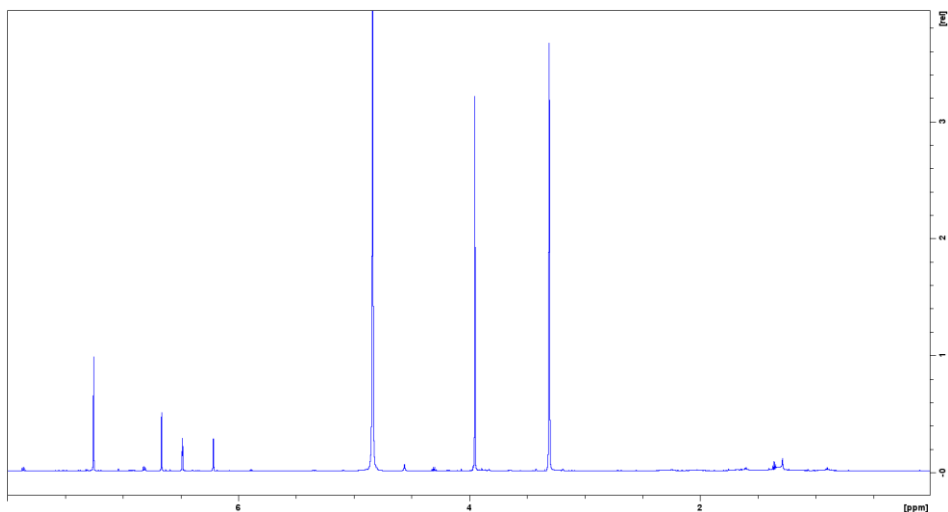


$^1\text{H}$  NMR spectrum (600 MHz) of rhodionin (**10**) in  $\text{CD}_3\text{OD}$

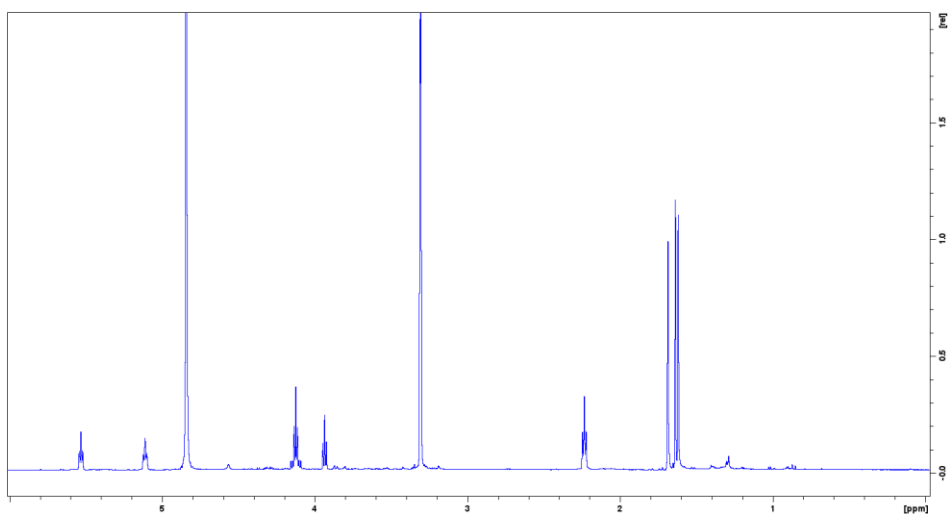


## Appendix B

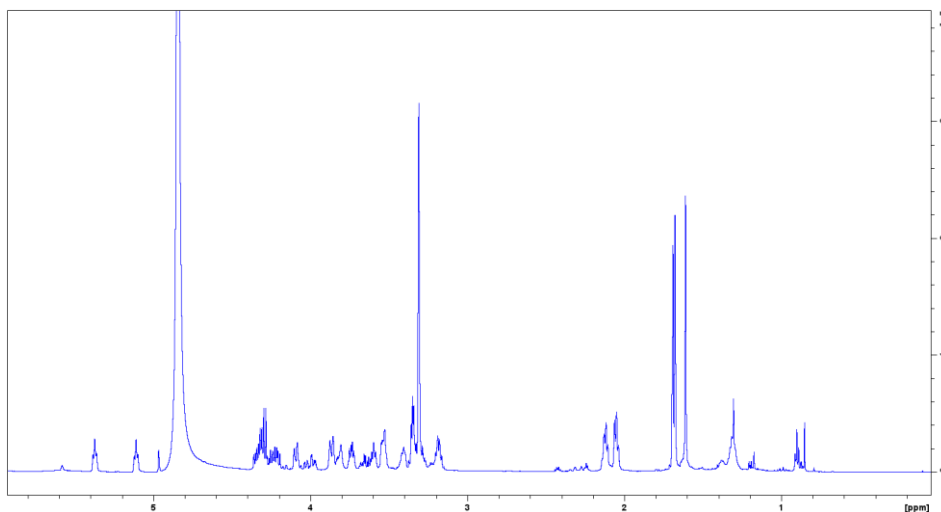
$^1\text{H}$  NMR spectrum (600 MHz) of triclin (**11**) in  $\text{CD}_3\text{OD}$



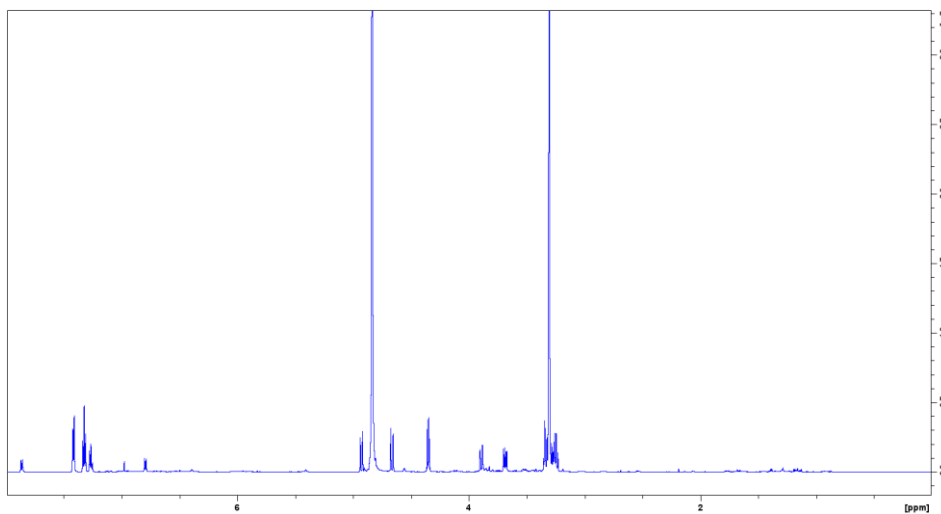
$^1\text{H}$  NMR spectrum (600 MHz) of rhosiridol (**12**) in  $\text{CD}_3\text{OD}$



$^1\text{H}$  NMR spectrum (600 MHz) of kenposide A (**12**) in  $\text{CD}_3\text{OD}$

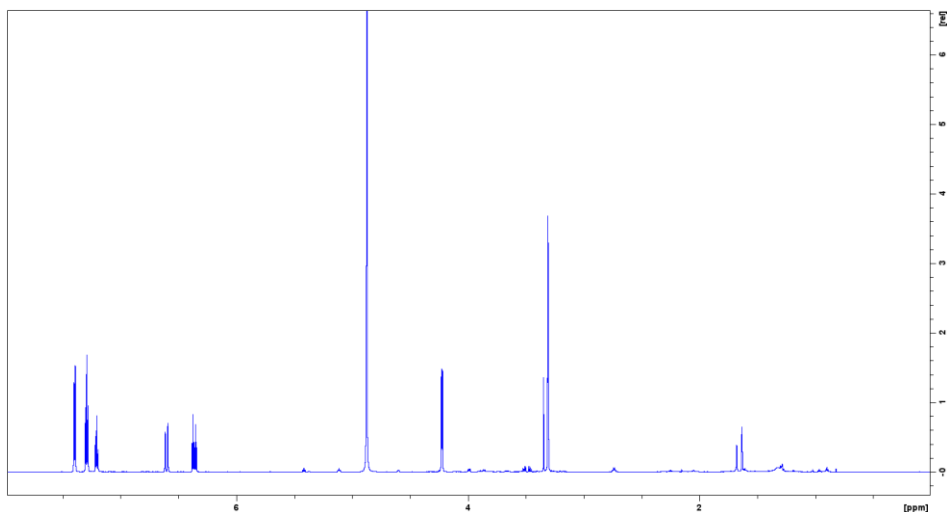


$^1\text{H}$  NMR spectrum (400 MHz) of benzyl-O-b-D-glucopyranoside (**14**) in  $\text{CD}_3\text{OD}$

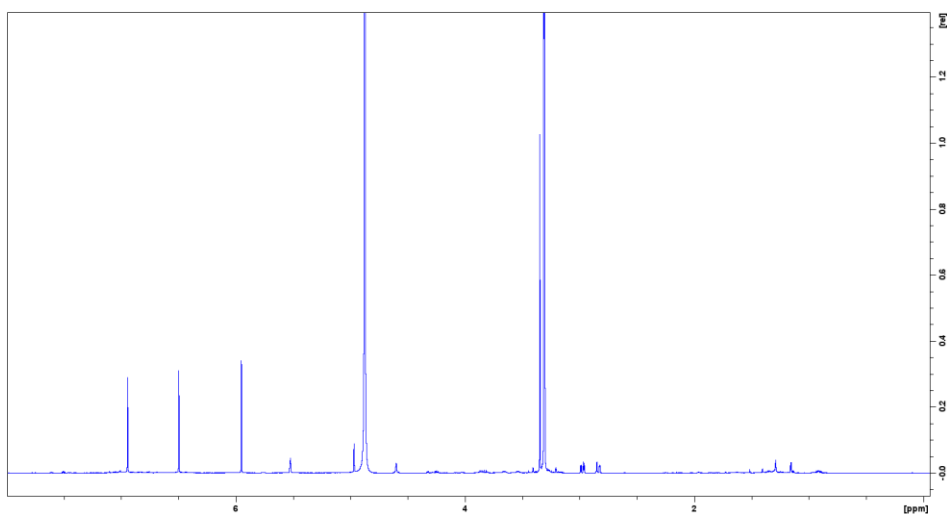


## Appendix B

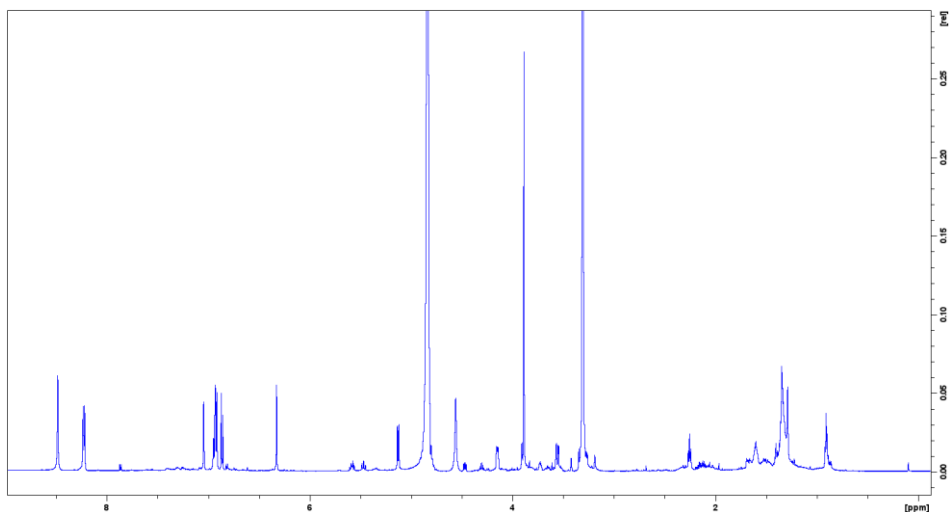
$^1\text{H}$  NMR spectrum (700 MHz) of cinnamic alcohol (**15**) in  $\text{CD}_3\text{OD}$



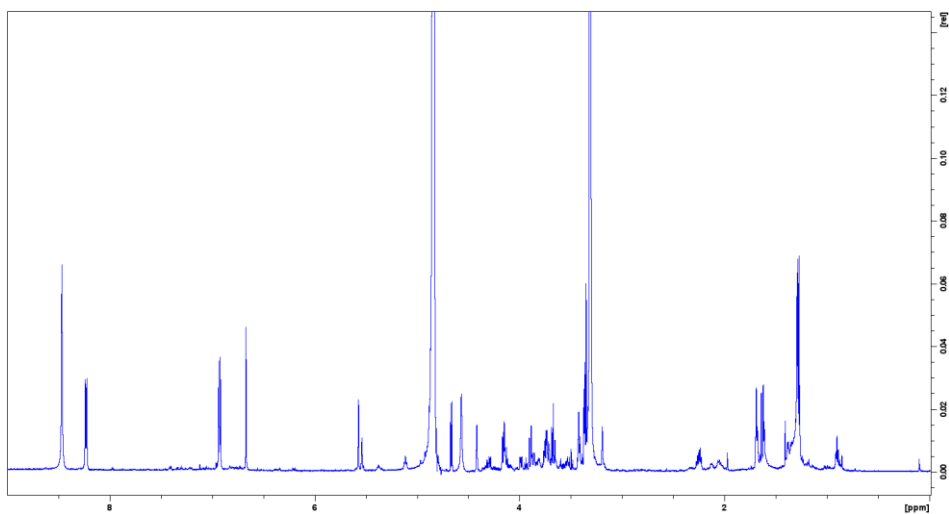
$^1\text{H}$  NMR spectrum (400 MHz) of epigallocatechin gallate (**16**) in  $\text{CD}_3\text{OD}$



$^1\text{H}$  NMR spectrum (600 MHz) of rhodiolinin (**17**) in  $\text{CD}_3\text{OD}$



$^1\text{H}$  NMR spectrum (600 MHz) of rhodiosin (**18**) in  $\text{CD}_3\text{OD}$





## **Chapter 4: Towards an annurcoic acid-rich apple standardized extract**

---

*Some experimental details and some data related to the objective of this chapter could not be disclosed due to the confidentiality reasons.*

### **4.1 Introduction**

The apple tree (*Malus domestica* Borkh., Rosaceae) originated in Central Asia, from its ancestor *Malus sieversii*. Apples have been grown for millennia in Asia and Europe and then brought to North America by European colonists.<sup>1</sup>

All *Malus* species (**Figure 4.1**) are trees or shrubs 3 to 12 m tall, with a twiggy, broad crown, deciduous or semi-evergreen, and usually unarmed. Leaves are alternate, simple, petiolate, and merely toothed, margin serrate or lobed. Blossoms are produced in spring simultaneously with the budding of the leaves and are produced on spurs and some long shoots. Pomes do not contain stone-cells or they are present in a few species. Fruits have 1 or 2 seeds in each cell, with a cartilaginous endocarp (core). Seeds are brown or black, and cotyledons plano-convex.

Apple trees have a long generation time, 3–8 years, producing up to 700 (5–10 per fruit) seeds. They are hermaphrodites, with both sexes within the same flower, usually self-incompatible, with moderate to severe inbreeding depression. Several researchers suggest that seeds are mostly dispersed by large herbivores which additionally provided seed beds for germination.<sup>2</sup>



**Figure 4.1.** *Malus domestica*.

To date, the apple is one of the most economically and culturally significant nutrient-rich fruits,<sup>3</sup> and it is irreplaceable in human nutrition as they increase immunity and have a positive effect on stress resistance.<sup>4</sup> The whole fruit is edible, except for seeds, and many other products are produced from them, such as ciders and juices, jams, compotes, wine, tea, or dry apples.

Apples contain several bioactive substances, mainly concentrated in the pulp and peel, and they include polyphenols, polysaccharides, sterols, and pentacyclic triterpenes. These compounds jointly contribute to most of the positive effects on human health, such as antioxidants, anti-cancer, and anti-inflammatory.<sup>5,6</sup> Organic acids have also been found in apples, with significantly different presence in pulp and skin.

Phenolic compounds are contained in a large number and high levels mainly in the peel, although it contains, compared to pulp, a higher concentration of substances from environmental pollution.<sup>7</sup>

Moreover, their profile is frequently and significantly different in apple varieties and in different parts of the apple.<sup>8</sup> Apple polyphenols include phenolic acids, dihydrochalcones, and flavonoids (**Figure 4.2**). Phenolic compounds have antioxidant activity, and for this reason, apple functional foods consumption develops anti-inflammatory and antioxidant activities in the organism and helps in fighting against cancer and cardiovascular diseases.<sup>9</sup>

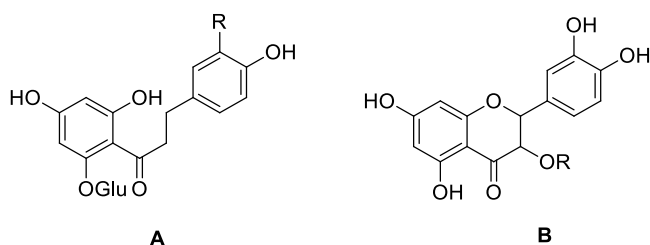


**Figure 4.2.** Dihydrochalcones (**A**) and flavonoids (**B**) derivatives.  
*R = H or sugar.*

Triterpenes, especially pentacyclic ones, represent a significant part of the bioactive substances of apples,<sup>10,11</sup> and, among them, the main constituents are ursolic acid and oleanolic acid (**Figure 4.3**).<sup>12</sup> Pentacyclic triterpenes are considered potential drugs for tumour diseases<sup>13,14</sup> with remarkable effects in the prevention and therapy of malignancies.<sup>15</sup> Nowadays, the treatment of cancer does not only consist of the elimination of tumour cells, inducing apoptosis. In fact, the new therapeutic strategies also modify the microenvironment of the tumour to prevent angiogenesis, modulation of the immune response, or chronic inflammation, which is often associated with cancer.<sup>16</sup>

## Chapter 4

Moreover, pentacyclic triterpenes exhibit other interesting effects on humans, such as anabolic effects on skeletal muscles, which play a vital role in the process of ageing.<sup>17</sup>

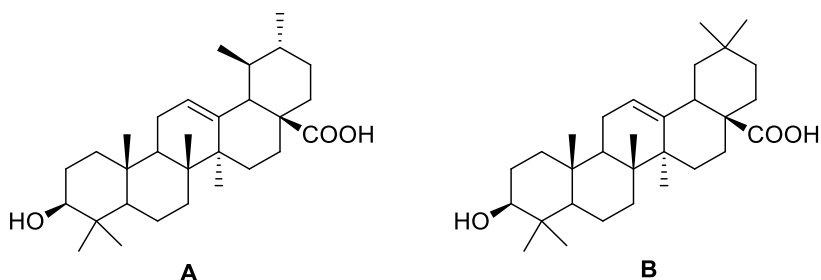


**Figure 4.3.** Chemical structures of ursolic acid (A) and oleanolic acid (B).

Very recently, a new ursane triterpene was identified as 1 $\alpha$ , 19 $\alpha$ -dihydroxy-3-oxours-12-en-28-oic acid, and named annurcoic acid, by D'Abrosca et al.<sup>18</sup> (**Figure 4.4**). Pharmacological studies on annurcoic acid showed its antioxidant activity, identifying it as a significant component in the pool of apple antioxidant triterpenes.<sup>18,19</sup>

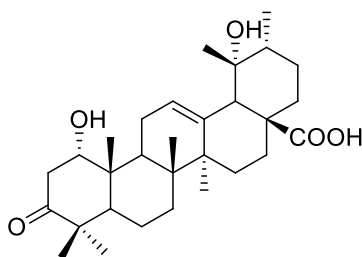


**Figure 4.4.** Chemical structure of annurcoic acid.

As a result, bioactive constituents have multiple medicinal and healthcare functions, and they can be used in the development of healthy foods and beverages with unique functions. For example, apple juice can be developed as a functional food that assists in suppressing tumors, lowering blood pressure, anti-ageing, and losing weight, or nutritional products for improving growth, memory, and sleep quality.<sup>20</sup>

#### **4.2 *Malus domestica* for the nutraceutical extract**

As already discussed in the first chapter (*Natural products and human health 1.1*), besides the investigation of the phytochemical profile of a natural extract, the implementation of scientific protocols characterized by low variability and high recovery yields of the metabolites of interest represents the first crucial step to obtain high-quality standardized products. To this regard, this chapter deals with the preliminary studies and the relevant scientific activities for the development and optimization of a procedure to obtain a nutraceutical product from apple. Particularly, the main aim was to obtain a standardized extract enriched in annurcoic acid. In parallel, a further procedure was set up to obtain the annurcoic acid to be used as a reference standard.

The Botanical Raw material (BRM) has been selected based on the analytical quality of apple waste biomasses from the industrial apple juice manufacture. It should be noted that this choice has a strong innovative connotation since it is committed to promoting cultural change towards the different aspects of sustainable development, starting from the awareness that the environmental dimension of

sustainability is important, as well as the economy and sociality. For this purpose, the project follows the bio-circular-green economic model which aims at taking the most of every resource. Accordingly, nothing must be wasted and abandoned as waste but reintroduced into the production cycle for a new use.

### **4.2.1 Starting material and phytochemical profile of apple waste biomass**

The starting material was selected at Indena laboratories (Milan, Italy) through preliminary analyses conducted on two types of apple waste biomasses: pressing residues (including pulp, skin, core, and seeds) and peeling residues both from different apple varieties (RED delicious, Golden delicious, and a material resulting from the processing of a “mix” of varieties).

The analytical characterization of the biomasses showed the presence of triterpenic acids, while no flavonoids were detected. In addition, further tests were carried out to evaluate the stability of the detected metabolites under different experimental conditions. As a result, the variety of the apple, the physical state (fresh or dry) and different drying temperatures (45°, 60°, 75°) did not affect the total triterpenic acids content. Moreover, the samples consisting of "peeling residues" were characterized by a lower amount of annurcoic acid (w/w %) compared to the "whole" pressing residues (which include the core). **Table 4.1** reports the analytical results of the biomass with a higher amount of annurcoic acid (**1**), so this biomass was chosen for the R&D activity. A total of six pentacyclic triterpenes were detected, in deep: i) five triterpene structures were

## *Towards an annurcoic acid-rich apple standardized extract*

identified (vs analytical standards) and quantified, and ii) one pentacyclic triterpene structures was identified as unknown compound with a molecular weight (MW) of 472.

**Table 4.1.** *Indena HPLC analytical results of apple waste biomass.*

annurcoic acid	MW 472	maslinic acid	corosolic acid	oleanolic acid	ursolic acid
0.21	0.10	0.02	0.02	0.15	0.72

Subsequently, a representative raw extract coming from the selected biomass was sent to the Department of Pharmacy of the University of Naples and analyzed. The raw extract was subjected to a purification by chromatographic technique (RP-18) using as mobile phases acidified water, acetonitrile and methanol. The subsequent HPLC chromatographic purifications of the fractions of interest afforded pure compounds from the sample. The NMR experiments and HRMS direct infusion of the purified compounds allowed the characterization of the phytochemical profile of the sample. As a result, the presence of the six pentacyclic terpene acids was confirmed: annurcoic acid (AA, **1**),<sup>18</sup> tormentic acid (TA, **2**),<sup>21</sup> maslinic acid (MA, **3**),<sup>21</sup> corosolic acid (CA, **4**),<sup>22</sup> oleanolic acid (OA, **5**)<sup>23</sup> and ursolic acid (UA, **6**),<sup>24</sup> meanwhile the unknown compound MW 472, was identified as pomolic acid (PA, **7**) (**Figure 4.5**).<sup>25</sup> In addition, during the purification steps, a structural congener of the annurcoic acid was detected and identified as 3-epi-2-oxopomolic acid (OPA, **8**) (**Figure 4.5**).<sup>26</sup>

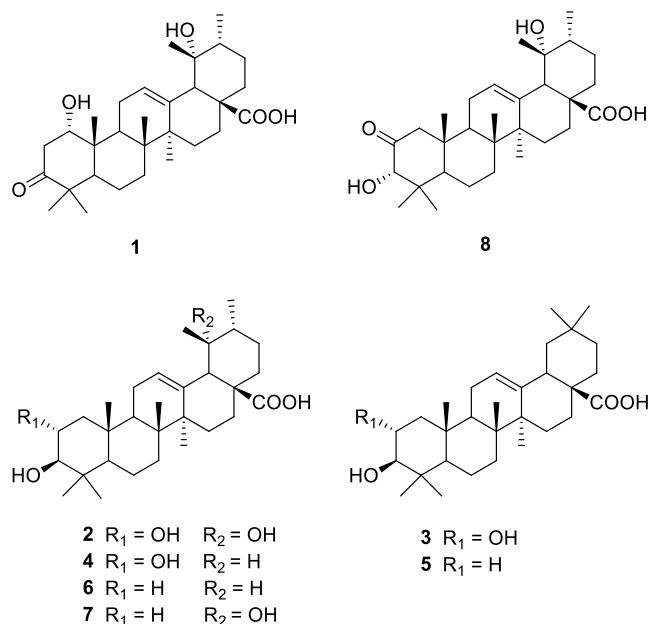


**Figure 4.5.** Chemical structures of the triterpenic acids (1-7) isolated and characterized from the raw extract.

#### 4.2.2 Anurcoic acid-enriched standardized extract: method development

Apple waste biomass was subjected to a laboratory scale feasibility test aimed at the development and optimization of a process to obtain a nutraceutical extract enriched in anurcoic acid (1). The first step of this research was to subject BRM to a laboratory scale feasibility test, keeping into consideration the E.U. directives 2009/32/EC and 2016/1855 of the European Parliament and the Council. With a view to protecting human health, these Directives lay down provisions concerning extraction solvents used or intended for use in the production and processing of raw materials, foodstuffs, food components, or food ingredients. The

preliminary studies were carried out at Indena SpA laboratories (Milan, Italy), and were focused on the preparation of a standardized extract characterized by a high content of triterpene acids, and especially of annurcoic acid (**1**) as the main component. Preliminary analytical results showed that the total content of triterpenic components was around 1.2% w/w and, among them, annurcoic acid (**1**) content was only 0.2% w/w (**Table 4.1**). Therefore, an effective method of extraction and purification had to be developed.

An evaluation of the best extraction conditions was carried out, considering both the polarity of the pentacyclic triterpenes and the limits of the directives above mentioned (2009/32/EC and 2016/1855), in terms of solvents to be used. Consequently, extractions with several mixtures of hydroalcoholic solutions at different temperatures and an extraction with ethyl acetate were studied. This preliminary investigation showed a correlation between the molar yield and process yield and the extraction conditions, namely the ethanolic grade and temperature. Particularly, the higher was the ethanolic grade of the extraction solution and higher was the operative temperatures, the higher was the molar yield (quantitative both for the sum of triterpenes, and for **1**) and the lower was the extraction selectivity (yield of 57.1% w/w) (1236/45/A, **Table 4.2**). On the other hand, the use of ethyl acetate as extraction solvent allowed to obtain a quantitatively molar yield of triterpene acids (approx. 90.6% w/w as sum of triterpenes, and 93% w/w of **1**) with a high selectivity (process yield of 3.9% w/w) (1270/11/A, **Table 4.2**).

## Chapter 4

**Table 4.2.** HPLC analysis of the apple extract in high-grade ethanol (1236/45/A) and the apple extract in ethyl acetate (1270/11/A).

Batch	TA 2	OPA 8	AA 1	PA 7	MA 3	CA 4	OA 5	UA 6	Sum of acids
1236/45/A	0.06	-	<b>0.33</b>	0.13	0.06	0.04	0.19	0.67	<b>1.48</b>
1270/11/A	1.2	0.1	<b>5.0</b>	1.7	1.1	0.6	3.4	15.0	<b>28.2</b>

Although the ethyl acetate extraction improves the selectivity, the optimization of the extraction process was carried out with ethanol, for its lower flammability, considering that the process will be developed at industrial scale. For this purpose, the extraction conditions were tested according two different extraction procedures: i) static extraction by percolation until exhaustion (**Table 4.3**); ii) extraction in reactor under stirring (1236/45/A, **Table 4.2**). Based on the analytical (HPLC) and molar yield results of the extraction technique both conditions allowed to obtain a raw extract with a comparable molar yield and process yield. However, due to the higher productivity the static extraction system was chosen for the preparation of the extract. Hence, the biomass was extracted at high temperature (three hours as time of contact) and the leachates were cooled to room temperature, obtaining a precipitation of a solid which was filtered by a Büchner funnel. **Table 4.3** shows the extraction trend of three percolations (1270/35/A, 1270/35/B, 1270/35/C), which allowed a quantitative molar yield in annurcoic acid (**1**).

**Table 4.3.** HPLC analysis of 1<sup>st</sup> (1270/35/A), 2<sup>nd</sup> (1270/35/B), and 3<sup>rd</sup> (1270/35/C) percolations.

Batch	TA 2	OPA 8	AA 1	PA 7	MA 3	CA 4	OA 5	UA 6	Sum of acids
1270/35/A	0.03	-	<b>0.52</b>	0.12	0.05	0.08	0.21	0.83	<b>1.84</b>
1270/35/B	0.02	-	<b>0.32</b>	0.10	0.03	0.06	0.17	0.91	<b>1.61</b>
1270/35/C	0.03	-	<b>0.18</b>	0.05	0.02	0.03	0.07	0.48	<b>0.86</b>

The amount % of the triterpene compounds (as sum of triterpenes) was still far from the target as shown in **Table 4.3**, so a further purification step (by adsorption resin) was investigated to enrich the terpenoid fraction with a focus on a quantitative molar yield. For this purpose, three matrices were studied: a divinylbenzene (DVB, 1270/35/F), an aromatic polymer (1270/35/G), and an aliphatic polymer (1270/35/H) (**Table 4.4**).

**Table 4.4.** HPLC analysis of purification step with divinylbenzene (1270/35/F), aromatic polymer (1270/35/G), and aliphatic polymer (1270/35/H) resins.

Batch	TA 2	OPA 8	AA 1	PA 7	MA 3	CA 4	OA 5	UA 6	Sum of acids
1270/35/F	1.2	-	<b>19.2</b>	4.9	2.9	3.5	9.5	35.6	<b>76.8</b>
1270/35/G	0.5	-	<b>14.5</b>	3.1	1.9	2.6	7.8	30.8	<b>61.2</b>
1270/35/H	1.2	-	<b>4.1</b>	1.2	0.5	0.8	2.1	8.0	<b>17.9</b>

The analytical results in **Table 4.4** showed that the divinylbenzene resin provided the better results among the investigated matrix in term of sum of acids (amount 76.8% w/w) and annurcoic acid (**1**,

## Chapter 4

amount 19.2% w/w). The process allowed to purify the sample by the polar phase (eluted loading solution) and the lipophilic phase retained by the resin (discarded with high-grade ethanolic elution) and concentrate annurcoic acid (**1**) in the elution phase with a medium-grade ethanolic solution. As regards, the aromatic polymer resin had shown a lower capacity, while the aliphatic polymer had a lower selectivity. Once the resin was identified, a study of the column parameters was conducted, in particular: a resin saturation, column loading, washing and elution and linear velocity study. **Figure 4.6** shows a general HPLC-UV chromatogram of the purified extract after resin DVB purification step (1270/40/D).

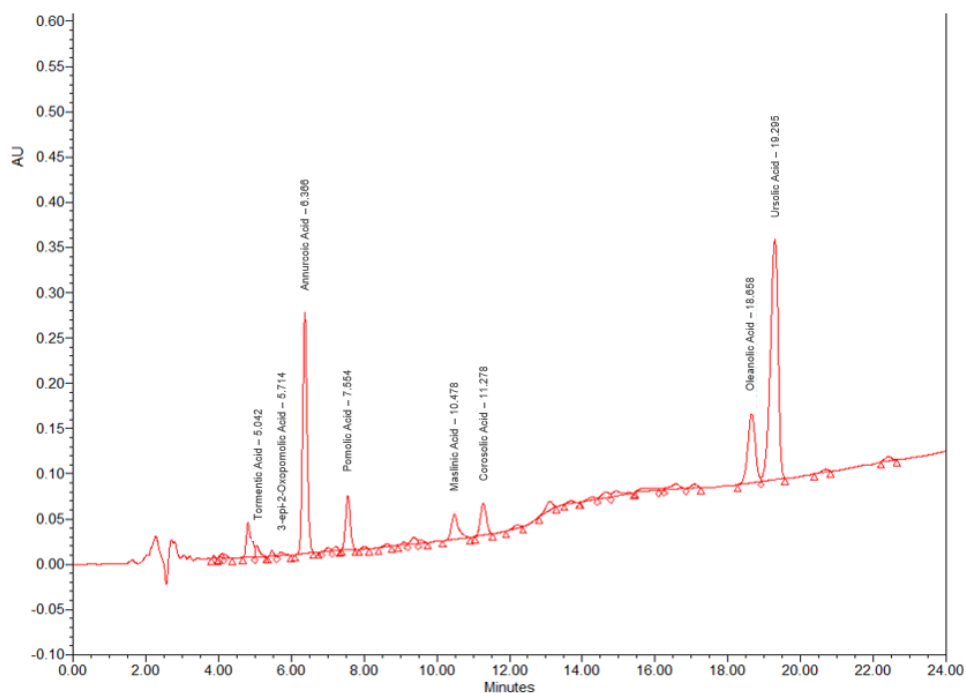


**Figure 4.6.** HPLC-UV chromatogram of the extract after purification with DVB resin (1270/40/D).

## *Towards an annurcoic acid-rich apple standardized extract*

After that the extraction and purification conditions were set up, a further activity was carried out in order to increase the purity of annurcoic acid (**1**) in the extract. The analysis of the column purified extract showed ursolic acid (**6**) as the mainly component of the sample, so crystallization was performed. In fact, as reported by Fan et al.<sup>27</sup> a purified form of ursolic acid (**6**) can be obtained from apple waste pomace using the crystallization technique, consisting of a first crystallization in ethanol 96% v/v, following by a second crystallization step.<sup>27</sup> Therefore, starting from the conditions described by these Authors, optimization studies were carried out on parameters such as: i) temperature and ii) concentration of the purified extract, in order to obtain a product low in ursolic acid (**6**), which can be used in other industrial processes, and enrich the annurcoic acid extract (**1**) (**Table 4.5**). As described in the literature the current optimized crystallization step allowed to remove ursolic acid (**6**, crystal form) with a molar yield of approximately 70% w/w while annurcoic acid (**1**) was enriched in the mother liquor phase as described in **Table 4.5**.

**Table 4.5.** *HPLC analysis of mother liquors after enrichment step by crystallization of ursolic acid (**6**).*

Batch	TA 2	OPA 8	AA 1	PA 7	MA 3	CA 4	OA 5	UA 6	Sum of acids
1270/40/F	1.7	0.4	<b>25.8</b>	5.5	4.3	2.3	12.4	19.3	<b>71.7</b>

The current developed process involved in just one crystallization step allowing to obtain **1** in a concentration of 25.8% w/w with a molar yield of 78% w/w with respect to the starting biomass. The

## Chapter 4

process showed a significant reduction of ursolic and (6) corosolic acid (4) as shown in **Table 4.5** (1270/40/F). **Figure 4.7** shows the chromatogram of a mother liquors after crystallization of ursolic acid (6) (1270/40/F).

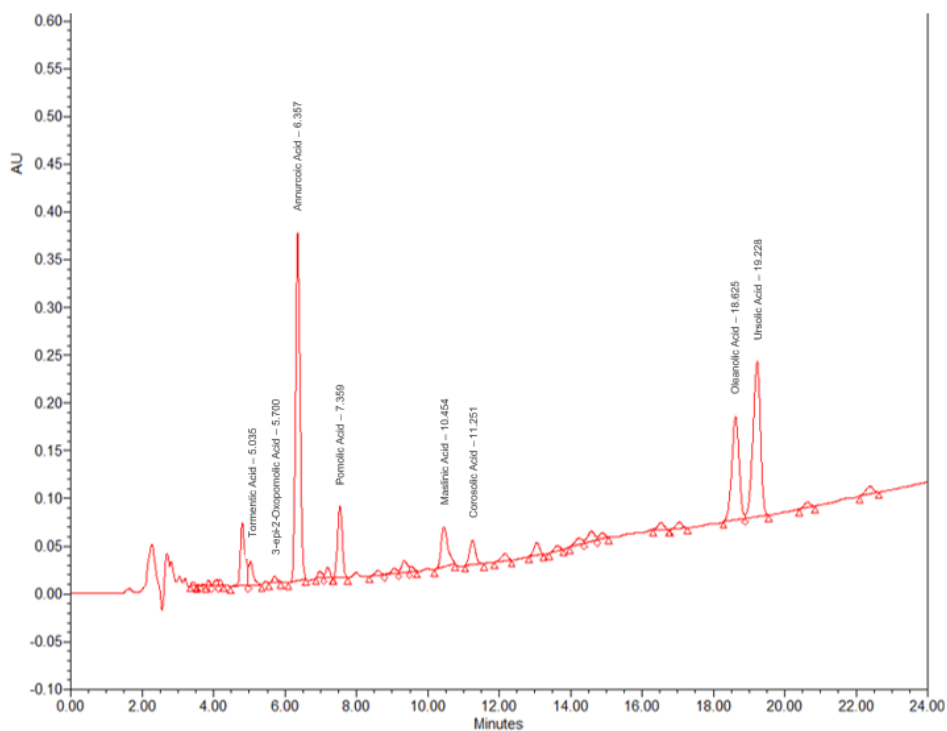


**Figure 4.7.** HPLC-UV chromatogram of the extract after enrichment step by crystallization of ursolic acid (6) in ethanol.

In summary, the process can be summarized as in the following flowchart (**Figure 4.8**).

## *Towards an annurcoic acid-rich apple standardized extract*

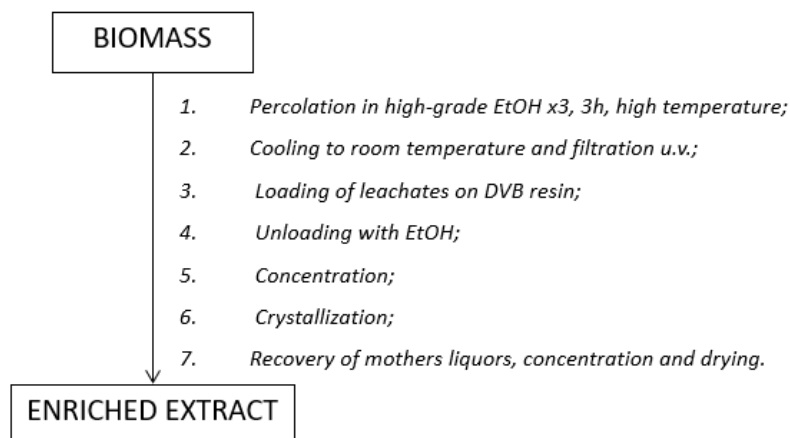


**Figure 4.8.** *Process steps from the biomass to the final enriched product.*

### **4.2.3 Development of annurcoic acid reference standard**

The R&D activities at Indena SpA (Milan, Italy) included the development of a further process consisting of the isolation in high purity of annurcoic acid. The aim of this work was to obtain pure annurcoic acid (**1**) to be used as a reference standard in chemical analyses, replacing ursolic acid (**6**).

For this purpose, several attempts have been carried out including crystallization, solubility, and chromatography in normal (SiO<sub>2</sub>) and reversed- (RP-18) phases studies. The outcomes of the lab. scale tests showed that the reversed-phase chromatographic technique led to a product with annurcoic acid (**1**) concentration of approximately 86% w/w. This result was in line with the expectation based on the chromatographic theory in which the difference in polarity between triterpene compounds led to a different interaction with stationary and mobile phases, therefore a different retention

time. As the matter of the fact, the terpenic acids are structural analogues that differ in the methyl substitution pattern on C-19 and C-20, of the ursane (**1**, **2**, **4**, **6**, **7**) and the oleanane series (**3**, **5**), and hydroxylation in different positions of the rings. Tormentic acid (**2**) is the most polar compound among the triterpenes series of the apple, as it is a derivative of hydroxylated ursane in both C-2, C-3 and C-19. Annurcoic acid (**1**) differs from other apple triterpenes in the oxidation to ketone of the hydroxyl group at C-3 (e.g).

For this purpose, the extract enriched in annurcoic acid (1270/40/F, **Table 4.5**) obtained from the process described in the previous paragraph (4.2.2) was subjected to a reversed-phase purification step. The conditions studied included: i) the stationary phase, ii) the mobile phase, and iii) the flow rate.

The promising results were obtained using as a *stationary phase* Zeobeads®100 (20-30 µm), C18 reversed-phase, fifty parts vs the sample amount. The *mobile phase* was chosen as a ternary mixture consisting of 25% water, 10% acetonitrile, and 65% methanol. The choice of the ternary mixture allowed to increase in the separation efficiency, since it has been shown that a small proportion of acetonitrile added in a methanol-water system remarkably improves the separation efficiency of a complex mixture of natural products in the RP phase.<sup>28</sup> Regarding the *flow rate*, the choice to work under pressure with nitrogen flow was further undertaken to increase the separation efficiency.

**Table 4.6** reports the analytical results of the annurcoic acid (**1**) fraction (1270/40/L). In fact, the main compound was annurcoic acid (85% w/w), although two minor compounds were still present (**Figure 4.9**). Tormentic acid (**2**) represented 3.4% w/w of the

## Towards an annurcoic acid-rich apple standardized extract

sample while 3-epi-2-oxopomolic acid (isomer of annurcoic acid, **8**) constituted 2.6% w/w. The method to separate the minor analogues is *under evaluation*.

**Table 4.6.** HPLC-UV assay of column fraction of annurcoic acid (**1**) (1270/40/L).

Batch	TA 2	OPA 8	AA 1	PA 7	MA 3	CA 4	OA 5	UA 6
1270/40/L	3.4	2.6	85.1	-	-	-	-	-

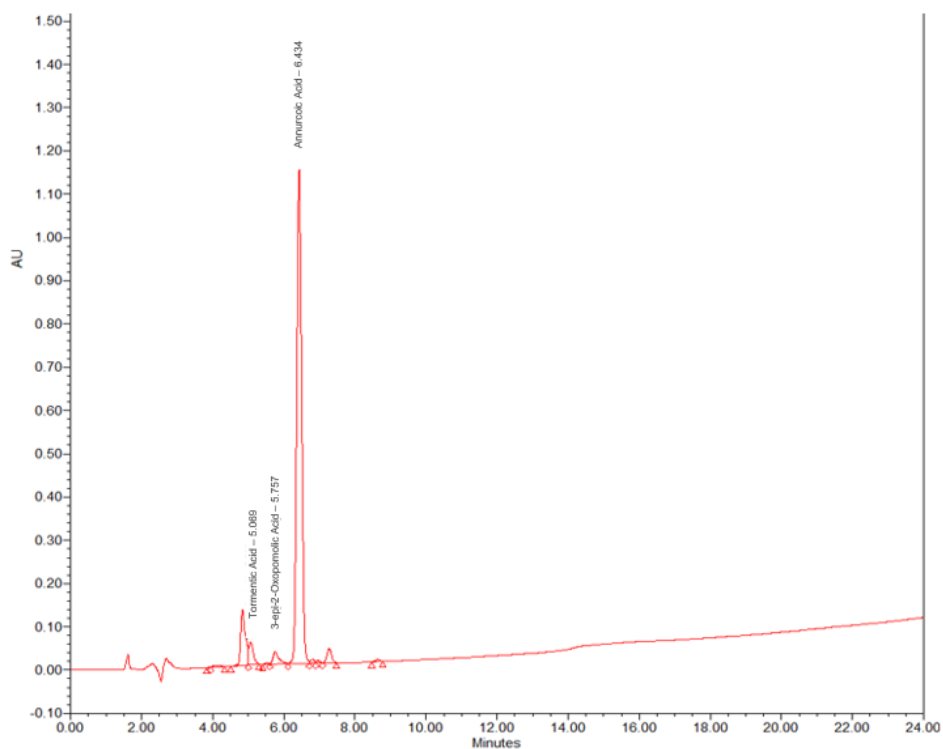


**Figure 4.9.** HPLC-UV chromatogram of a column fraction of annurcoic acid (**1**) (1270/40/L).

### 4.3 Conclusions

The apple is one of the most economically and culturally significant nutrient-rich fruits in human nutrition for its many bioactive constituents. They mainly include polyphenols and pentacyclic triterpene acids which have multiple medicinal and health promotion functions, and they can be exploited in the development of healthy foods and beverages with unique functions. To this end, apple waste biomass derived from the pressing residues (including pulp, skin, core, and seeds) of an industrial apple juice processing was chosen for the development and optimization of a procedure to obtain a nutraceutical product from apples.

Apple waste biomass was first subjected to phytochemical investigation carried out firstly at Indena SpA laboratories (Milan, Italy) and completed at the Department of Pharmacy of the University of Naples. This analysis allowed the identification of seven triterpene acids including: annurcoic acid (AA, **1**), tormentic acid (TA, **2**), maslinic acid (MA, **3**), corosolic acid (CA, **4**), oleanolic acid (OA, **5**), ursolic acid (UA, **6**), and pomolic acid (PA, **7**). In addition, a structural congener of the annurcoic acid emerged during the purification phases, identified as 3-epi-2-oxopomolic acid (OPA, **8**).

The laboratory scale feasibility carried out at Indena SpA led to the development of a seven-step procedure (**Figure 4.8**) obtaining a standardized extract characterized by a high content of triterpene acids, of which annurcoic acid (**1**) was the main component (25% w/w) (1270/40/F, **Table 4.5**, **Figure 4.7**). In parallel, a further process was developed to obtain annurcoic acid as a reference

standard to be implemented in chemical analyses, in view to replace ursolic acid (**6**). The R&D activities led to a process able to obtain annurcoic acid (**1**) (85% w/w) batch, the main impurities were identified as tormentic acid (**2**) (3.4% w/w) and 3-epi-2-oxopomolic acid (2.6% w/w) (1270/40/L, **Table 4.6**, **Figure 4.9**).

## **4.4 Experimental section**

### **4.4.1 Starting material**

The starting material was provided by "Società Agricola Melavi", Società Cooperativa", Ponte in Valtellina (Sondrio), a Cooperative dedicated to apple production. Two main types of apple waste biomasses were processed: pressing residues (including pulp, skin, core, and seeds), and peeling residues, both derived from the industrial apple juice processing. The processed apple varieties were: RED delicious, Golden delicious and a "Mix" of varieties. These samples were dried in Indena SpA laboratories under different conditions (45 °C for 4-5 days, 60 °C for 3 days, 75 °C for 3 days) and then analyzed by HPLC.

### **4.4.2 HPLC-UV analysis**

All HPLC analyzes were performed using a HPLC system consisting of Quaternary pump, Thermostated column compartment, Thermostated autosampler and UV/VIS Detector, connected to Empower software (Empower System Enterprise Client/Server), or equivalent. The reference standard used for the quantitative analyzes was ursolic acid (Chemieliva pharmaceutical).

## Chapter 4

Chromatographic separation was achieved using a Synergi Polar RP (250 x 4.6 mm, 80Å, 4 µm) (Phenomenex). The UV detection was at 210 nm, the column temperature was 15°C, while the autosampler temperature was 20°C. Gradient elution was performed using a mobile phase consisting of water (solvent A) and acetonitrile (solvent B), both containing 0.01% v/v formic acid, and methanol (solvent C). The injection volume was 10 µL and the flow rate was 1 mL/min. The chromatographic procedure lasted 32 min, and the gradient design was as follows: at 0 min a mixture of 60% B and 20% C, from 0 to 23 min B, reached 78%, hold at 78% B from 23 to 26, then from 26 to 28 min B reached 60% and hold at 60% B from 28 to 32 min.

### **4.4.3 Chromatographic separations of raw extract from apple waste biomass**

A sample of the raw extract (500 mg) was first subjected to chromatographic purification by gravity column chromatography using 20 g ( $V_0 = 20\text{ml}$ ) C18 0.7 – 0.9  $\text{cm}^3/\text{g}$  pore volume (97727-U Sigma- Aldrick). The mobile phase was a mixture of (A) water with a 0.1% formic acid, (B) acetonitrile and (C) methanol with a gradient method as follows: starting conditions: 20%A – 30%B – 50% C for ten CV; 10%A – 40%B – 50% C for 20 CV; 100% C for 10 CV. The flow rate was 3.0 mL/min. A total of 7 fractions (1–7) were obtained and further purified by HPLC. Fraction 2 (eluted with a mixture of A: B:C 20:30:50) was separated by RP-18 HPLC-UV using an isocratic mixture of solvent of 20% A - 30% B – 50% C, Kinetex C18 250 x 4.6 mm column, flow rate 1.0 mL/min, affording in the pure form of

### *Towards an annurcoic acid-rich apple standardized extract*

tormentic acid (**2**, 0.8 mg,  $t_R$  5.2 min) and annurcoic acid (**1**, 2.7 mg,  $t_R$  6.1 min). Fraction 3 (eluted with a mixture of A:B:C 15:35:50) was purified by RP-HPLC-UV using an isocratic eluent of 25% A – 30% B – 45% C, Kinetex C18 250 x 4.6 mm column, flow rate 1.0 mL/min, to yield 3-epi-2-oxopomolic acid (**8**, 0.6 mg,  $t_R$  7.9 min) and annurcoic acid (**1**, 4.2 mg,  $t_R$  8.2 min). Fraction 4 (eluted with a mixture of A: B:C 10:40:50) was purified by RP-HPLC-UV using an isocratic eluent of 20% A – 30% B – 50% C, Kinetex C18 250 x 4.6 mm column, flow rate 1.0 mL/min, to yield tormentic acid (**2**, 3.2 mg,  $t_R$  4.9 min), annurcoic acid (**1**, 12.5 mg,  $t_R$  5.1 min), pomolic acid (**7**, 12.8 mg,  $t_R$  7.3 min), maslinic acid (**3**, 3.2 mg,  $t_R$  11.9 min), corosolic acid (**4**, 4.6 mg,  $t_R$  12.8 min), and oleanolic acid (**5**, 3.1 mg,  $t_R$  17.2 min). Fraction 7 (eluted with a mixture of A: B:C 10:40:50) was chromatographed on RP-HPLC-UV using an isocratic eluent of 15% A – 35% B – 50% C, Kinetex C18 250 x 4.6 mm column, flow rate 1.0 mL/min, to yield tormentic acid (**2**, 0.9 mg,  $t_R$  2.8 min), annurcoic acid (**1**, 1.6 mg,  $t_R$  4.0 min), pomolic acid (**7**, 1.1 mg,  $t_R$  5.2 min), maslinic acid (**3**, 1.0 mg,  $t_R$  8.0 min), corosolic acid (**4**, 1.0 mg,  $t_R$  8.3 min), and ursolic acid (**6**, 14.9 mg,  $t_R$  18.0 min).

## References

---

1. Brite, E. B. (2021). The origins of the apple in central Asia. *Journal of World Prehistory*, 34(2), 159-193.
2. Ignatov, A., & Bodishevskaya, A. (2011). Malus. In *Wild crop relatives: genomic and breeding resources* (pp. 45-64). Springer, Berlin, Heidelberg.
3. Spengler, R. N. (2019). Origins of the apple: the role of megafaunal mutualism in the domestication of Malus and rosaceous trees. *Frontiers in plant science*, 10, 617.
4. Boyer, J., & Liu, R. H. (2004). Apple phytochemicals and their health benefits. *Nutrition journal*, 3(1), 1-15.
5. Can, Z., Dincer, B., Sahin, H., Baltas, N., Yildiz, O., & Kolayli, S. (2014). Polyphenol oxidase activity and antioxidant properties of Yomra apple (*Malus communis* L.) from Turkey. *Journal of enzyme inhibition and medicinal chemistry*, 29(6), 829-835.
6. Pádua, T. A., de Abreu, B. S., Costa, T. E., Nakamura, M. J., Valente, L. M., Henriques, M. D. G., ... & Rosas, E. C. (2014). Anti-inflammatory effects of methyl ursolate obtained from a chemically derived crude extract of apple peels: potential use in rheumatoid arthritis. *Archives of pharmacal research*, 37(11), 1487-1495.
7. Tsao, R., Yang, R., Young, J. C., & Zhu, H. (2003). Polyphenolic profiles in eight apple cultivars using high-

- performance liquid chromatography (HPLC). *Journal of agricultural and food chemistry*, 51(21), 6347-6353.
8. Le Deun, E., Van der Werf, R., Le Bail, G., Le Quere, J. M., & Guyot, S. (2015). HPLC-DAD-MS profiling of polyphenols responsible for the yellow-orange color in apple juices of different French cider apple varieties. *Journal of agricultural and food chemistry*, 63(35), 7675-7684.
  9. Cencic, A., & Chingwaru, W. (2010). The role of functional foods, nutraceuticals, and food supplements in intestinal health. *Nutrients*, 2(6), 611-625.
  10. Brieskorn, C. H., & Süß, H. P. (1974). Triterpenoids from the peels of pear and apple (author's transl). *Archiv der Pharmazie*, 307(12), 949-960.
  11. McGhie, T.K.; Hudault, S.; Lunken, R.C.; Christeller, J.T. Apple peel, from seven cultivars, have lipase-inhibitory activity and contain numerous ursenoic acids as identified by LC-ESI-QTOF-HRMS. *J. Agric. Food Chem.* 2012, 60, 482–491.
  12. He, Q. Q., Yang, L., Zhang, J. Y., Ma, J. N., & Ma, C. M. (2014). Chemical Constituents of Gold-red Apple and Their  $\alpha$ -Glucosidase Inhibitory Activities. *Journal of food science*, 79(10), C1970-C1983.
  13. Patocka, J., & Stiborova, M. (2004). Betulinic acid: Prospective cytostatic agent. *Chemické listy*, 98(4).

## Chapter 4

14. Patocka, J. (2003). Biologically active pentacyclic triterpenes and their current medicine signification. *J Appl Biomed*, 1(1), 7-12.
15. Shanmugam, M.K.; Nguyen, A.H.; Kumar, A.P.; Tan, B.K.; Sethi, G. Targeted inhibition of tumor proliferation, survival, and metastasis by pentacyclic triterpenoids: Potential role in prevention and therapy of cancer. *Cancer Lett.* 2012, 320, 158–170.
16. Laszczyk, M. N. (2009). Pentacyclic triterpenes of the lupane, oleanane and ursane group as tools in cancer therapy. *Planta medica*, 75(15), 1549-1560.
17. Bakhtiari, N., Hosseinkhani, S., Tashakor, A., & Hemmati, R. (2015). Ursolic acid ameliorates aging-metabolic phenotype through promoting of skeletal muscle rejuvenation. *Medical hypotheses*, 85(1), 1-6.
18. D'Abrosca, B., Fiorentino, A., Monaco, P., Oriano, P., & Pacifico, S. (2006). Annurcoic acid: A new antioxidant ursane triterpene from fruits of cv. Annurca apple. *Food Chemistry*, 98(2), 285-290.
19. Cefarelli, G., D'Abrosca, B., Fiorentino, A., Izzo, A., Mastellone, C., Pacifico, S., & Piscopo, V. (2006). Free-radical-scavenging and antioxidant activities of secondary metabolites from reddened cv. Annurca apple fruits. *Journal of agricultural and food chemistry*, 54(3), 803-809.
20. Patocka, J., Bhardwaj, K., Klimova, B., Nepovimova, E., Wu, Q., Landi, M., ... & Wu, W. (2020). *Malus domestica*: A review

- on nutritional features, chemical composition, traditional and medicinal value. *Plants*, 9(11), 1408.
21. Yamagishi, T., Zhang, D. C., Chang, J. J., McPhail, D. R., McPhail, A. T., & Lee, K. H. (1988). The cytotoxic principles of *Hyptis capitata* and the structures of the new triterpenes hyptatic acid-A and-B. *Phytochemistry*, 27(10), 3213-3216.
22. Park, S. H., Oh, S. R., Ahn, K. S., Kim, J. G., & Lee, H. K. (2002). Structure determination of a new lupane-type triterpene, tiarellic acid, isolated from *Tiarella polyphylla*. *Archives of pharmacal research*, 25(1), 57-60.
23. Verma, S. C., Jain, C. L., Nigam, S., & Padhi, M. M. (2013). Rapid extraction, isolation, and quantification of oleanolic acid from *Lantana camara* L. Roots using microwave and HPLC-PDA techniques. *Acta Chromatographica*, 25(1), 181-199.
24. Gnoatto, S. C., Dassonville-Klimpt, A., Da Nascimento, S., Galéra, P., Boumediene, K., Gosmann, G., ... & Moslemi, S. (2008). Evaluation of ursolic acid isolated from *Ilex paraguariensis* and derivatives on aromatase inhibition. *European journal of medicinal chemistry*, 43(9), 1865-1877.
25. Cheng, J. J., Zhang, L. J., Cheng, H. L., Chiou, C. T., Lee, I. J., & Kuo, Y. H. (2010). Cytotoxic hexacyclic triterpene acids from *Euscaphis japonica*. *Journal of Natural Products*, 73(10), 1655-1658.

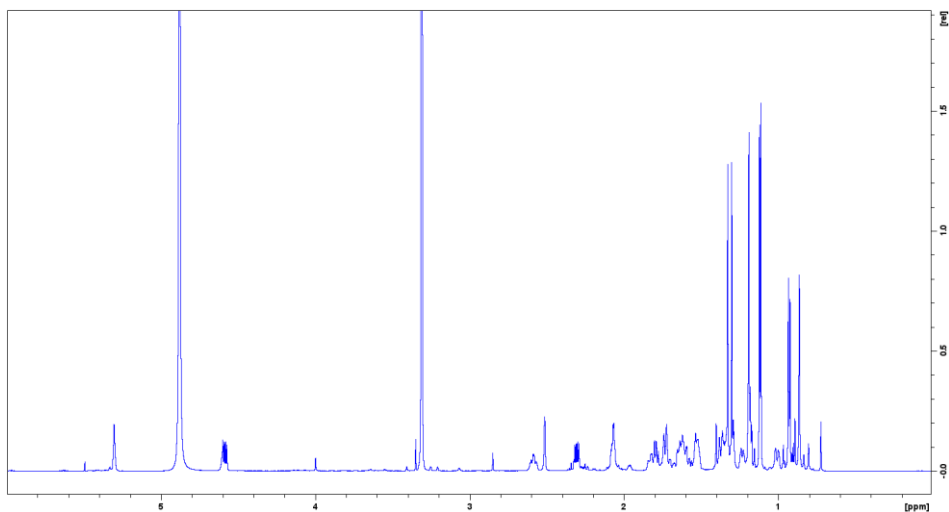
## Chapter 4

26. D'Abrosca, B., Fiorentino, A., Monaco, P., & Pacifico, S. (2005). Radical-Scavenging Activities of New Hydroxylated Ursane Triterpenes from cv. Annurca Apples. *Chemistry & biodiversity*, 2(7), 953-958.
27. Fan, J. P., Liao, D. D., & Zhang, X. H. (2016). Ultrasonic assisted extraction of ursolic acid from apple pomace: A novel and facile technique. *Separation Science and Technology*, 51(8), 1344-1350.
28. Qiao, X., Ye, M., Liang, Y. H., Yang, W. Z., & Guo, D. A. (2011). Retention behaviors of natural products in reversed-phase liquid chromatography using mobile phase comprising methanol, acetonitrile and water. *Journal of separation science*, 34(2), 169-175.

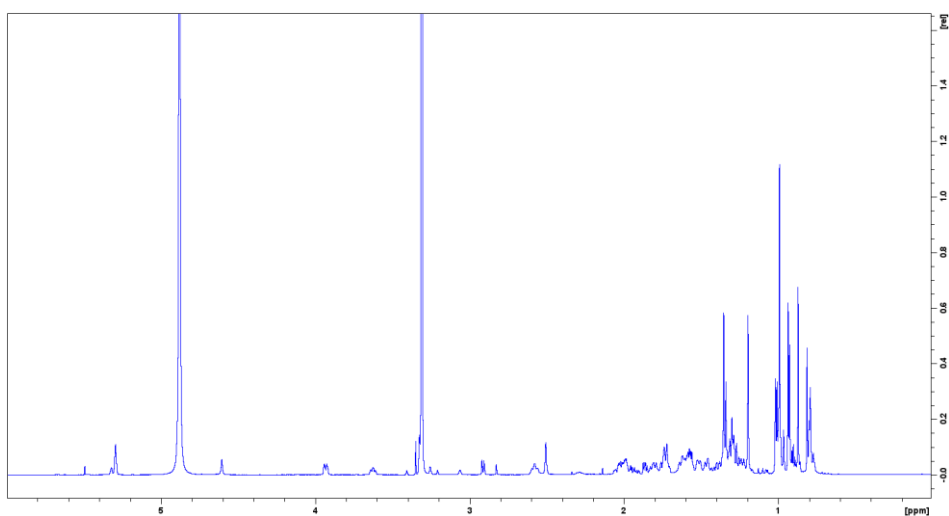
## Appendix C: Spectral data of chapter 4

---

$^1\text{H}$  NMR spectrum (600 MHz) of annurcoic acid (**1**) in  $\text{CD}_3\text{OD}$

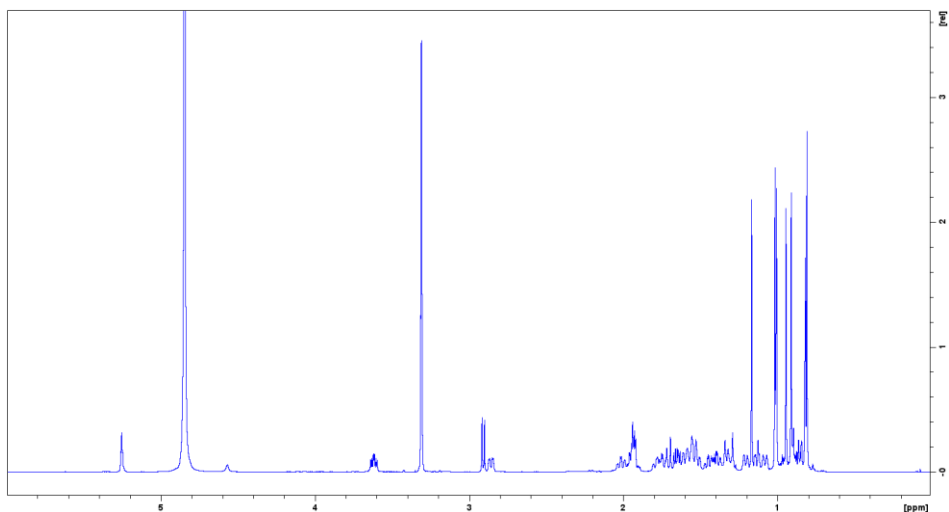


$^1\text{H}$  NMR spectrum (600 MHz) of tormentic acid (**2**) in  $\text{CD}_3\text{OD}$

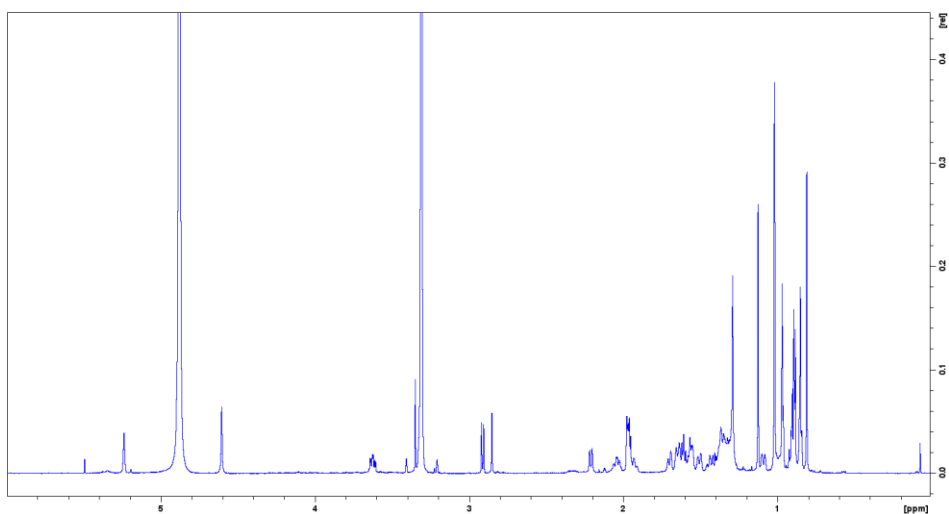


## Appendix C

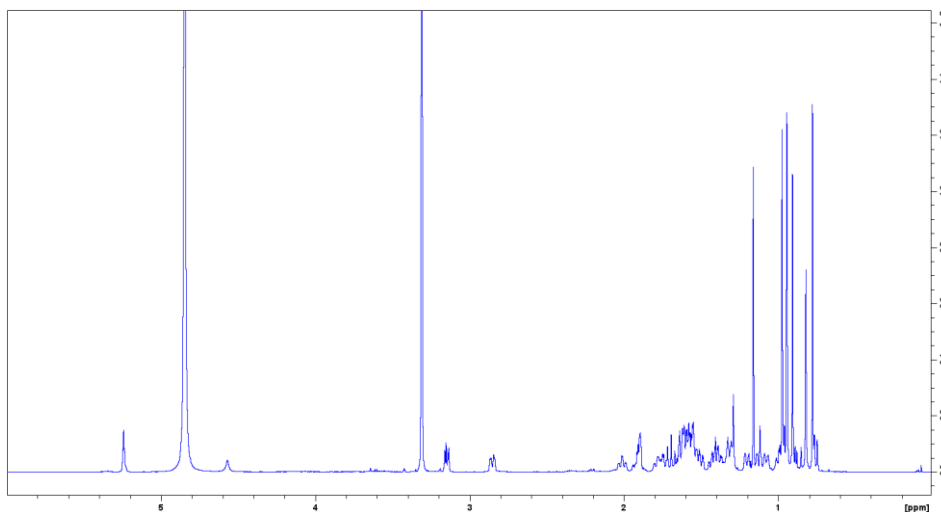
$^1\text{H}$  NMR spectrum (600 MHz) of maslinic acid (**3**) in  $\text{CD}_3\text{OD}$



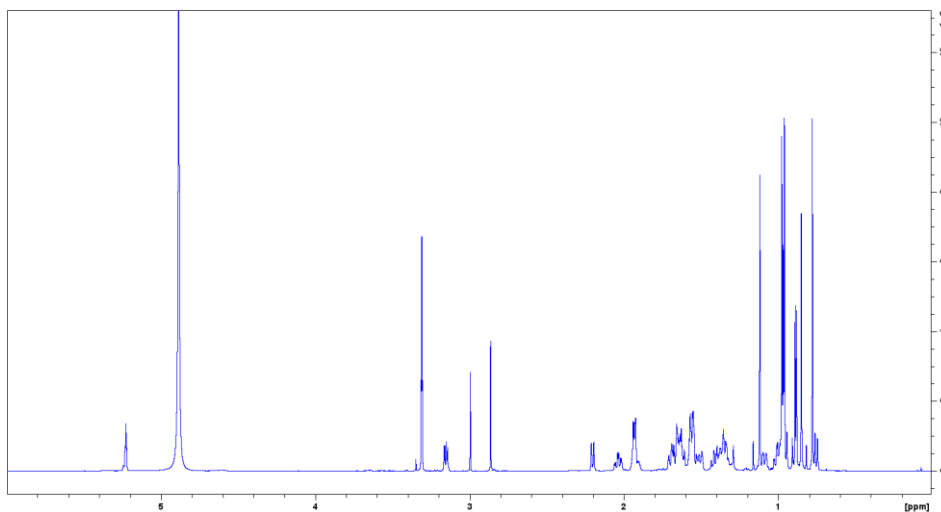
$^1\text{H}$  NMR spectrum (600 MHz) of corosolic acid (**4**) in  $\text{CD}_3\text{OD}$



$^1\text{H}$  NMR spectrum (600 MHz) of oleanolic acid (**5**) in  $\text{CD}_3\text{OD}$

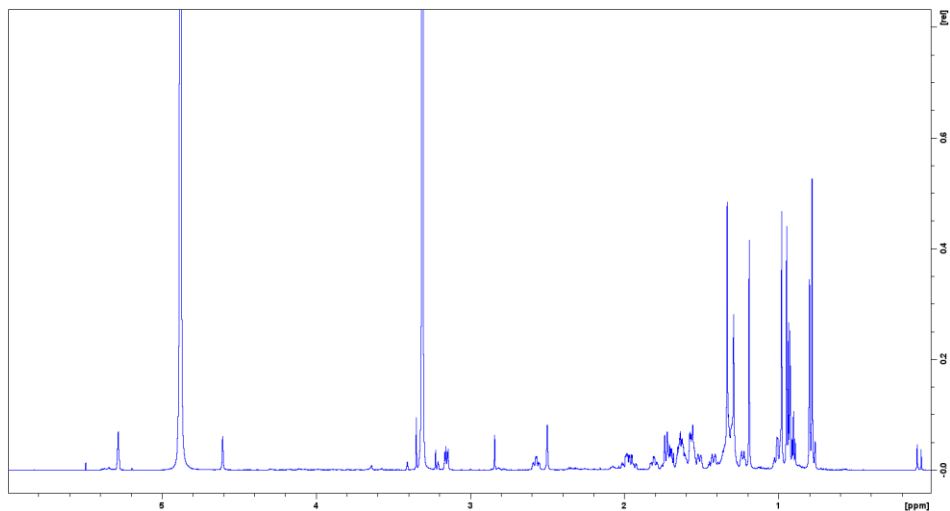


$^1\text{H}$  NMR spectrum (600 MHz) of ursolic acid (**6**) in  $\text{CD}_3\text{OD}$

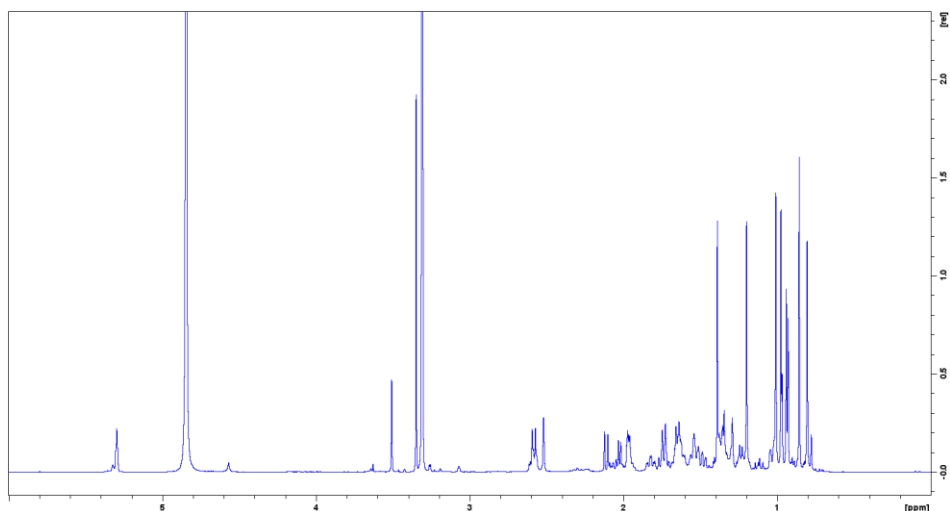


## Appendix C

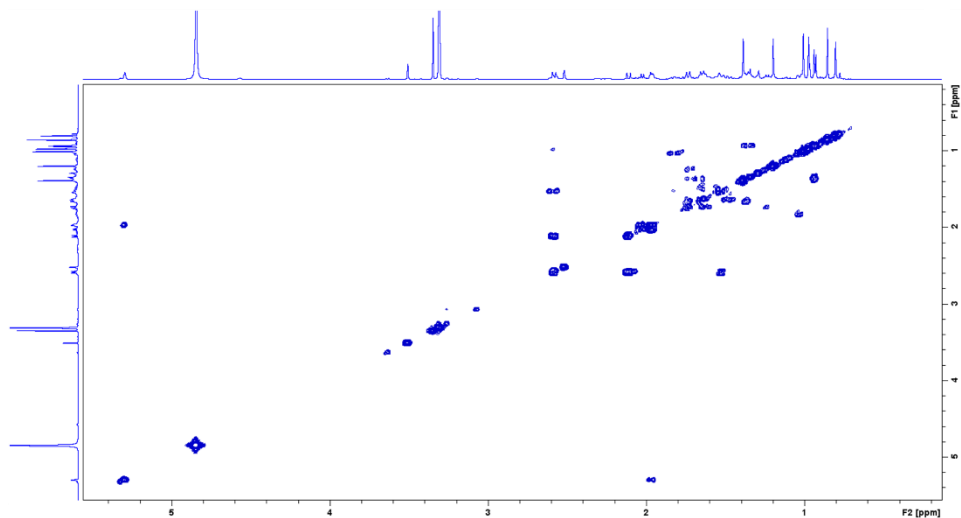
$^1\text{H}$  NMR spectrum (600 MHz) of pomolic acid (**7**) in  $\text{CD}_3\text{OD}$



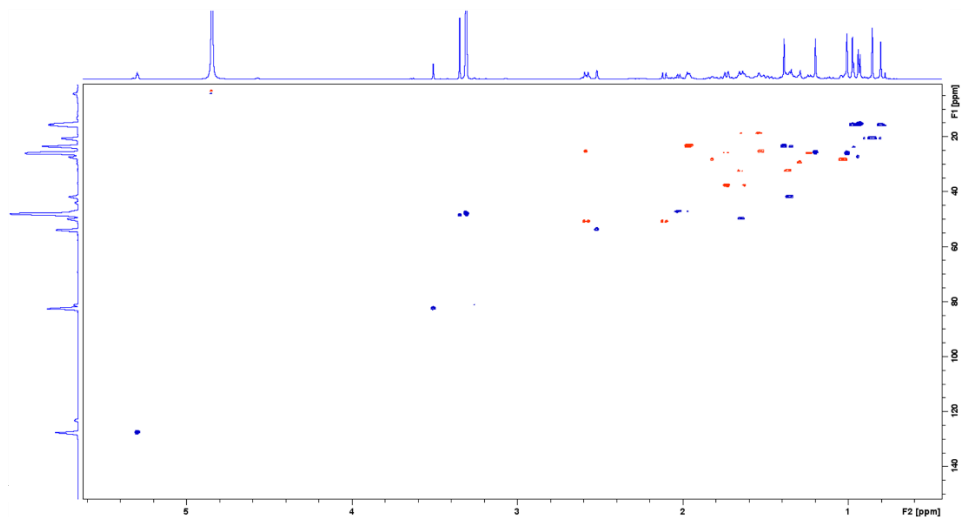
$^1\text{H}$  NMR spectrum (600 MHz) of 3-epi-2-oxopomolic acid (**8**) in  $\text{CD}_3\text{OD}$



COSY NMR spectrum (600 MHz) of 3-epi-2-oxopomolic acid (**8**) in CD<sub>3</sub>OD

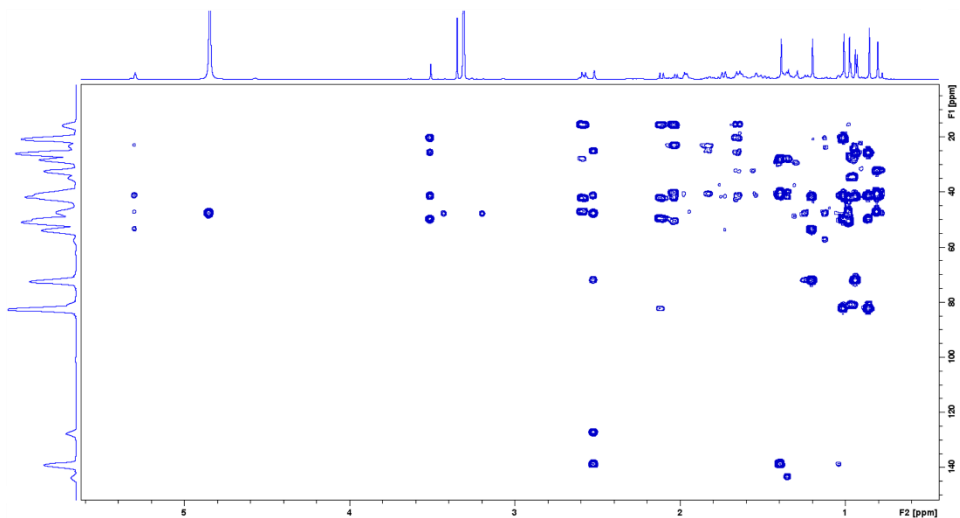


HSQC NMR spectrum (600 MHz) of 3-epi-2-oxopomolic acid (**8**) in CD<sub>3</sub>OD



## Appendix C

HMBC NMR spectrum (600 MHz) of 3-epi-2-oxopomolic acid (**8**) in CD<sub>3</sub>OD



## Chapter 5: Conclusions

---

Natural products can bring several benefits to human health, as well as mitigate health problems. For this reason, their role includes being a "support tool" for personal well-being to date, since they are focused on preventive healthcare strategies, rather than treatment and disease management. A large variety of natural products have been used in health promotion, including nutraceuticals, functional food, and medicinal foods. Among all of these, nutraceuticals have received an unexpected worldwide response, and their market is constantly growing since the nutraceutical industry is flourishing and diversifying rapidly. However, natural matrices are complex, and their chemical composition can strongly vary according to different factors. The work in the present thesis work was carried out in collaboration with Indena SpA (Milan, Italy) and it aimed at the phytochemical characterization of commercial products obtained from different plant extracts and the development and optimization of an extraction method to obtain a nutraceutical product to be placed on the market.

From the chemical point of view, the above-mentioned processes represent the two objectives indispensable to obtain high-quality standardized products.

For this purpose, two commercial products obtained from two plant species were phytochemically investigated to discover the minor compounds that can impact the pharmacological activity of the final product. Regarding Centevita<sup>®</sup>, a nutraceutical product of *Centella asiatica* leaves, its madecassoside-enriched fraction contains significant amounts of the new saponin isomadecassoside, in

## Chapter 5

addition to the main madecassoside and terminoloside. From the LC-MS guided phytochemical investigation on the commercial *C. asiatica* leaves extract named Centevita<sup>®</sup>, 24 secondary metabolites have been identified and quantified, belonging to two structural classes, triterpenoids (and their glycosides) and polyphenolic derivatives. The total amounts found for these components (ab. 43% for triterpenoids and 6% for polyphenols) well correspond to the values reported for the standardized extract. The metabolomic characterization also resulted in the discovery of isoterminoloside, a new triglycoside saponin of the unprecedented  $2\alpha,3\beta,6\beta,23$ -tetrahydroxyolean-13(18)-en-28-oic acid (isoterminolic acid).

As to Rhodiola 5%, a nutraceutical product of *Rhodiola rosea* roots, the LC-MS guided phytochemical investigation allowed the putative identification of some of the main components. Thus, from the chromatographic analysis, 18 secondary metabolites were identified. These belong to two main structural classes, monoterpenoids (and their glycosides) and phenolic derivatives. From the analysis, the ratio between these classes of components seems to follow the industrial specifications, confirming the title of 5% of rosavins and 1.8% of salidroside. The metabolomic characterization also resulted in the discovery of rhodiosidin, a new rosiridin derivative with *trans*-cinnamoyl ester at CH<sub>2</sub>-6'- of glucose. In addition, the 5-lipoxygenase inhibition activity of the main components was characterized, revealing rosiridin, kenposide A and rosavins mainly responsible for the activity of the extract.

On the other hand, a development and optimization of extraction method to obtain a nutraceutical product enriched in annurcoic acid

was investigated. Apple waste was first subjected to a phytochemical investigation that allowed to the identification of seven terpene acids including: annurcoic acid, tormentic acid, maslinic acid, corosolic acid, oleanolic acid, ursolic acid, and pomolic acid. The R&D subsequent activities were carried out at Indena SpA laboratories and led to the development of a seven-step procedure to obtain a standardized extract enriched in annurcoic acid (25% w/w). In parallel, a further procedure was set up to obtain the annurcoic acid to be used as a reference standard. The research process led to the isolation of annurcoic acid (85% w/w), together with two minor compounds: tormentic acid (3.4% w/w) and 3-epi-2-oxopomolic acid (2.6% w/w).

Taken together, these results illustrate the complexity of natural matrices used in the phytotherapeutic and nutraceutical preparations. In parallel, this stimulates the need for a detailed characterization of these extracts trying to identify and possibly quantify all the detectable components, even those present in minor amounts. Indeed, even trace products can give a significant contribution to the activity or to the toxicity and their presence must be monitored and taken into account. In this context, the present research work demonstrates also that even well characterized extracts, such as *Centella asiatica* and *Rhodiola rosea*, can contain compounds that are still waiting to be identified and structurally characterized.